

**LAYER-BY-LAYER SURFACE MODIFICATION OF POLYMER
FILAMENT FOR CATALYTIC 3D PRINTED PARTS**

Pornnutcha Thadasri

A Thesis Submitted in Partial Fulfillment of the Requirements
for the Degree of Master of Science
The Petroleum and Petrochemical College, Chulalongkorn University
in Academic Partnership with
The University of Michigan, The University of Oklahoma,
and Case Western Reserve University

2021



2287006321

CU :Thesis 6272032063 thesis / recv : 19072564 14:14:29 / seq : 8



2287006321

Layer-by-layer Surface Modification of Polymer Filament for Catalytic 3D Printed Parts

Miss Pornnutcha Thadasri

A Thesis Submitted in Partial Fulfillment of the Requirement
for the Degree of Master of Science in Polymer Science
Common Course
The Petroleum and Petrochemical College
Chulalongkorn University
Academic Year 2020
Copyright of Chulalongkorn University

การปรับปรุงพื้นผิวของเส้นใยโพลีเมอร์สำหรับการพิมพ์ตัวเร่งปฏิกิริยาในรูปแบบสามมิติ

น.ส.พรณัชชา ธาดาสีห์

วิทยานิพนธ์นี้เป็นส่วนหนึ่งของการศึกษาตามหลักสูตรปริญญาวิทยาศาสตรมหาบัณฑิต
สาขาวิชาวิทยาศาสตร์พอลิเมอร์ ไม่สังกัดภาควิชา/...
วิทยาลัยปิโตรเลียมและปิโตรเคมี จุฬาลงกรณ์มหาวิทยาลัย
ปีการศึกษา 2563
ลิขสิทธิ์ของจุฬาลงกรณ์มหาวิทยาลัย

พรรณษา ธาตาสีห์ : การปรับปรุงพื้นผิวของเส้นใยโพลิเมอร์สำหรับการพิมพ์ตัวเร่งปฏิกิริยาในรูปแบบสามมิติ. (Layer-by-layer Surface Modification of Polymer Filament for Catalytic 3D Printed Parts) อ.ที่ปรึกษาหลัก : รศ.ดร.สเดฟาน ที ดุบาส

แคตาลิสถูกขึ้นรูปให้อยู่ในรูปแบบของไมโครรีแอ็กเตอร์โดยการหลอมขึ้นรูปโมเดลหรือการพิมพ์ขึ้นรูป 3 มิติที่สามารถปรับแต่งในระดับไมโครเพื่อให้การขึ้นรูปนั้นมีความละเอียดสูง วัสดุที่นำมาใช้ในการขึ้นรูปคือเส้นใยโพลีแลคติกแอซิด (PLA) และโพลีเอทิลีน เทเรฟทาเลต (PET) การปรับแต่งพื้นผิวถูกนำมาใช้ในการปรับปรุงการยึดเกาะของพื้นผิวเส้นใย โดยการใช้ค่าและโพลีเอทิลีนอีมีนที่ใช้เวลาและความเข้มข้นต่างกัน จากนั้นจึงชุบด้วยโพลีเอทิลีน เทเรฟทาเลต มัลติเลเยอร์โดยเทคนิคเลเยอร์สลับเลเยอร์ก่อนที่จะนำไปบรรจุแคตาลิส แคตาลิสถูกสังเคราะห์โดยปฏิกิริยาระหว่างซิลเวอร์ไนเตรตและโซเดียมโบโรไฮไดรด์ด้วยการใช้โพลีโพรพิลีน ซัลโฟเนต โพลีเอทิลีน-โค-มาเลอิกแอซิดเป็นตัวช่วยในการผลิตซิลเวอร์นาโนพาทิกัลที่มีความเป็นแคตาลิสสูง เส้นใยที่บรรจุแคตาลิสแล้วถูกนำมาพิมพ์ขึ้นรูปสามมิติเพื่อนำไปวิเคราะห์คุณสมบัติต่างๆ โดยกล้องจุลทรรศน์อิเล็กตรอนแบบส่องกราด, การทดสอบการลอก, เครื่องทดสอบยูนิเวอร์แซล, เครื่องฟูเรียร์ทรานส์ฟอร์มอินฟราเรดสเปกโตรมิเตอร์, เทคนิคเอ็กซ์เรย์ดิฟแฟรกชัน ค่าและโพลีเอทิลีนอีมีนสามารถเพิ่มการยึดเกาะของพื้นผิวของวัสดุได้เป็นอย่างดีมีประสิทธิภาพ ผลลัพธ์คือการเกาะติดของซิลเวอร์นาโนพาทิกัลที่เพิ่มมากขึ้นอย่างมีนัยสำคัญ

สาขาวิชา	วิทยาศาสตร์พอลิเมอร์	ลายมือชื่อนิสิต
	
ปีการศึกษา	2563	ลายมือชื่อ อ.ที่ปรึกษาหลัก
	



2287006321

CU :Thesis 6272032063 thesis / rev: 19072564 14:14:29 / seq: 8

6272032063 : MAJOR POLYMER SCIENCE

KEYWORD 3D printing, Polyelectrolyte multilayers, Silver nanoparticles

D:

Pornnutcha Thadasri : Layer-by-layer Surface Modification of Polymer Filament for Catalytic 3D Printed Parts. Advisor: Assoc. Prof. STEPHAN T.DUBAS, Ph.D.

Catalyst was constructed in form of microreactor by fused deposition modeling (FDM) or 3D printing method that allow micro scale customization in order to achieve high detail construction. Poly (lactic acid) (PLA) and Poly (acrylonitrile-butadiene-styrene) (ABS) filaments were used as a built-up material. The surface modification was introduced to improve filaments surface adhesion by using alkaline treatment and Polyethyleneimine with variation of time and concentration and then deposited with polyelectrolyte multilayers by layer-by-layer technique before catalyst loading. Catalyst were synthesized by reduction reaction of Silver nitrate (AgNO_3) and sodium borohydride (NaBH_4) with using poly (4-styrenesulfonic acid-co-maleic acid) as a capping agent to produce silver nanoparticles that is supercatalytic. Catalyst loaded filaments were 3D printed out to characterize various properties by Field scanning electron microscopy (FE-SEM), Peeling test, Universal testing machine (UTM), Fourier-transform infrared spectroscopy (FTIR), X-Ray Diffractometer (XRD). Alkaline and Polyethylenimine can effectively increase built up materials surface adhesion resulting in increasing of silver nanoparticles attachment significantly.

Field of Study: Polymer Science

Student's Signature

Academic Year: 2020

Advisor's Signature

Year:

.....

ACKNOWLEDGEMENTS

First, I would like to sincerely thanks to my thesis advisor, Assoc. Prof. Stephan T. Dubas, Ph.D. for his advice and encouragement throughout this research. I am grateful for his help and this thesis would not have achieved without all the support that I have always received from him.

In addition, I would like to thanks external committee Assist. Prof. Bussarin Ksapabutr, Ph.D. and chairman Assoc. Prof. Thanyalak Chaisuwan, Ph.D. for all suggestion and their help.

Finally, I most gratefully acknowledge The Petroleum and Petrochemical College for all equipment and system support throughout the period of this research.

Pornnutcha Thadasri

TABLE OF CONTENTS

	Page
ABSTRACT (THAI)	iii
ABSTRACT (ENGLISH).....	iv
ACKNOWLEDGEMENTS	v
TABLE OF CONTENTS.....	vi
LIST OF TABLES	x
LIST OF FIGURES	xi
CHAPTER 1 INTRODUCTION	1
CHAPTER 2 LITERATURE REVIEW	2
2.1 3D Printing.....	2
2.1.1 Type of 3D Printing.....	2
2.1.2 The Operation of Fused Deposition Modelling.....	3
2.1.3 Parameters of 3D Printing	4
2.1.3.1 Nozzle Size	4
2.1.3.2 Nozzle Temperature	4
2.1.3.3 Bed Temperature	5
2.1.3.4 Printing Speed	5
2.1.4 Materials used for Fused Deposition Modelling	5
2.1.4.1 Poly (lactic acid) (PLA)	5
2.1.4.2 Poly (Acrylonitrile-Butadiene-Styrene) (ABS).....	6
2.1.4.3 Polyethylene Terephthalate Glycol-modified (PETG).....	6
2.2 Polyelectrolyte Multilayers (PEMs)	7
2.2.1 Polycation	8
2.2.2 Polyanion.....	8
2.2.3 Polyelectrolyte Multilayers Construction.....	9
2.3 Metallic Coating	10

2.4 Surface Modification	12
2.4.1 Alkaline Surface Treatment.....	12
2.4.2 Plasma Treatment	12
2.4.3 Polyethylenimine (PEI) Treatment.....	13
2.5 Electrocatalyst.....	13
2.5.1 Silver Nanoparticles (AgNPs).....	14
2.5.2 Zeolitic Imidazole Framework (ZIF-8)	15
2.6 Microreactor	16
CHAPTER 3 METHODOLOGY	20
3.1 Materials and Equipment.....	20
3.2 Experimental Procedures	21
3.2.1 Preparation of Polyelectrolyte Multilayers (PEMs)	21
3.2.2 Silver Nanoparticles Coating.....	21
3.2.2.1 Exsitu.....	21
3.2.2.2 Insitu	22
3.2.3 Surface Treatment	22
3.2.4 Characterization.....	23
3.2.5 3D Printing	25
3.2.6 Preparation of Polyelectrolytes Multilayers (PEMs).....	30
3.2.7 ZIF-8 Synthesis	31
3.2.8 ZIF-8 Coating	31
3.2.9 Surface Characterization	32
3.2.10 3D Printing	32
CHAPTER 4 RESULT AND DISCUSSION	33
4.1 Synthesis of Silver Nanoparticles (AgNPs).....	33
4.2 Silver Nanoparticles Coating on Polyelectrolyte Multilayers	34
4.2.1 Exsitu.....	35
4.2.2 Insitu	37

4.3 Layer-by-layer Assembly of Polyelectrolyte Multilayers (PEMs) on Filaments	39
4.3.1 PEMs Deposition	39
4.3.2 3D printing PEMs Coated Filaments	40
4.4 Silver Nanoparticles Exsitu Loading on Polymer Filament	43
4.4.1 Silver Nanoparticles Loading	44
4.4.2 3D Printing Silver Nanoparticles Coated Filaments	46
4.5 Silver Nanoparticles Insitu Loading on Polymer Filament	48
4.5.1 Silver Nanoparticles Loading	48
4.5.2 3D Printing Silver Nanoparticles Coated Filaments	52
4.6 Surface Treatment of Poly (lactic acid) and Poly (Acrylonitrile-Butadiene Styrene) Filament for Exsitu Silver Nanoparticles Loading	52
4.6.1. NaOH Treatment	53
4.6.1.1 PLA Filament	53
4.6.1.2 ABS Filament	59
4.6.1.3 3D Printed NaOH Treated PLA and ABS	64
4.6.2 Polyethylenimine (PEI) Treatment	65
4.6.2.1 AgNPs Loading on PEI Treated PLA and ABS Filament	65
4.6.2.2 3D Printed PEI Treated PLA and ABS	67
4.7 Surface Treatment of Poly (lactic acid) and Poly (Acrylonitrile-Butadiene Styrene) Filament for Insitu Silver Nanoparticles Loading.	68
4.7.1 Alkaline Treatment	68
4.7.2 PEI Treatment	69
4.7.2.1 AgNPs Loading on PEI Treated PLA and ABS Filament	69
4.7.2.2 3D Printed PEI Treated PLA and ABS	70
4.8 3D Printing Confirmation	71
4.9 ZIF-8 Particles Size Distribution	74
4.10 ZIF-8 Crystal Morphology	75
4.11 ZIF-8 Dispersion on Filaments	76
4.12 3D Printing	80

CHAPTER 5 CONCLUSION.....83

APPENDIX.....85

 Appendix A.....85

REFERENCES86

VITA.....89



2287006921

CU IThesis 6272032063 thesis / recv: 19072564 14:14:29 / seq: 8

LIST OF TABLES

	Page
Table 2.1 Diagram of widely used 3D printing technology (Karakurt and Lin 2020)..	3
Table 2.2 Materials operating temperature	5
Table 3.1 Built-up materials properties.....	29
Table 4.1 Maximum tensile stress of PLA.....	46
Table 4.2 NaOH concentration variation and result of PLA filament after modification	53
Table 4.3 Maximum Tensile Stress of PLA.....	57
Table 4.4 Maximum Tensile Stress of ABS.....	62



2287006921

LIST OF FIGURES

	Page
Figure 2.1 Computer-aided design (CAD) software.....	3
Figure 2.2 Fused deposition modelling process. (Jose, GV et al. 2018).....	4
Figure 2.3 Various nozzle size.....	4
Figure 2.4 PLA structure.....	6
Figure 2.5 ABS structure.	6
Figure 2.6 PETG structure.	7
Figure 2.7 Schematic of the deposition of alternate polyelectrolyte solution.....	8
Figure 2.8 Polycation structure.	8
Figure 2.9 Polyanion structure.	9
Figure 2.10 SEM image of Poly(ethyleneimine) and Poly(acrylic acid) deposition. ...	9
Figure 2.11 Schematic drawing of polyanion/polycation bilayers prepared without (left) and with (right) supporting salt. (Merlin L. Bruening 2020).....	10
Figure 2.12 Thickness as a function of the number of layers for a PSS/PDADMAC with 1.0 M NaCl. (Odd layers are PDADMAC and even layers are PSS.).....	10
Figure 2.13 The incorporation of metal nanoparticles on polyelectrolyte multilayer. (Yuan, Weng et al. 2020).....	11
Figure 2.14 Schematic of Ag-Au bimetallic synthesis by galvanic replacement method. (Zhang, Zhang et al. 2013).....	11
Figure 2.15 The mechanism of PLA hydrolysis in basic solution. (Tham, Hamid et al. 2014).....	12
Figure 2.16 Repeating unit of Polyethylenimine.	13
Figure 2.17 Linear PEIs and branched PEIs structure.	13
Figure 2.18 Illustration of typical pathways of oxygen reduction reaction in an alkaline fuel cell and three categories of the electrocatalysts used for oxygen reduction reaction (ORR). (Song, Cheng et al. 2016).....	14
Figure 2.19 Transmission electron microscopy (TEM) images of silver nanoparticles with diameters of 20 nm, 60 nm, and 100 nm respectively with scale bars of 50 nm. 15	

Figure 2.20 Mechanism of the formation of ZIF-8 crystals in water. (Jian, Liu et al. 2015).....	16
Figure 2.21 General concept of microreactor. (Ramanjaneyulu, Vishwakarma et al. 2018).....	17
Figure 2.22 a) CAD design of microreactor 3D model b) 3D printed microreactor by FDM. (Neumaier, Madani et al. 2019)	17
Figure 2.23 a) glass microreactor fabricated by wet chemical etching. b) PDA coated microreactor by dip coating. c) AgNPs coated microreactor by insitu immobilization. (Zhang, Liu et al. 2017)	18
Figure 2.24 Reduction reaction of 4-NP to 4-AP by NaBH ₄ and AgNO ₃ performed in glass microreactor.	19
Figure 3.1 PEMs procedure.	21
Figure 3.2 Exsitu coating.	22
Figure 3.3 Insitu coating.	22
Figure 3.4 Peeling test.....	24
Figure 3.5 Image J program.	24
Figure 3.6 Anet A8 3D printer.	29
Figure 3.7 Set up process of 3D printer.	30
Figure 4.1 AgNPs solution.....	33
Figure 4.2 UV-vis spectrum of AgNPs solution.	34
Figure 4.3 9 (top) and 10 (bottom) layers of PEMs deposited glass slide appearance.	35
Figure 4.4 Diagram of exsitu (left) and insitu (right) AgNPs loading method.	35
Figure 4.5 Silver nanoparticles coating on PEMs at different concentration of PSS-co-MA 0.25, 0.1, 0.05, 0.01, 0.005 mM respectively.	36
Figure 4.6 UV-vis spectrum of AgNPs coated glass at various concentration of capping agent.	36
Figure 4.7 Silver nanoparticles coating on different layers of PEMs 3,5,7,9,11 layers.	37
Figure 4.8 PSS 50 mM with NaCl concentration of 0,1,2 M respectively.	37
Figure 4.9 PSS concentration of 0,5,10,30,50,100 mM with NaCl 2 M respectively.	38

Figure 4.10 DI water, PSS 50 mM → NaCl 2 M, NaCl 2 M → PSS 50 mM respectively.	38
Figure 4.11 3,4,5,6,7,8,9,10 layers of PEMs deposited filament appearance respectively.	39
Figure 4.12 PLA (left) and ABS (right) filament with 2,4,6,8 layers of PEMs.....	40
Figure 4.13 ATR-FTIR spectra of bare PLA, PLA with PDAD top layer, and PLA with PSS top layer.....	41
Figure 4.14 ATR-FTIR spectra of bare PLA, Polyelectrolyte multilayers coated PLA odd layer and even layer.	43
Figure 4.15 Dye absorption of before (left) and after (right) 3D printed polyelectrolyte multilayers coated filament. a) Untreated b) NaOH treated c) PEI treated.....	43
Figure 4.16 PLA and ABS filament respectively.	44
Figure 4.17 AgNPs coated PLA and ABS filament respectively.	44
Figure 4.18 The morphology of AgNPs dispersion on PLA and ABS filament respectively.	45
Figure 4.19 Stress and % strain curve of AgNPs coated PLA.....	45
Figure 4.20 Printed normal PLA and ABS filament respectively.....	46
Figure 4.21 Printed AgNPs exsitu coated PLA and ABS filament respectively.	47
Figure 4.22 FE-SEM surface image of printed AgNPs exsitu coated PLA and ABS filament respectively.	47
Figure 4.23 FE-SEM cross-section image of printed AgNPs exsitu coated PLA at x5.00k and x15.0k.....	47
Figure 4.24 PDAD and PSS 10 mM in NaCl 1 M, AgNO ₃ 10 mM, NaBH ₄ 5 mM. ...	48
Figure 4.25 PDAD and PSS 50 mM in NaCl 2 M, AgNO ₃ 10 mM, NaBH ₄ 5 mM. ...	49
Figure 4.26 PDAD and PSS 50 mM in NaCl 2 M, AgNO ₃ 20,30 mM respectively, NaBH ₄ 5 mM.	49
Figure 4.27 PLA that soaked into 50 and 100 mM AgNO ₃	50
Figure 4.28 PLA with 8,10,12,14,16 PEMs layers using 10 mM AgNO ₃ respectively.	50
Figure 4.29 PLA with 8 PEMs using 30,50,100 mM AgNO ₃ respectively.	51
Figure 4.30 The morphology of AgNPs insitu synthesized on PLA.	51

Figure 4.31	The morphology of AgNPs insitu synthesized on ABS.	52
Figure 4.32	Broken PLA filament from modification.	54
Figure 4.33	FE-SEM image of PLA filament cross section at different magnification.	54
Figure 4.34	% weight loss of PLA after treated at various times.	55
Figure 4.35	FE-SEM image of NaOH treated surface of PLA filament at different magnification.	56
Figure 4.36	Stress and % strain curve of bare PLA and NaOH PLA.	57
Figure 4.37	Untreated and Alkaline treated PLA	58
Figure 4.38	The morphology of AgNPs dispersion on alkaline treated PLA on low and high surface roughness respectively.....	58
Figure 4.39	Peeling test of NaOH treated PLA.	59
Figure 4.40	FE-SEM image of NaOH treated surface of ABS filament at different magnification.	61
Figure 4.41	% weight loss of ABS after treated at various concentration of NaOH. .	61
Figure 4.42	Stress and % strain curve of ABS.....	62
Figure 4.43	The morphology of AgNPs dispersion on alkaline treated ABS.....	63
Figure 4.44	Peeling test of NaOH treated ABS.	63
Figure 4.45	FE-SEM image of printed AgNPs exsitu coated on NaOH treated PLA and ABS.	64
Figure 4.46	FE-SEM cross-section image of printed AgNPs exsitu coated on NaOH treated PLA at x5.00k and x15.0k.	64
Figure 4.47	PEI treated PLA and ABS filament respectively.....	65
Figure 4.48	The morphology of AgNPs dispersion on PEI treated PLA and ABS.	66
Figure 4.49	Peeling test of PEI monolayer treated PLA and ABS.	66
Figure 4.50	Peeling test of PEI multilayer treated PLA.	67
Figure 4.51	FE-SEM image of printed AgNPs exsitu coated on PEI treated PLA and ABS.....	67
Figure 4.52	FE-SEM cross-section image of printed AgNPs exsitu coated on NaOH treated PLA at x5.00k and x15.0k.	68
Figure 4.53	NaOH treated insitu coating.	68



2287006921

Figure 4.54 AgNPs insitu loaded PEI treated PLA and ABS respectively.....	69
Figure 4.55 The morphology of AgNPs insitu synthesized on PEI treated PLA.....	70
Figure 4.56 The morphology of AgNPs insitu synthesized on PEI treated ABS.	70
Figure 4.57 Printed AgNPs insitu coated PLA filament with and respectively.....	71
Figure 4.58 FE-SEM image of printed AgNPs insitu coated on PEI treated PLA and ABS.....	71
Figure 4.59 Printed AgNPs coated sample. a) Untreated b) NaOH treated c) PEI treated.....	72
Figure 4.60 XRD patterns of printed samples. (Shameli, Ahmad et al. 2012)	73
Figure 4.61 SEM image of synthesized ZIF-8.....	74
Figure 4.62 Size distribution of ZIF-8 particles.....	75
Figure 4.63 ZIF-8 solutions.	75
Figure 4.64 XRD patterns of synthesized ZIF-8 sample.	76
Figure 4.65 Optical images of PLA and ABS filaments; seed layer, and secondary growth.	77
Figure 4.66 Optical images of PETG filaments; bare filament, seed layer, and secondary growth.	77
Figure 4.67 SEM images of ZIF-8 seed layer at different magnification; a) PLA x5.00k, b) PLA x10.0k, c) ABS x5.00k, d) ABS x10.0k, e) PETG 5.00k, and f) PETG x10.0k.....	79
Figure 4.68 ZIF-8 dense thin film coated on PETG filaments obtained from secondary growth process in different growth time; a) 1 hr., b) 2 hr., c) 3 hr.	79
Figure 4.69 FE-SEM image of printed PETG surface.	80
Figure 4.70 FE-SEM image of printed seed layer and growth layer of ZIF-8 coated PETG.....	80
Figure 4.71 FE-SEM image of growth layer of ZIF-8 coated printed seed layer of ZIF-8 coated PETG.....	81
Figure 4.72 XRD patterns of printed samples.....	82



2287006921

CU IThesis 6272032063 thesis / rev: 19072564 14:14:29 / seq: 8

CHAPTER 1

INTRODUCTION

It is known today that 3D printing or additive manufacturing is technology that can construct three dimensional objects. This technology first emerged in 1981; printed model was built up using polymer. After that, printing was developed to be widely used in printing materials such as metal, ceramics, hydrogel, and composite.

Nowadays, 3D printing technology has been developed to be usable in chemical engineering because its performance is the key to produce super complex shapes or geometries that would be otherwise impossible to construct by hand. Therefor it is an option to construct chemical engineering device like microreactor which transports gaseous precursor and gaseous products are mostly made from glass, quartz, silicon, and metals such as stainless steel that has disadvantages such as poor corrosion resistance and high cost. The 3D printing can construct microreactor from plastic as a built-up material that light weight, low cost, and easy to modify and customize. Built up materials in use to fabricate microreactor is surface modified by layer-by-layer technique, deposition of polyelectrolyte multilayer and addition of treatment such as alkaline and Polyethylenimine in order to increase adhesion between built up materials and metal nanoparticles that act as catalyst.

The aim of this research is to introduce surface modification to improve surface adhesion of built up materials used in 3D printing technology and metallization to functionalize built up materials for catalyst.

The morphology of metal nanoparticles dispersion on substrate was analyzed by Field scanning electron microscopy (FE-SEM), the adhesion between metal nanoparticles and substrate was demonstrated by Peeling test, the effect of surface treatment to modified built up materials was investigated by Universal testing machine (UTM), the effect of 3D printing process to polyelectrolyte multilayers was characterized by Fourier-transform infrared spectroscopy (FTIR), and the effect of 3D printing process to metal nanoparticle was characterized by X-Ray Diffractometer (XRD)

CHAPTER 2

LITERATURE REVIEW

2.1 3D Printing

3D printing or additive manufacturing is advance technology with a high degree of customization of product. 3D printing can construct three-dimensional object by layer by layer deposition of material designed by computer program. And can fabricate very complex shape in micro scale which is impossible to construct with manmade. Nowadays, 3D printing technology is widely used in the world for the decade in the field of agriculture in healthcare, automotive, and biomedical. (Shahrubudin, Lee et al. 2019)

2.1.1 Type of 3D Printing

3D printing technologies have variety types differentiate by material used, process, and function. According to ASTM standard F2792 (Shahrubudin, Lee et al. 2019) that categorized 3D printing into seven group, including the binding jetting, directed energy deposition, material extrusion, material jetting, powder bed fusion, sheet lamination and vat photopolymerization. The commonly used 3D printing is fused deposition modeling (FDM) that in the group of materials extrusions. FDM method uses thermoplastic polymer filament (such as PLA and ABS) as the main material and fabricate product by layer-by-layer from the bottom to the top by heating while extrusion. Process can be applied with fabrication of composite filament by embedding ceramic or metal particles. (Karakurt and Lin 2020)



2287006921

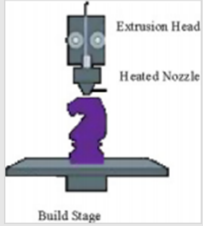
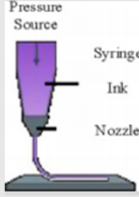
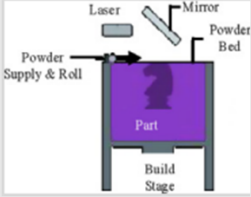
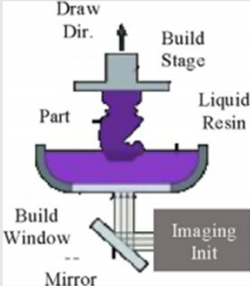
	Fused deposition modelling (FDM)	Direct ink writing	Selective laser sintering (SLS)	Stereolithography (SLA)
Illustration				
Materials	Thermoplastics polymer	Hydrogels, composites	Metals and polymers powder	Photopolymer resin
Application	- Microfluidic devices - automotive and aerospace	- Hydrogels for drug encapsulation - Electronic devices	- Medical and healthcare - Electronic devices	- Dental and healthcare - Engineering

Table 2.1 Diagram of widely used 3D printing technology (Karakurt and Lin 2020)

2.1.2 The Operation of Fused Deposition Modelling

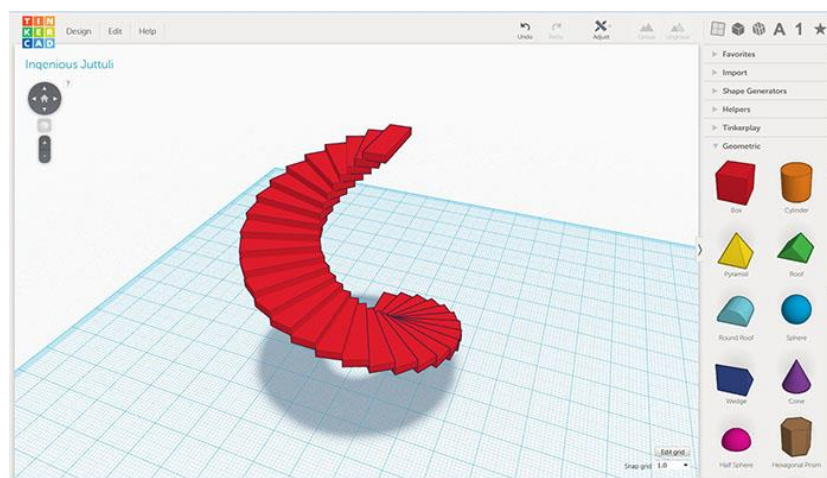


Figure 2.1 Computer-aided design (CAD) software.

3D object creation starts with digital 3D model designed in computer-aided design (CAD) software. And 3D model design file must be converted to a format that 3D printer can understand before printing.

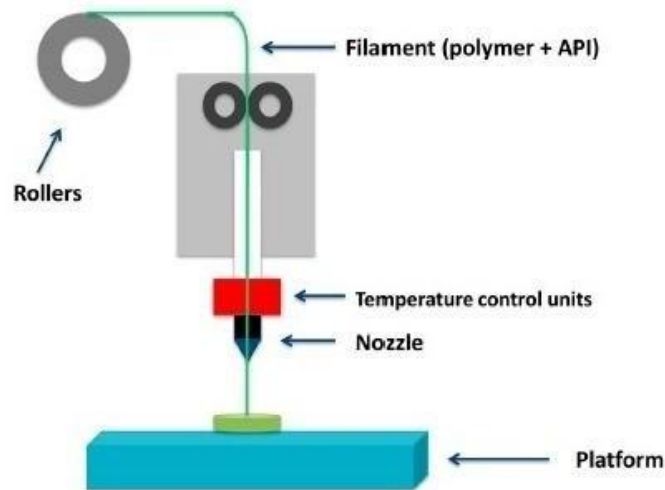


Figure 2.2 Fused deposition modelling process. (Jose, GV et al. 2018)

Plastic filament is fed through printer's head while nozzle is heated to above materials softening point which is then extruded through a moving nozzle on a moving platform, and deposited layer by layer from the bottom to the top in the desired shape. Printed filament is solidified by air.

2.1.3 Parameters of 3D Printing

2.1.3.1 Nozzle Size

A smaller nozzle size obtains great for detailed but slower print, while bigger nozzles size can print faster, but the quality is poorer. The nozzle size correlate with layer height thus nozzle size should be chosen appropriately with layer height.



Figure 2.3 Various nozzle size.

2.1.3.2 Nozzle Temperature

Printing process require appropriate nozzle temperature set up in order to soften plastic filament through the extrusion process. Thus, nozzle

temperature range depend on plastic filament type that commonly set up above softening point of plastic. If nozzle is too hot, the filament can become extra soft and flimsy. This can cause printed sample to be messy and droopy. If nozzle is too cold, nozzle will be clogged by hardened filament.

2.1.3.3 Bed Temperature

Bed or platform temperature need to be set up in proper range depend on type of plastic filament in order to adhere printed sample on 3D printer platform to avoid shifting or warping. If temperature is too low, printed sample cannot adhere on platform cause inaccurate deposition.

Materials	Nozzle temperature (°C)	Bed temperature (°C)
PLA	180 – 230	80
ABS	210 – 250	100 – 110
PETG	220 – 250	100
PC	290 - 315	140 – 145
Nylon	220 - 250	70 - 90

Table 2.2 Materials operating temperature

2.1.3.4 Printing Speed

3D printing speed is usually set in the slicing software that use to create 3D model in order to control the nozzle moving around the part to print each layer of filament depends on type of filament and 3D printer. Too high printing speed can cause low quality of printed sample and to slow printing speed can overheat the nozzle head and cause major print imperfections. Appropriate printing speed can help improving print quality and helping reduce problems such as warping or curling.

2.1.4 Materials used for Fused Deposition Modelling

2.1.4.1 *Poly (lactic acid) (PLA)*

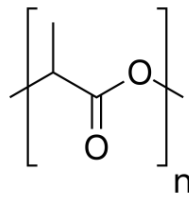


Figure 2.4 PLA structure.

PLA filament is commonly used to be build up material for 3D printing because of characteristic of ease of printing, glossiness, multicolor appearance. (Baran and Erbil 2019) A high accuracy of printing can be achieved with PLA because of proper glass transition and melting temperature and viscosity for layering when it melts. However, PLA filaments have some disadvantages such as poor toughness and brittle.

2.1.4.2 Poly (Acrylonitrile-Butadiene-Styrene) (ABS)

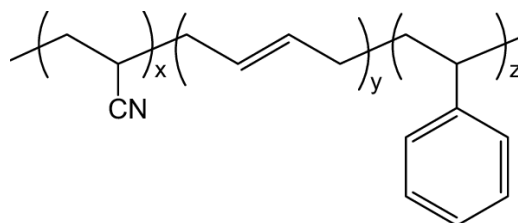


Figure 2.5 ABS structure.

ABS is amorphous thermoplastic that consist of three types of monomer such as Acrylonitrile, Styrene, and 1,3-butadiene. ABS properties are high toughness from butadiene and resistance to acid or alkali and flammable when exposed to high temperature. Product that made from ABS such as toys, musical instrument, container, bumper.

ABS is suitable for using in 3D printing due to high stability and various post-processing but commonly used less than PLA because PLA can be achieved higher accuracy than ABS and poses less warp because PLA has more proper melting temperature.

2.1.4.3 Polyethylene Terephthalate Glycol-modified (PETG)

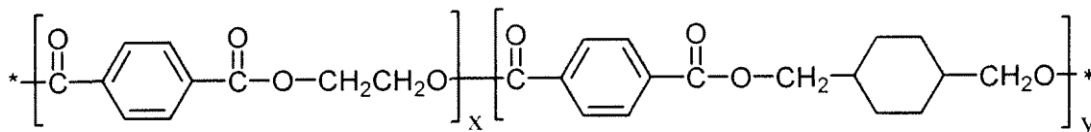


Figure 2.6 PETG structure.

PETG is a copolymer of the synthetic polymer Polyethylene Terephthalate (PET) that made from made from 3 components such as terephthalic acid (TPA), ethylene glycol (EG) and cyclohexane dimethanol (CHDM). PETG is the material used to make water bottles and plastic bottles because has a clear, semi-transparent color. PETG are extremely tough, durable and strength equivalent to ABS, but easy to print like PLA therefor it is suitable for use as a replacement for PLA in applications requiring high strength and heat resistance.

2.2 Polyelectrolyte Multilayers (PEMs)

The deposition of polycation and polyanion on substrate by layer-by-layer assembly technique. The surface of substrate is treated to negatively charge by appropriate technique and dipped into a solution of polycation and polyanion alternately, rinsing by deionized water during dipping the other solution to remove the excess solution. Electrostatic force between oppositely charges makes each layer of polyelectrolyte stick to each other leading to reversal of the surface charge.

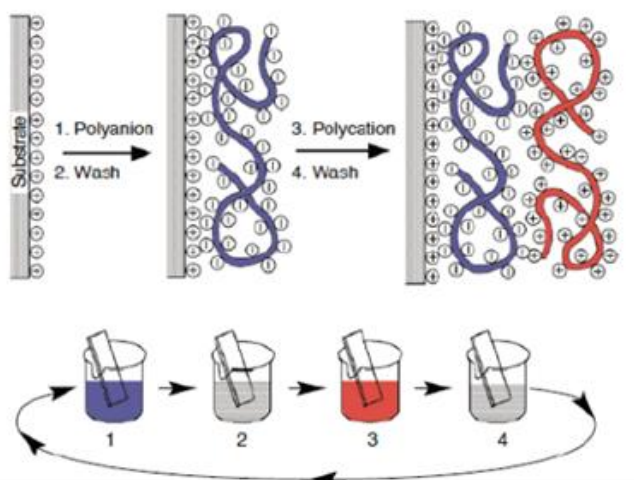


Figure 2.7 Schematic of the deposition of alternate polyelectrolyte solution.

(Merindol 2014)

2.2.1 Polycation

A polymer or chemical complex having positive charges at several sites. Example of Polydiallyldimethylammonium chloride (PDADMAC), Poly (allylamine hydrochloride).

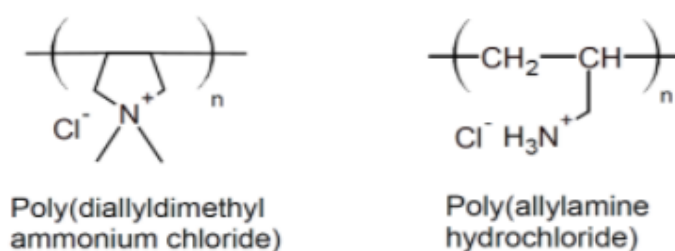


Figure 2.8 Polycation structure.

2.2.2 Polyanion

A polymer or chemical complex having negative charges at several sites. Example of Polyacrylate, Poly(styrenesulfonate), Polyacrylamide, Poly (acrylamide-2-methyl-1-propanesulfonate).

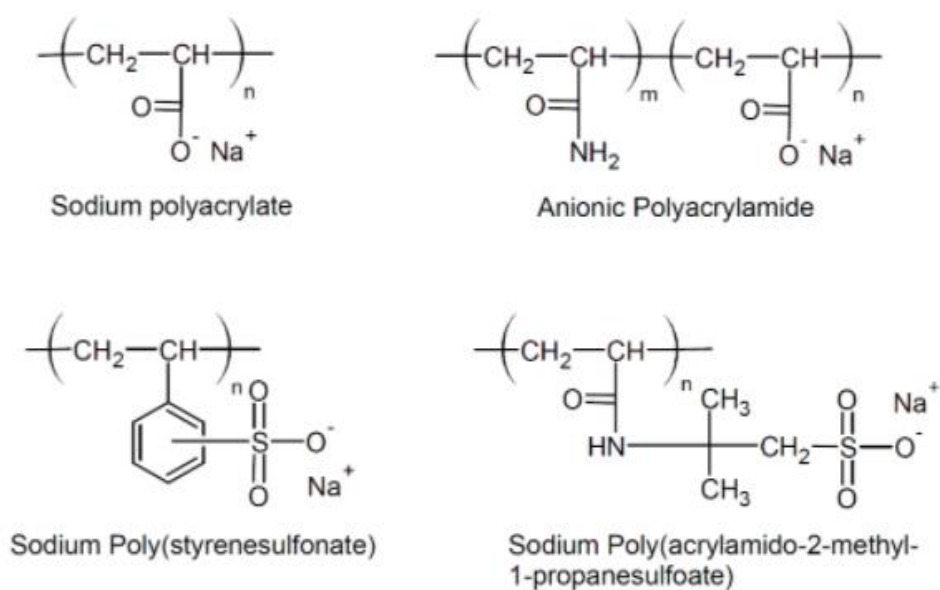
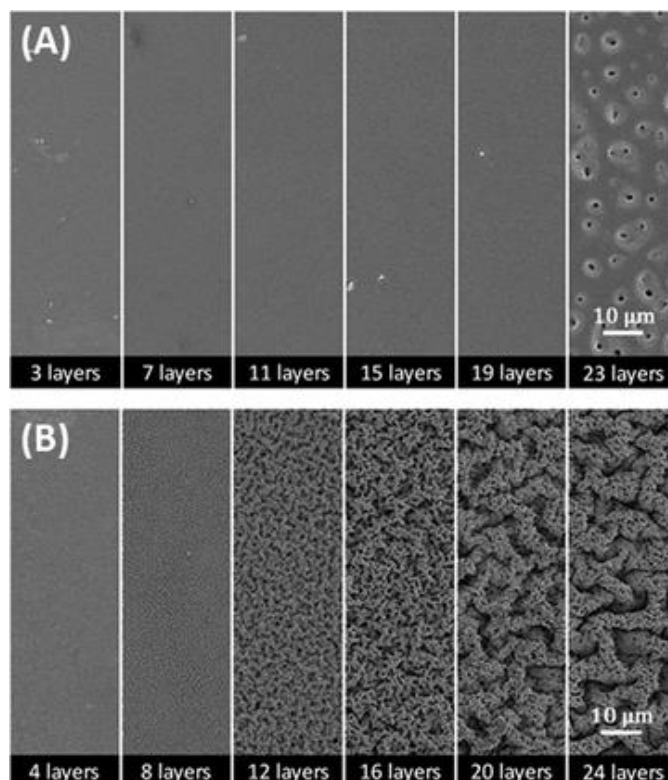
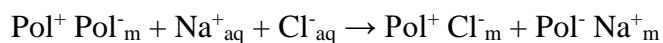


Figure 2.9 Polyanion structure.**Figure 2.10** SEM image of Poly(ethyleneimine) and Poly(acrylic acid) deposition.

(A) PEI is on top (B) PAA is on top. (Chen, Ren et al. 2016)

2.2.3 Polyelectrolyte Multilayers Construction

The most important parameter is the thickness of PEMs deposition. Exactly, the thickness of PEMs deposition increases proportional to the number of layers of polyelectrolyte. But the increment of the thickness is in the extremely small scale. For example, the thickness of a 10 bilayer PSS/PDADMAC prepared is about 60 Å, the average thickness per layer is only 3 Å. (Dubas and Schlenoff 1999) Thus charge compensation has been introduced by addition of salt into polyelectrolyte solution. (Dubas and Schlenoff 2001) Salt function is to create charge compensation form by neutralize polycation and polyanion that is shown in equation:



Result to swelling of each layer, the thickness of the corresponding 10 bilayer is more than 3,000Å.

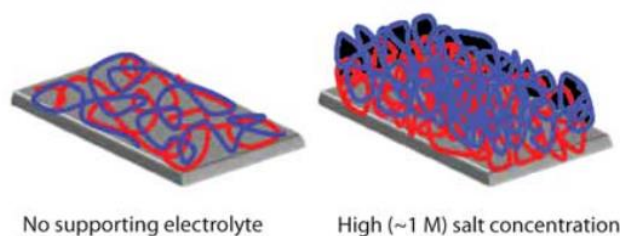


Figure 2.11 Schematic drawing of polyanion/polycation bilayers prepared without (left) and with (right) supporting salt. (Merlin L. Bruening 2020)

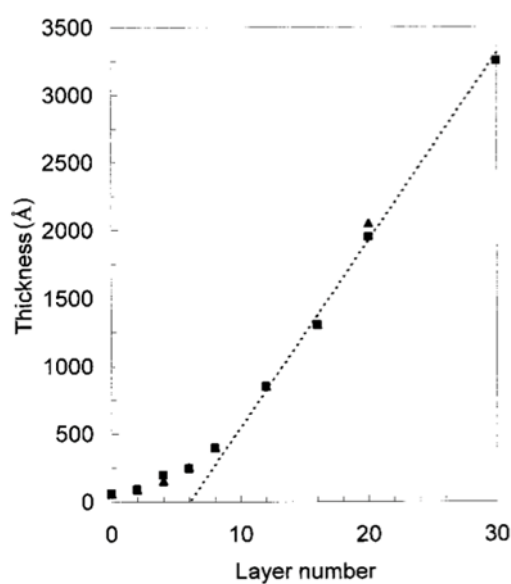


Figure 2.12 Thickness as a function of the number of layers for a PSS/PDADMAC with 1.0 M NaCl. (Odd layers are PDADMAC and even layers are PSS.)
(Dubas and Schlenoff 1999)

2.3 Metallic Coating

PEMs can be fabricated on variety substrates by layer-by-layer assembly and can be surface functionalized by various metallic nanoparticles such as Au, Ag, Pt, Pd. This functionalization can be also called surface metallization. The modified

substrates have found application in antimicrobial coating, catalyst, electrocatalyst, optics, electrical engineering, magnetism. (Kong, Rui et al. 2017)

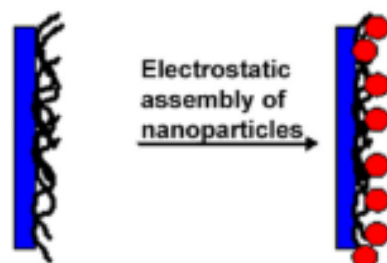


Figure 2.13 The incorporation of metal nanoparticles on polyelectrolyte multilayer. (Yuan, Weng et al. 2020)

Surface metallization should load appropriate sort of catalyst to achieve desire chemical reaction and can apply with application. Monometallic and bimetallic system is the key enabling target application. The system of Pt, Pd, Ag, Au, Ru, Ir nanoparticles and Pt-Ru, Pt-Pd, Ag-Au, Ag-Pd are example of monometallic and bimetallic system respectively. (Açıkyıldız, Gürses et al. 2014)

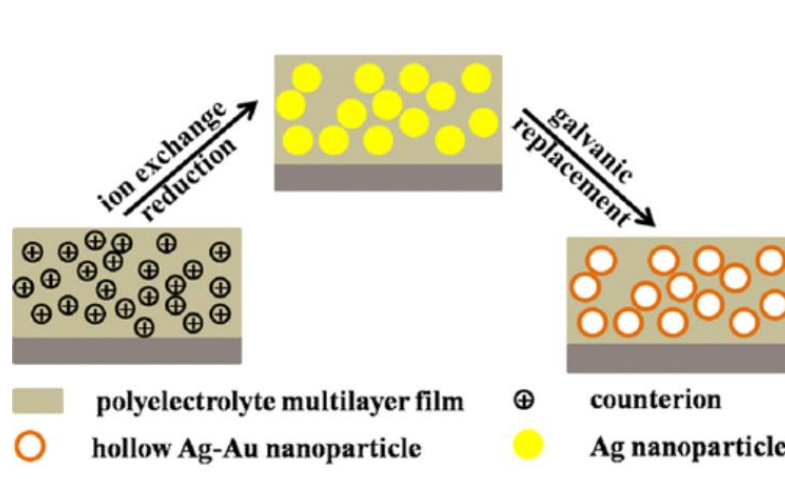


Figure 2.14 Schematic of Ag-Au bimetallic synthesis by galvanic replacement method. (Zhang, Zhang et al. 2013)

2.4 Surface Modification

2.4.1 Alkaline Surface Treatment

PLA consist of ester bond that is not reactive. The alkaline solution such as NaOH and KOH can modify the surface properties of PLA such as surface hydrophilicity, surface energy by hydroxide nucleophilic attack on the ester bond. However, increase surface roughness because degradation from strong alkaline. Thus, low concentration of alkaline solution can success the surface modification of PLA.

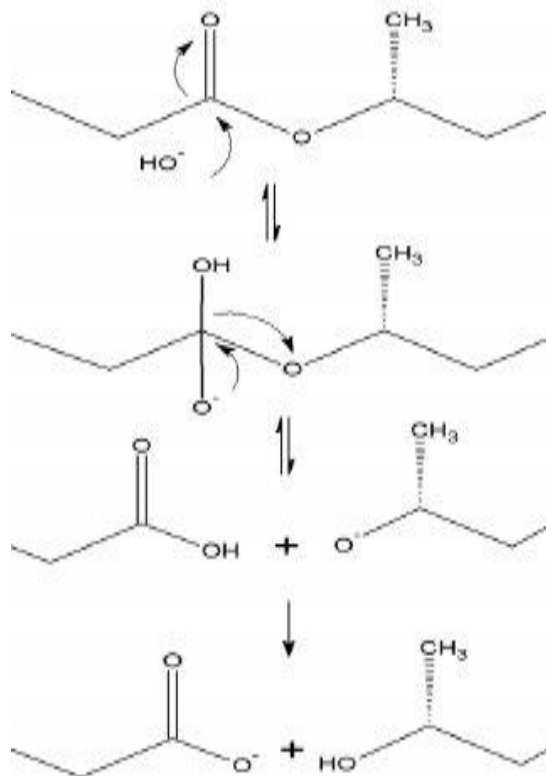


Figure 2.15 The mechanism of PLA hydrolysis in basic solution. (Tham, Hamid et al. 2014)

2.4.2 Plasma Treatment

Plasma treatment is activation of positive ions and electrons produced by ionization (Rasal, Janorkar et al. 2010) to improve PLA surface hydrophilicity by treated PLA surface with oxygen, helium, and nitrogen. (Baran and Erbil 2019) NH_3 plasma created reactive amine groups on PLA through polar and hydrogen bond.

2.4.3 Polyethylenimine (PEI) Treatment

Polyethylenimine (PEI) or polyaziridine is hydrophilic polymers that compose of monomer of CH_2CH_2 and amine group. PEI structure can be either linear or branch. The linear PEIs are solids and branched PEIs are liquids at room temperature.

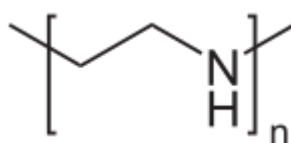


Figure 2.16 Repeating unit of Polyethylenimine.

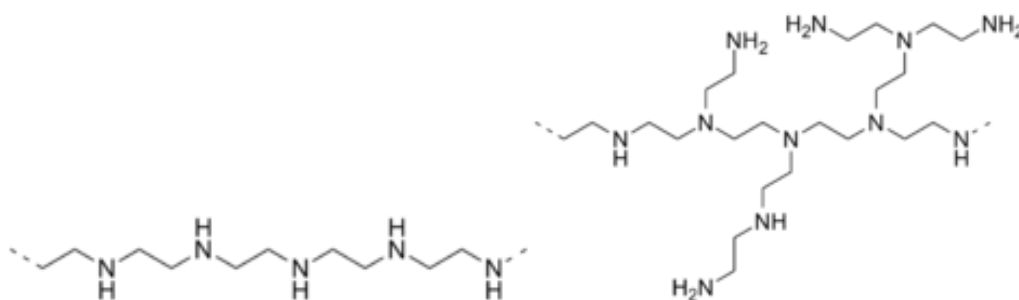


Figure 2.17 Linear PEIs and branched PEIs structure.

PEIs is cationic polymer and has strong positively charge thus PEIs is commonly used as polyelectrolyte multilayer to modify the surface for many substrates such as fiber, polymer to enhance the adhesion, wettability.

2.5 Electrocatalyst

Electrocatalyst is catalysts that is an electrochemical reaction involved and generate electrical power. Electrocatalyst can be fabricated by surface metallization with metal nanoparticles to functionalize electrode surface using as an intermediate chemical transformation to increase chemical reaction rate. The catalytic activity of an electrocatalyst can be tuned with size of metal particles, surface area, and type of

substrate. Electrocatalyst can be used in the field of electrochemical devices such as fuel cells, batteries, sensors, solar cells, and electrolysis cell.

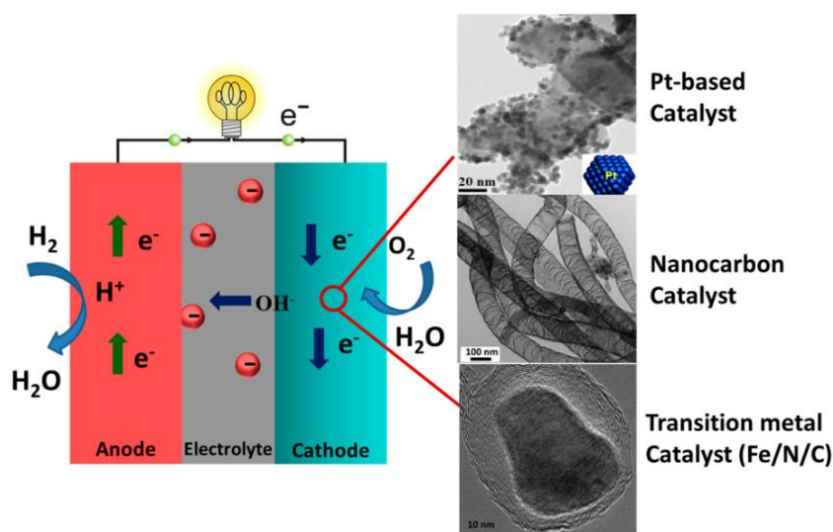
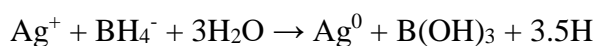


Figure 2.18 Illustration of typical pathways of oxygen reduction reaction in an alkaline fuel cell and three categories of the electrocatalysts used for oxygen reduction reaction (ORR). (Song, Cheng et al. 2016)

2.5.1 Silver Nanoparticles (AgNPs)

S. Iravani and co-worker synthesized Ag nanoparticles. Ag nanoparticles was synthesized by reduction of silver ions (Ag^+) in aqueous or non-aqueous solutions to the formation of metallic silver (Ag^0) by reducing agent such as sodium citrate, ascorbate, sodium borohydride (NaBH_4), elemental hydrogen, polyol process, Tollens reagent, N,N-dimethylformamide (DMF), and poly (ethylene glycol)-block copolymers. (Iravani, Korbekandi et al. 2014) The synthesis of silver nanoparticles by sodium borohydride (NaBH_4) reduction occurs by the following reaction:



In order to stabilize NPs growth, and avoid NPs from agglomeration, the stabilizer such as poly (4-styrenesulfonic acid-co-maleic acid), Humic acid, poly (methacrylic acid), and polymethylmethacrylate have been introduced to stabilize NPs.

AgNPs is used in various technologies because properties of conductive, antibacterial, optical in application of conductive composite, biosensors, paints, and wound dressings.

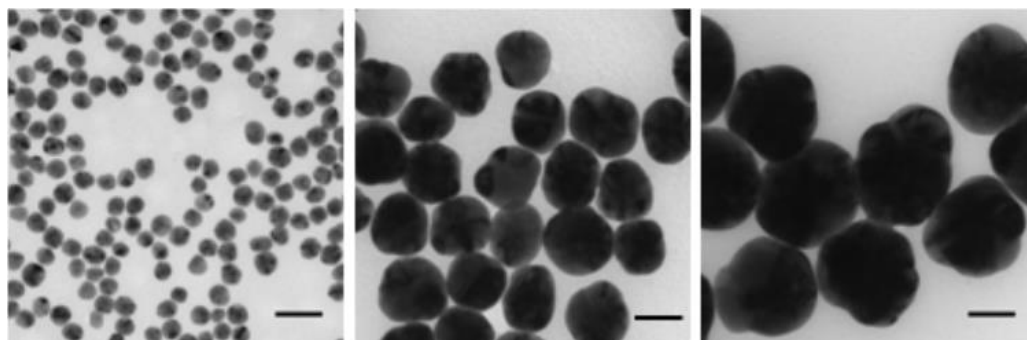


Figure 2.19 Transmission electron microscopy (TEM) images of silver nanoparticles with diameters of 20 nm, 60 nm, and 100 nm respectively with scale bars of 50 nm.

2.5.2 Zeolitic Imidazole Framework (ZIF-8)

ZIF-8 is a subclass of MOFs that is zeolite-type structure built by metal ions and imidazolate ligands. ZIF-8 is porous crystal structure that has properties of high crystallinity, large surface area, exceptional chemical, and functional tunability. It can be synthesized by using various zinc source such as $\text{Zn}(\text{OAc})_2$, ZnSO_4 , $\text{Zn}(\text{NO}_3)_2$, ZnCl_2 , ZnBr_2 , ZnI_2 to make a metal bridge with imidazolate ligand and commonly solvent used is organic solvent or water. The application filed including gas storage, CO_2 capture, separation, sensing, catalysis, drug delivery, and water treatment.(Zhang, Jia et al. 2018)

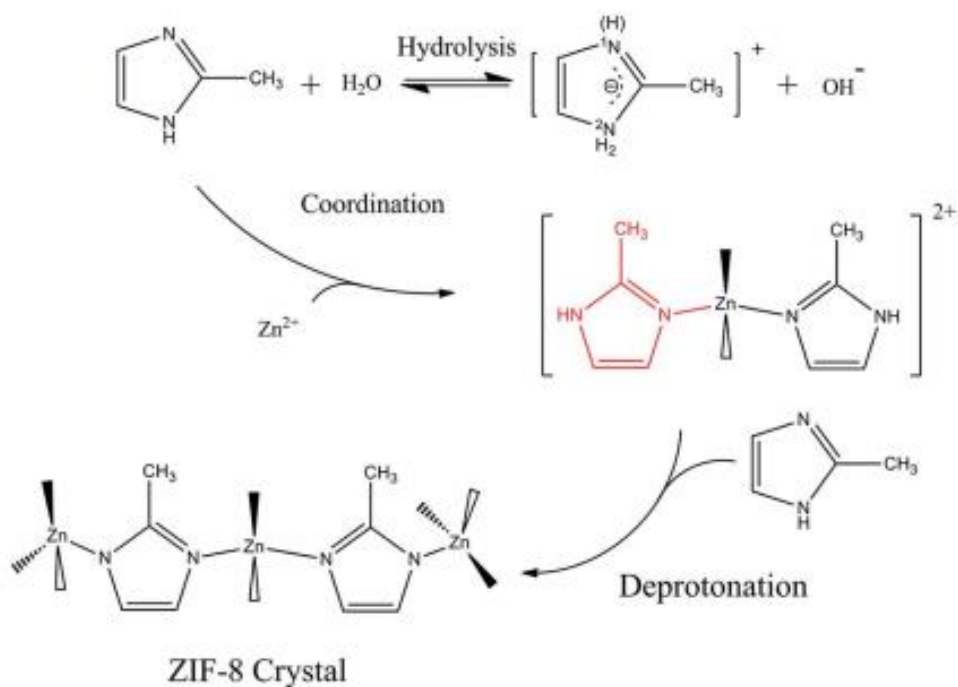


Figure 2.20 Mechanism of the formation of ZIF-8 crystals in water. (Jian, Liu et al. 2015)

2.6 Microreactor

Microreactor technology (MRT) is chemical engineering device that chemical reaction occur inside channel diameter below 1 mm. called microchannel. Microreactors are typically made out of glass, quartz, polymers, silicon, and metals such as stainless steel. Microreactors are generally operated in a continuous flow and flowing chemicals allow the adjustable volume flow rate synthesis. Miniaturized reaction operated by microreactor offer many advantages in the chemical engineering, pharmacy, medical, and biotechnology industries.

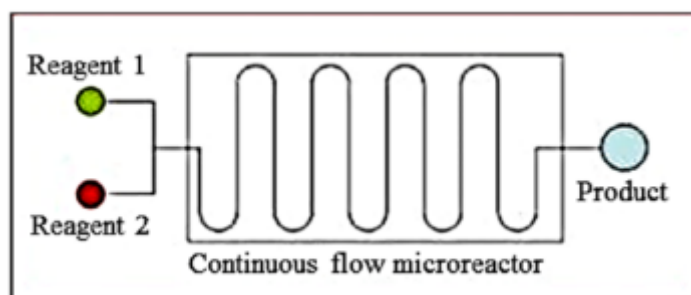


Figure 2.21 General concept of microreactor. (Ramanjaneyulu, Vishwakarma et al. 2018)

The concept of microreactor is the chemical is pulsed through the inlet of microchannel that coated with catalyst. The chemical reaction was performed by catalyst throughout the microchannel from inlet to outlet. And then obtain the final product.

Actually, 3D printing technology is unsuitable for reactor device applications, as they are not chemically compatible, or transparent. Nowadays there has the adoption of 3D printing technology for reactor device applications. Type of printers that can create microreactor devices are stereolithography (SLA), selective laser sintering (SLS) and fused deposition modeling (FDM). (Domínguez, Centeno et al. 2021)

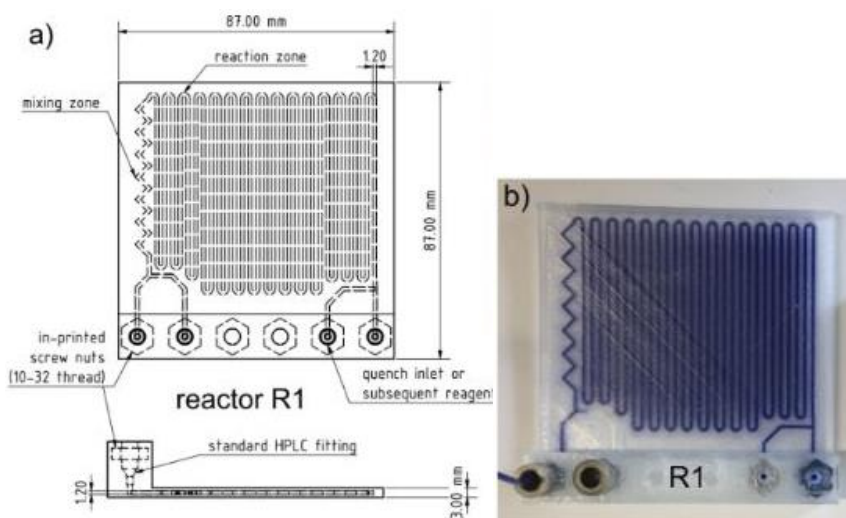


Figure 2.22 a) CAD design of microreactor 3D model b) 3D printed microreactor by FDM. (Neumaier, Madani et al. 2019)

Jochen and co-workers created microreactor 3D model by CAD program and then printed by Fused deposition modelling (FDM) 3D printer by using Polypropylene (PP) as a built-up material. The main advantage of FDM printed microreactors is inexpensive operation but significant disadvantage is low chemical resistance of the used built-up material towards most chemical reagents.

The microreactor can be functionalized with metal catalysts such as gold (Au), silver (Ag), and palladium (Pd) have shown great potential in the catalytic reactions. Based on the method of metal catalysts loading into the microreactor. Until now, several strategies have been developed to immobilize metal catalysts on the microchannel walls of microreactors.

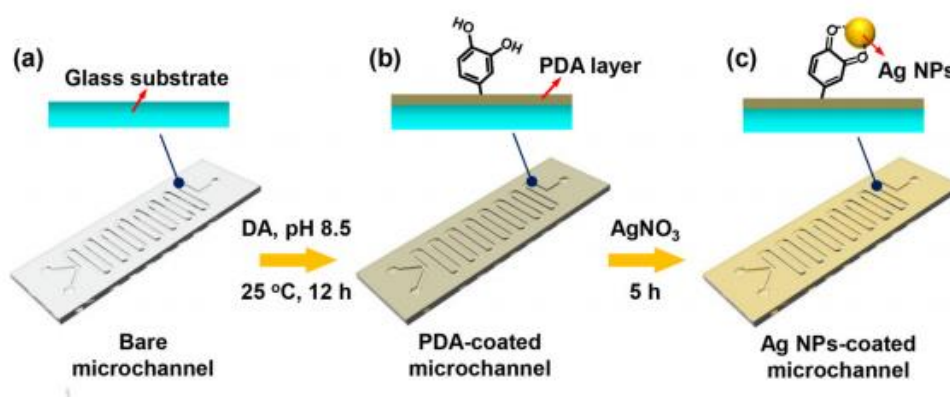


Figure 2.23 a) glass microreactor fabricated by wet chemical etching. b) PDA coated microreactor by dip coating. c) AgNPs coated microreactor by insitu immobilization. (Zhang, Liu et al. 2017)

For example, Lei Zhang and co-workers constructed glass microreactor by wet chemical etching method. Surface modification was applied by dip coating glass microreactor into dopamine (DA) solution which can self-polymerizes to polydopamine (PDA). And then was immersed in AgNO₃ solution. The silver ions were insitu immobilized or reduced to form silver nanoparticles (AgNPs) by PDA.

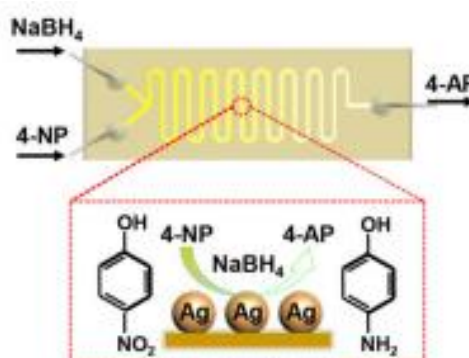


Figure 2.24 Reduction reaction of 4-NP to 4-AP by NaBH_4 and AgNO_3 performed in glass microreactor.

The model reaction that performed in glass microreactor is reduction reaction of 4-nitrophenol (4-NP) to 4-aminophenol (4-AP) by sodium borohydride (NaBH_4) and AgNPs that act as catalyst.



2287006921

CU Theses 6272032063 thesis / recv: 19072564 14:14:29 / seq: 8

CHAPTER 3

METHODOLOGY

3.1 Materials and Equipment

Equipment:

1. Field scanning electron microscopy (FE-SEM)
2. Fused Deposition Modeling (FDM)
3. UV-vis spectrophotometer (UV-vis)
4. Compression Molding
5. Peeling Test
6. Fourier-transform infrared spectroscopy (FTIR)
7. Universal testing machine (UTM)
8. X-Ray Diffractometer (XRD)

Software:

1. Tinkercad
2. Ultimaker Cura

Chemicals:

Polymer Chemicals

- Sodium Hydroxide (NaOH)
- Poly(ethyleneimine) (PEI) 0.1 g/ 100 ml
- Poly (diallyldimethylammonium chloride) (PDAD) solution 20 wt. % in H₂O
- Polystyrene sulfonate (PSS), C₈H₈O₃S, 184.209 g/mol
- Sodium chloride (NaCl), 58.44 g/mol
- Silver Nitrate (AgNO₃) 169.87 g/mol
- Sodiumbromohidride (NaBH₄) 37.83 g/mol
- Poly (4-styrenesulfonic acid-co-maleic acid) 189 g/mol
- Methylene blue 50 ppm
- Zinc acetate (Zn(OAc)₂.H₂O)
- 2-methylimidazole (Hmim)

Solvents

- Deionized (DI) water

3.2 Experimental Procedures

Part 1 Silver Nanoparticles Catalyst

3.2.1 Preparation of Polyelectrolyte Multilayers (PEMs)

The solution of PDAD and PSS were prepared with concentration of 10 mM and mix with 1 M NaCl. The solutions were dissolved in distilled water and dispersed by magnetic stirrer. The amount of substance to be used can be calculated by equation: $(g) = \text{Concentration (mM)} \times \text{Volume (L)} \times \text{Molecular weight (g/mol)}$

Procedure

- 1) Filament was sonicated in distilled water for 10 min.
- 2) Soak filament into PDAD/NaCl solution for 2 min.
- 3) Rinse filament with distilled water for 1 min.
- 4) Soak filament into PSS/NaCl solution for 2 min.
- 5) Rinse filament with distilled water for 1 min.
- 6) Repeat from 1) until obtain 7 layers of PEMs. (PDAD is on top.)
- 7) The filament was air blown.

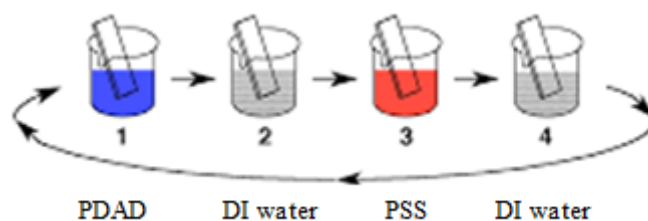


Figure 3.1 PEMs procedure.

3.2.2 Silver Nanoparticles Coating

3.2.2.1 *Exsitu*

- a. Silver nanoparticles were synthesized by mixing of 1 mM AgNO_3 solution and 0.01 mM PSS-co-MA (Poly (4-styrenesulfonic acid-co-maleic acid)) and 5 mM NaBH_4 was introduced to reduce from AgNO_3 to AgNPs. The solution was sealed with parafilm 6-8 hours for reduction reaction.

- b. PEMs coated filament was soaked into water bath for 10 min and then soak into AgNPs solution overnight.

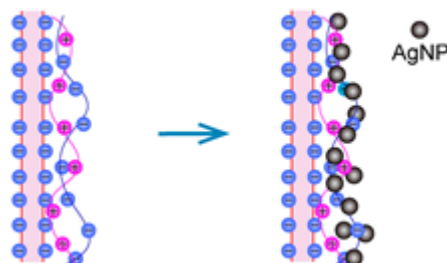


Figure 3.2 Exsitu coating.

3.2.2.2 *In situ*

- Preparation of PEMs onto filament 20 layers with PDAD and PSS concentration of 50 mM and 2 M NaCl.
- Soak filament into mixer of 50 mM PSS and 2 M NaCl for 30 min.
- Soak filament into 10 mM AgNO_3 for 10 min and then soak into 5 mM NaBH_4 for 5 min. (Soak into distilled water 3 times every step.)
- Repeat b. for 5 cycles.

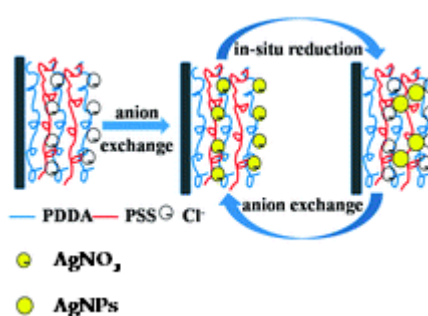


Figure 3.3 In situ coating.

3.2.3 Surface Treatment

- Alkaline treatment

- PLA filament was immersed into the mixture of 1 mM NaOH aqueous solution in ambient temperature for 1-5 hours. Then the PLA filament was rinsed by distilled water and dried by air blowing.
- ABS filament was immersed into the mixture of 1, 100, 1000 mM NaOH aqueous solution in ambient temperature for 3 hours. Then the ABS filament was rinsed by distilled water and dried by air blowing.

b. Polyethyleneimine treatment

PLA and ABS filaments were immersed in to PEI solution (0.1 % w/v) for 1-5 hour. Then the filaments were rinsed by distilled water and dried by air blowing.

3.2.4 Characterization

- a. Silver nanoparticles coated PLA and ABS filaments were characterized by Field scanning electron microscopy (FE-SEM) to investigate dispersion of silver nanoparticles on filaments before and after printing.
- b. To quantify adhesion quality of metal nanoparticles coating on PLA and ABS filament surface with Peeling test and to study effect of surface treatment to mechanical properties of PLA and ABS by Universal testing machine (UTM). Filaments were shape-shifted from rod shape to flat shape by Compression molding. The procedures are as follows.
 - PLA filament was shortened to pellet before compressed.
 - Preheat PLA pellet at 200°C for 15 min.
 - Compress PLA pellet ~ 20000 psi for 5 min. under heat.
 - Cool down PLA pellet at room temperature for 2 min.
 - ABS filament was shortened to pellet before compressed.
 - Preheat ABS pellet at 200°C for 15 min.
 - Compress ABS pellet ~ 20000 psi for 5 min. under heat.



2287006921

CU Theses 6272032063 thesis / rev: 19072564 14:14:29 / seq: 8

- Cool down ABS pellet at room temperature for 3 min.
- c. Flat filaments were cut to size 2 cm² to characterized the adhesion between the surface and metal nanoparticles by Peeling test. The procedures are as follows.
 - Place scotch tape on the metal nanoparticles coated flat filaments and then peel off the tape.

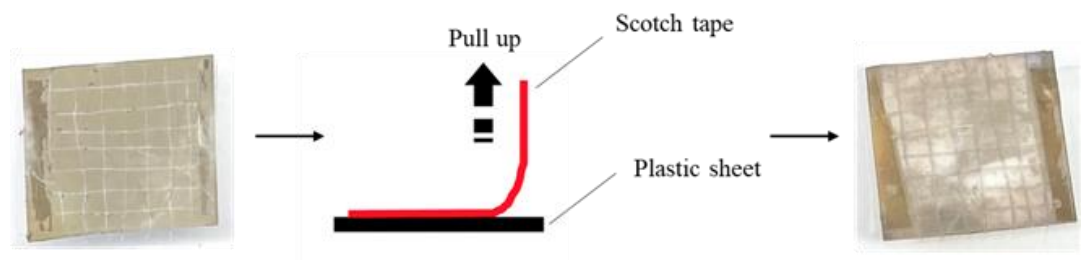


Figure 3.4 Peeling test.

- Calculate unremovable metal nanoparticles area by Image J program.

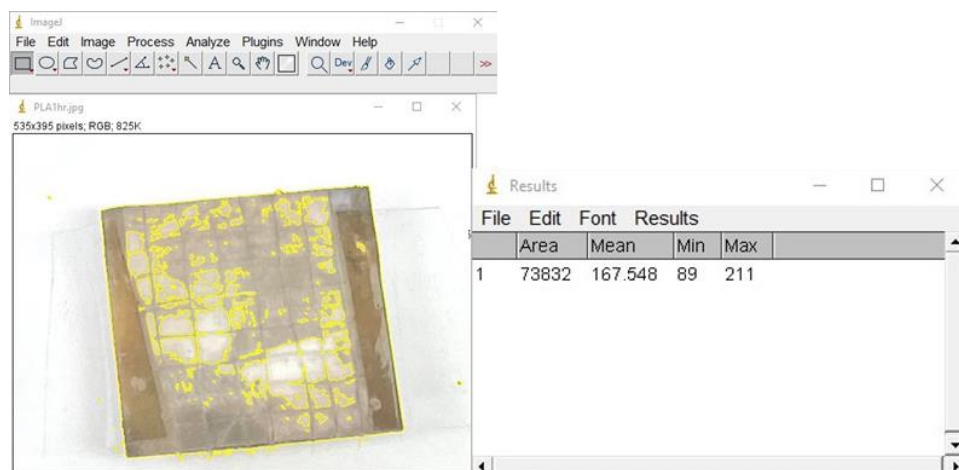


Figure 3.5 Image J program.

- d. Flat filaments were cut to size 1x12 cm² to investigate mechanical properties of alkaline treated filaments compared with untreated filaments by Universal testing machine (UTM).

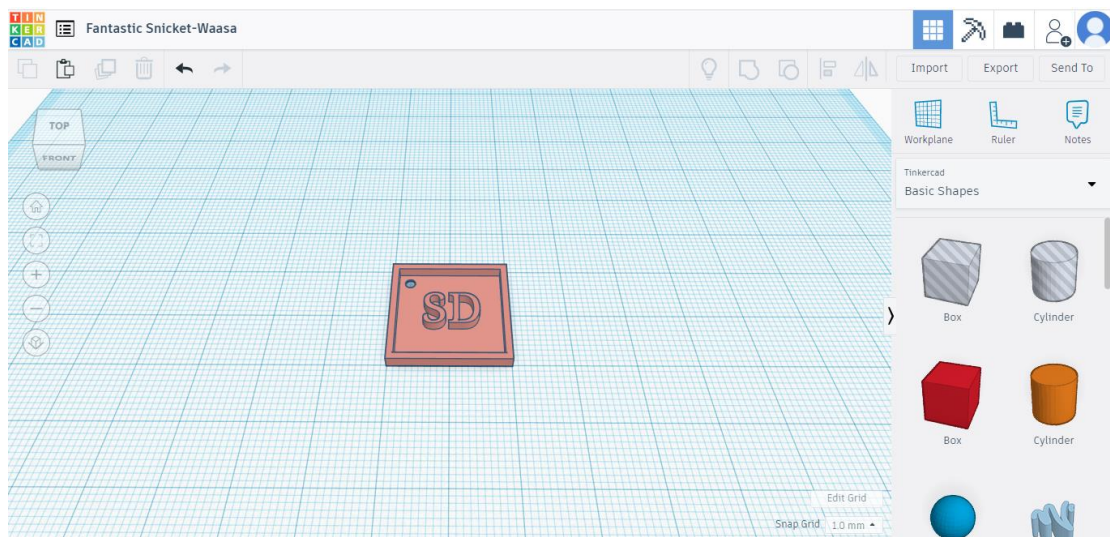
- e. The effect of 3D printing process to polyelectrolyte multilayers and Silver nanoparticles was analyzed by Fourier-transform infrared spectroscopy (FTIR), X-Ray Diffractometer (XRD).

3.2.5 3D Printing

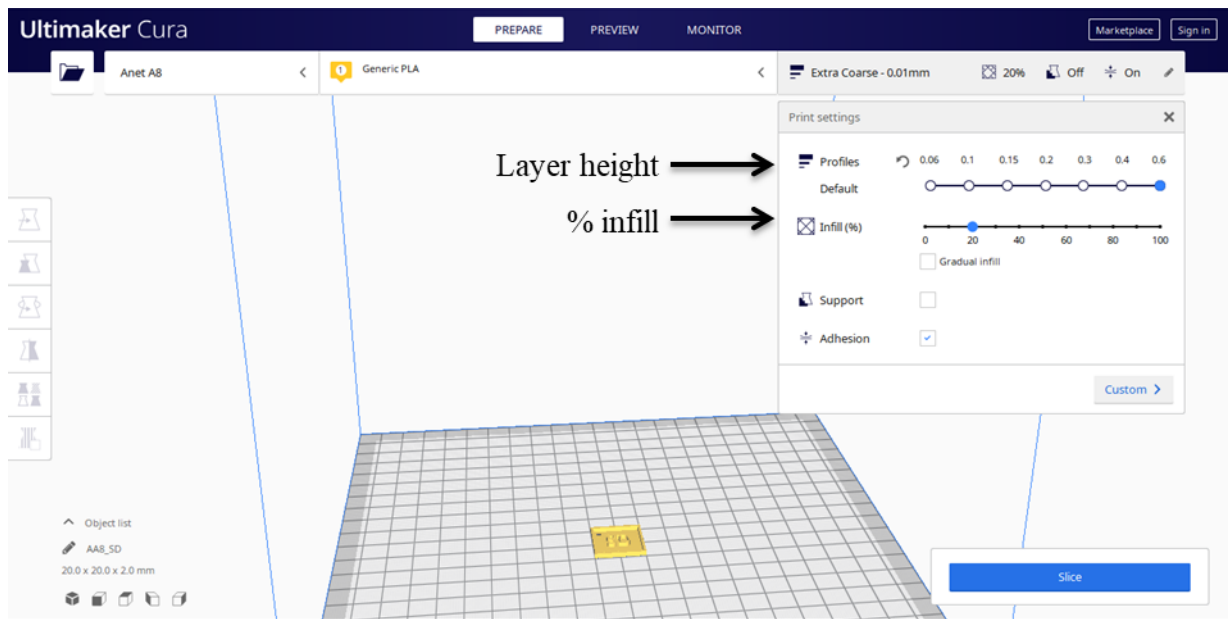
3D model was designed by Tinkercad and then customized printed parameters by Ultimaker Cura program. Designed 3D model was printed out with Anet A8 3D printer model.

Procedure

- 1) Design 3D model by Tinkercad program.



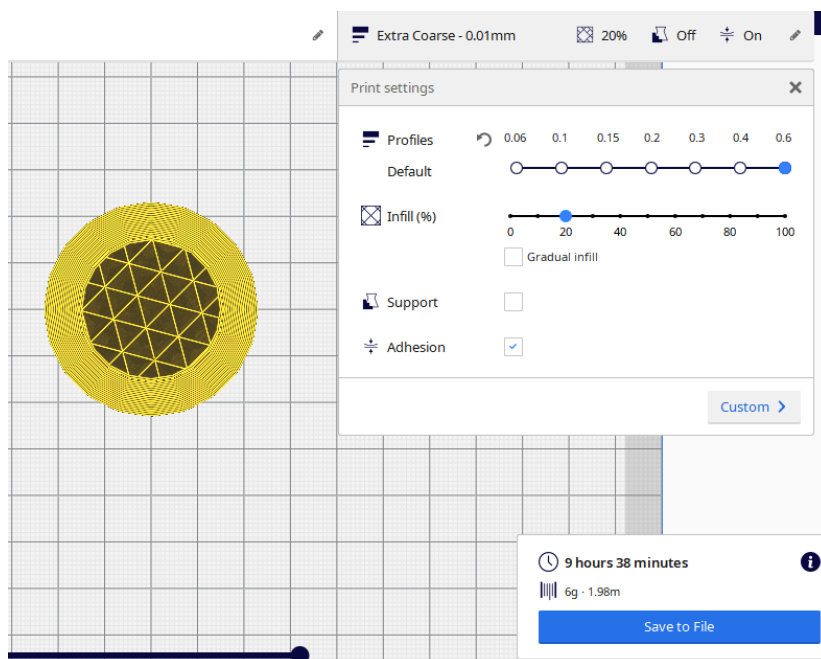
- 2) Import 3D model into Ultimaker Cura program in order to customize 3D model such as Layer height, Infill density, Nozzle diameter.



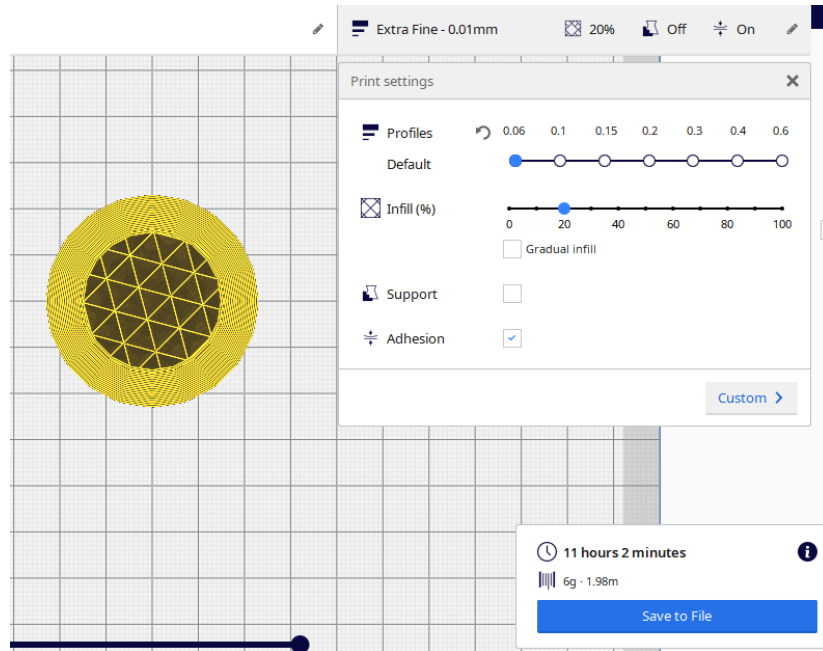
a. Layer height

The thickness of one printed layer in millimeters. The thinner layer height, the smoother surface and more detail visible in the Z-direction (height) of the model. On the other hand, the thicker layers height, the less print time substantially.

- Layer height = 0.6 mm.; It take 9 hr. and 38 min. to finish printing.



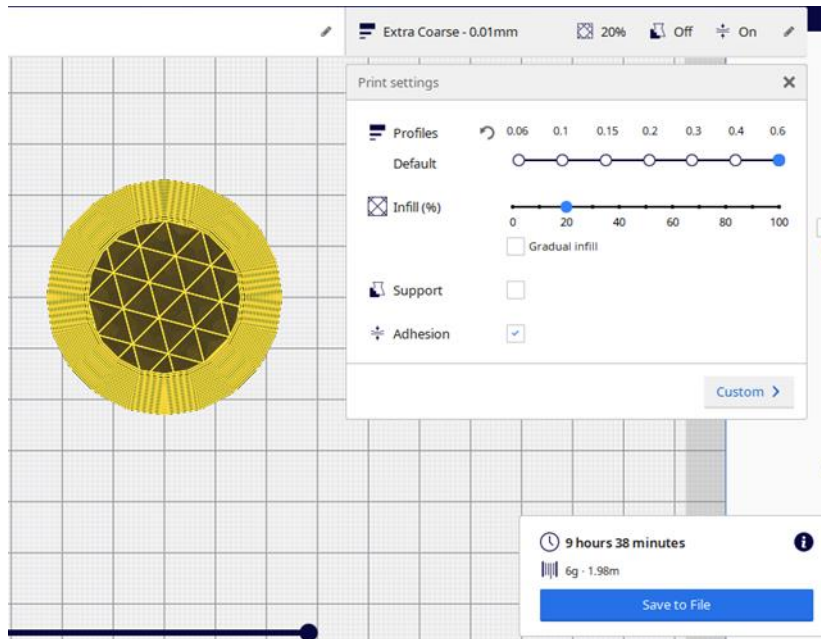
- Layer height = 0.06 mm.; It take 11 hr. and 2 min. to finish printing.



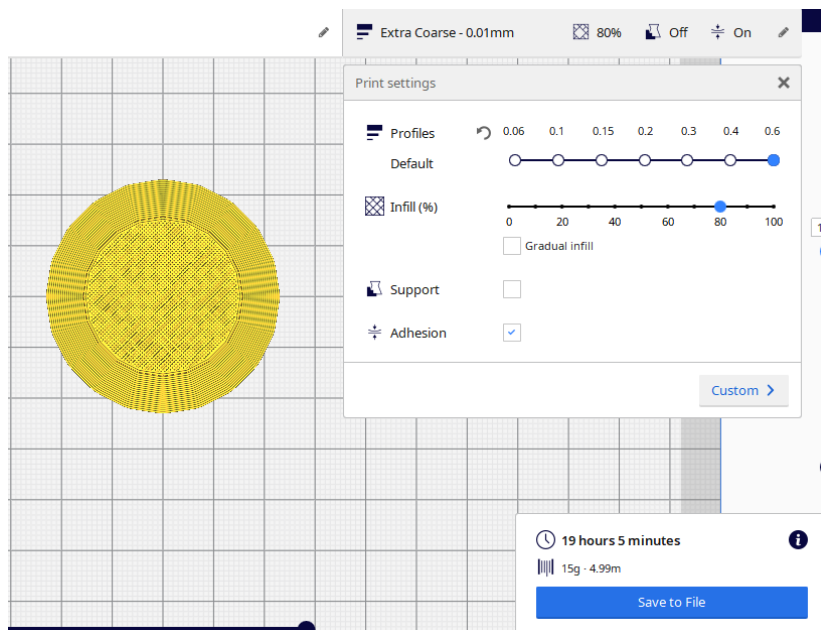
b. Infill density

The amount of plastic used inside of the printed sample. A higher infill density means that there is more plastic on the inside of your printed sample, leading to a stronger object.

- Infill density = 20 %; It take 9 hr. and 38 min. to finish printing.



- Infill density = 80 %; It take 19 hr. and 5 min. to finish printing.



3) 3D model was printed out by Anet A8 3D printer model.



Figure 3.6 Anet A8 3D printer.

Filament	Printing Properties	Strength	Flexibility	Durability	Print	Bed
					Temperature (°C)	Temperature (°C)
PLA	Easy to print	Medium	Low	Medium	180 – 230	80
ABS	Shrink while printing	Medium	Medium	High	210 – 250	100 – 110
PETG	More flexible than PLA or ABS durable	Medium	High	High	220 – 235	100

Table 3.1 Built-up materials properties

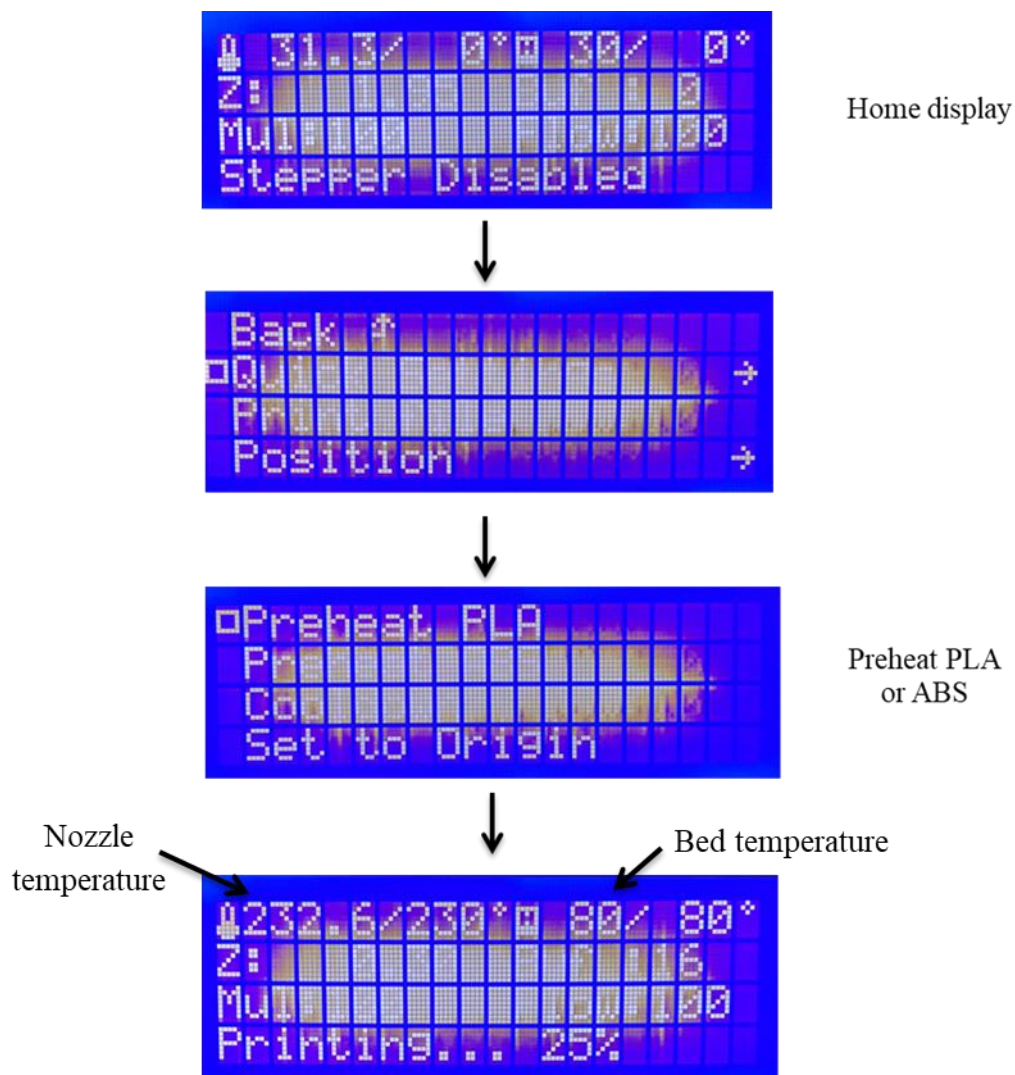


Figure 3.7 Set up process of 3D printer.

Part 2 ZIF-8 Particles Catalyst

3.2.6 Preparation of Polyelectrolytes Multilayers (PEMs)

- 1) Treated filament was sonicated in distilled water for 10 min.
- 2) Soak treated filament into PDAD/NaCl solution for 2 min.
- 3) Rinse treated filament with distilled water for 1 min.
- 4) Soak treated filament into PSS/NaCl solution for 2 min.
- 5) Rinse treated filament with distilled water for 1 min.

- 6) Repeat from 1) until obtain 10 layers of PEMs. (PSS is on top.)
- 7) The filament was air blown.

3.2.7 ZIF-8 Synthesis

- 1) Dissolve $\text{Zn}(\text{OAc})_2 \cdot \text{H}_2\text{O}$ and H_{mim} in DI water and use magnetic stirrer for 1 hour.
- 2) Contains equal quantities in centrifuge tubes and balance check.
- 3) Separate precipitate from solvent by centrifuge at 10000 rpm for 20 min.
- 4) Pour excess DI water out and refill fresh DI water.
- 5) Disperse precipitate in DI water by spoon or vortex mixer and sonicate for 15 min.
- 6) Repeat 3) to 5) more 2 times.
- 7) Open the centrifuge tubes cap and replace by perforated Aluminum foil.
- 8) Put it in the oven at 60°C for overnight.
- 9) Pound ZIF-8 powder with mortar and keep it in sealed container.

3.2.8 ZIF-8 Coating

- a. Seed layer deposition.
 - ZIF-8 particles ($\text{H}_{\text{mim}}:\text{Zn} = 45$); avg. particle size = 163 nm
 - 1) Immerse PEMs-mod filament into the ZIF-8 solution for 1 hour.
 - 2) Rinse with DI water, blow, and let it dry.
- b. Secondary growth thin film on filament.
 - ZIF-8 synthesis solution condition: $N = 0.0125\text{M}$, $\text{H}_{\text{mim}}/\text{Zn} = 60$, total vol. = 80

- Varied the growth time: 1, 2, and 3 hours
 - 1) Immerse seed layer coated filaments into 2-methylimidazole solution for 30 min (to induce the growth of ZIF-8 on seed crystals)
 - 2) Put zinc acetate solution into previous solution with stir well, then continuous immerse seed layer for 30 min, 90 min, and 150 min.
 - 3) Rinse filaments with DI water, blow, and let it dry.

3.2.9 Surface Characterization

- a. ZIF-8 particles coated PLA, ABS and PETG filaments were characterizes by using Field scanning electron microscopy (FE-SEM) to investigate dispersion on filaments before and after printing.
- b. The crystal morphology of ZIF-8 on filament was analyzed by X-Ray Diffractometer (XRD).

3.2.10 3D Printing

2 procedure variations

- a. Seed layer deposition → 3D printing → Secondary growth
- b. Seed layer deposition → Secondary growth → 3D printing



2287006921

CHAPTER 4

RESULT AND DISCUSSION

Part 1 Silver Nanoparticles Catalyst

4.1 Synthesis of Silver Nanoparticles (AgNPs)

Silver nanoparticles are sphere particles of silver in Nano size that disperse in a form of solution and can form solid with dispersion on solid substrate. AgNPs is good electrical, optical and thermal properties and high electrical conductivity, stability, and low sintering temperatures thus AgNPs is easy processing and also super catalytic that is significant property of AgNPs in this research.

The synthesis of AgNPs by sodium borohydride (NaBH_4) as a reducing agent and PSS-co-MA as a capping agent occurs by the following reaction:

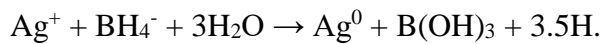


Figure 4.1 AgNPs solution.

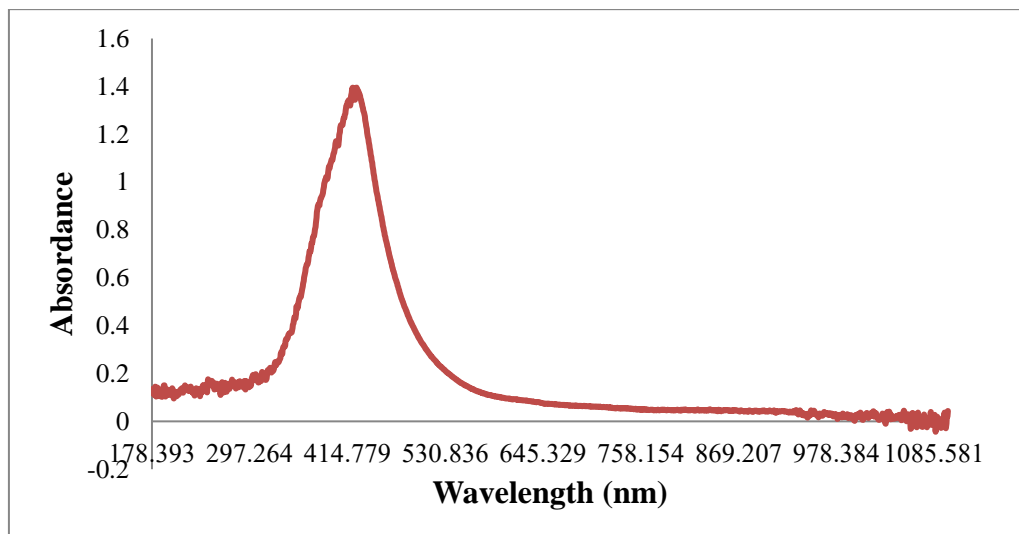


Figure 4.2 UV-vis spectrum of AgNPs solution.

The appearance of AgNPs is yellow solution and then was characterized by UV-vis spectrophotometer in visible range as shown in Figure 4.2 the absorbance peak of the AgNPs appear at around 400-420 nm

4.2 Silver Nanoparticles Coating on Polyelectrolyte Multilayers

Glass slides were used as a substrate in order to find the best condition of metal catalyst loading on filament. The polyelectrolyte multilayers used are 10 mM Poly (diallyldimethylammonium chloride) (PDAD) as a polycation and 10 mM Poly (styrene sulfonate) (PSS) as a polyanion.

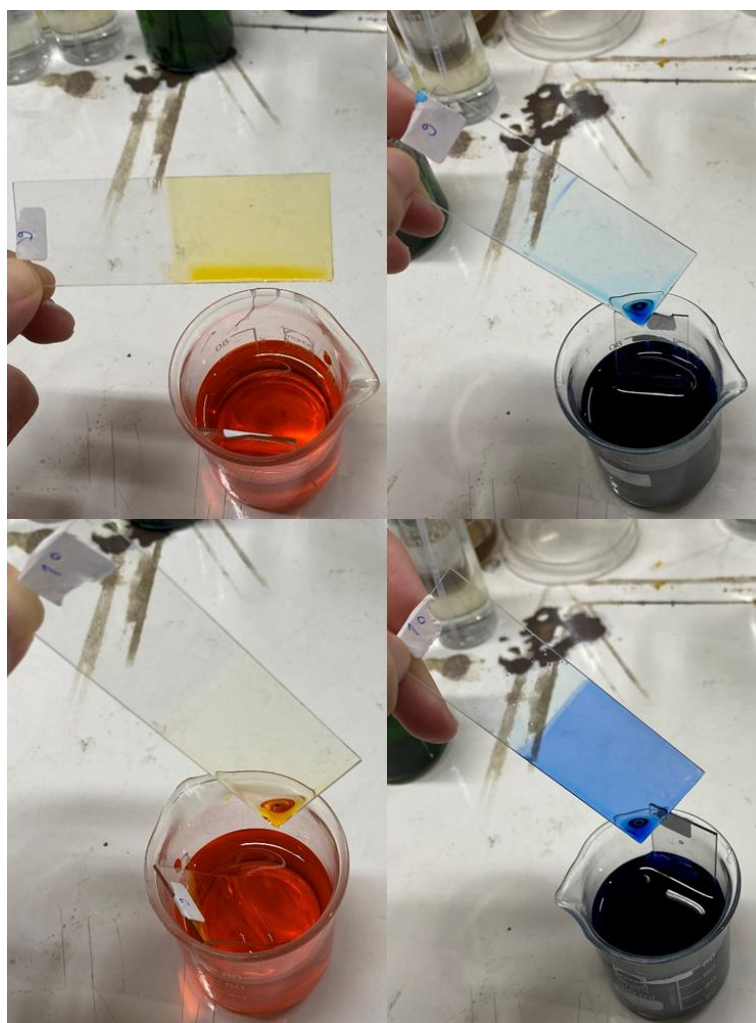


Figure 4.3 9 (top) and 10 (bottom) layers of PEMs deposited glass slide appearance.

To proof that polyelectrolyte multilayers can work well, Methyl orange and Methylene blue was used. 9 layers (PDAD is top layer) with positively charge can stick orange dye which is negatively charge but cannot stick blue dye that has the same charge. While 10 layers (PSS is top layer) with negatively charge can stick blue dye which is positively charge but cannot stick orange dye that has the same charge either.

Next step is AgNPs loading. 2 method of exsitu and insitu was demonstrated.

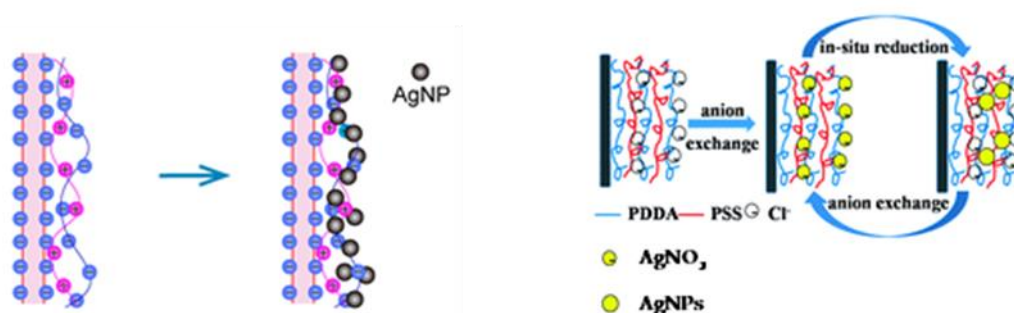


Figure 4.4 Diagram of exsitu (left) and insitu (right) AgNPs loading method.

For exsitu method that conducted simply by dip coating PEMs deposited substrate into AgNPs solution directly. AgNPs coating is performed by electrostatic force between positively charge of PEMs with PDAD top layer and negatively charge of AgNPs. And insitu method that conducted by dip coating PEMs deposited substrate into Ag ion solution and then dip coating into reducing agent for several cycles in order to synthesize or immobilize AgNPs throughout each layer of PEMs.

4.2.1 Exsitu

Silver nanoparticles solution was prepared by using 1 mM AgNO_3 , 5 mM NaBH_4 and PSS-co-MA was varied concentration such as 0.25,0.10,0.05,0.01, and 0.005 mM.



Figure 4.5 Silver nanoparticles coating on PEMs at different concentration of PSS-co-MA 0.25, 0.1, 0.05, 0.01, 0.005 mM respectively.

In Figure 4.5 glass slide was deposited with 7 layers of PEMs and coated with AgNPs for overnight. It is found that the different color is obtained with using different concentration of capping agent. The metallic color can be formed with low concentration of capping agent like 0.01 and 0.005 mM because the lower capping agent, the lower competition between AgNPs and capping agent to attach with positively charge of PDAD thus it can obtain higher yield of AgNPs coated.

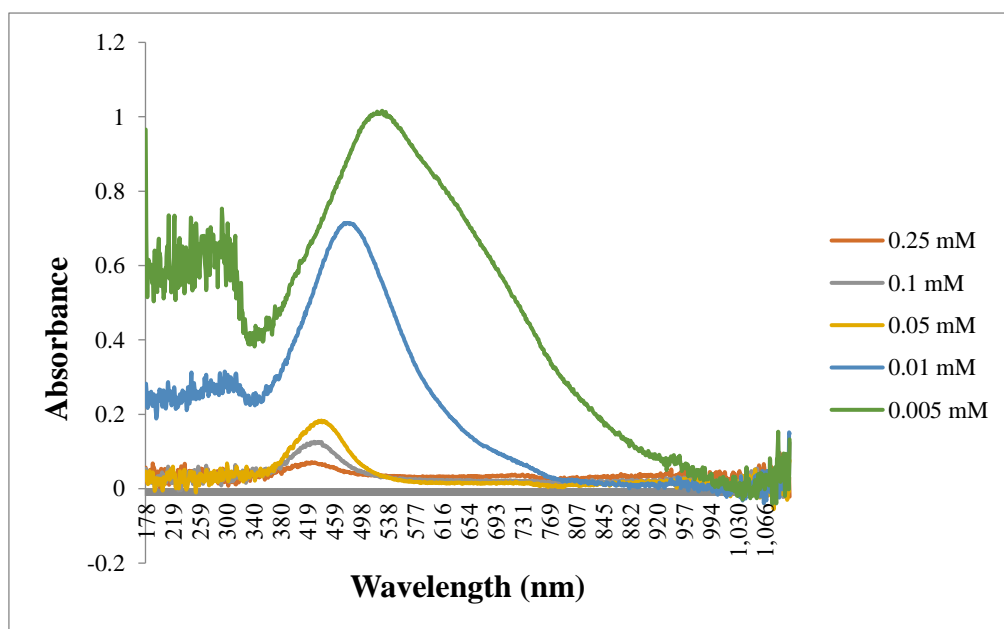


Figure 4.6 UV-vis spectrum of AgNPs coated glass at various concentration of capping agent.

AgNPs coated glass slides from figure 4.6 were detected absorbance by UV-vis spectrophotometer. The less concentration of capping agent, the higher peak absorbance because lower capping agent can obtain higher yield of AgNPs.

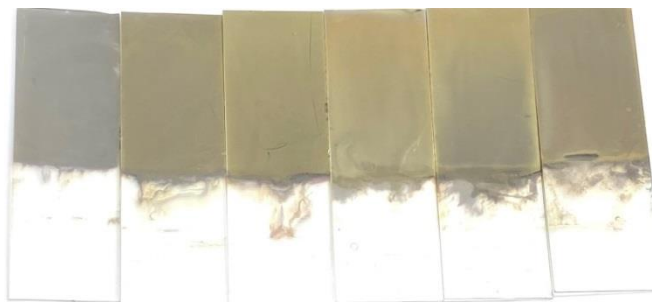


Figure 4.7 Silver nanoparticles coating on different layers of PEMs 3,5,7,9,11 layers.

In Figure 4.7 shows metallic coating on PEMs with different layers of 3,5,7,9,11 with 0.01 mM capping agent. The more PEMs layers, the more thickness of AgNPs.

4.2.2 In situ

PEMs was prepared on substrate 20 layers and then soaked in PSS/NaCl solution for increase negatively charge to catch Ag^- and annealing to obtain smoother surface. AgNO_3 10 mM and NaBH_4 5 mM were used to synthesize AgNPs inside layer of PEMs by soaking alternately for 5 cycles. The annealing step was varied for 3 ways.

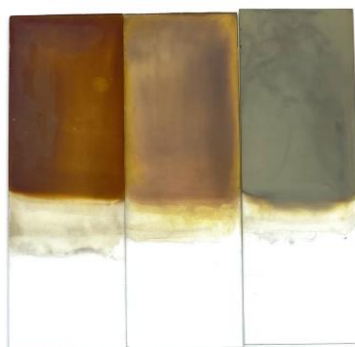


Figure 4.8 PSS 50 mM with NaCl concentration of 0,1,2 M respectively.

First, NaCl concentration variation of 0,1,2 M with PSS 50 mM. The metallic can form with NaCl 2 M only.

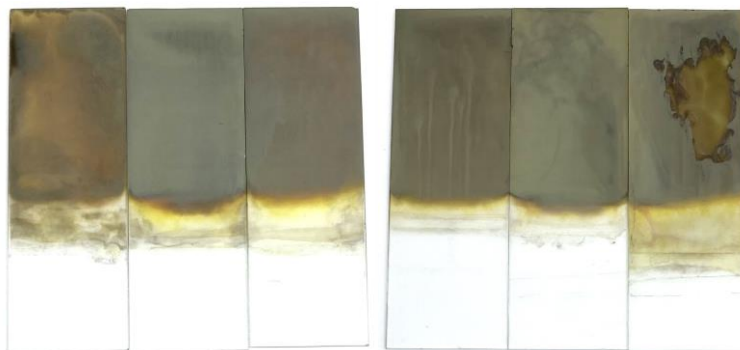


Figure 4.9 PSS concentration of 0,5,10,30,50,100 mM with NaCl 2 M respectively.

Second, PSS concentration variation of 0,5,10,30,50,100 mM with NaCl 2 M. For PSS 0 mM is not homogeneous metallic and the more PSS concentration, the more metallic color but for PSS 100 mM is peeled off easily because too high PSS concentration.



Figure 4.10 DI water, PSS 50 mM → NaCl 2 M, NaCl 2 M → PSS 50 mM respectively.

Third, procedure variation of no annealing (Di water), PSS 50 mM → NaCl 2 M, NaCl 2 M → PSS 50 mM. It is found that PSS 50 mM/NaCl 2 M solution is the best condition of metallic form.

4.3 Layer-by-layer Assembly of Polyelectrolyte Multilayers (PEMs) on Filaments

4.3.1 PEMs Deposition

The polyelectrolyte multilayers used are Poly (diallyldimethyl ammonium chloride) (PDAD) as a polycation and Poly (styrene sulfonate) (PSS) as a polyanion that were deposited on PLA and ABS filament via layer by layer techniques. This method can modify the filament surface to has more hydrophilicity that can be attached highly adhesion with various substance to obtain desire properties.



Figure 4.11 3,4,5,6,7,8,9,10 layers of PEMs deposited filament appearance respectively.

From Figure 4.11 The polymer filaments were deposited with PDAD and PSS for 3,4,5,6,7,8,9,10 layers. Odd number of layers is PDAD on top and even number of layers is PSS on top. Due to polyelectrolyte is transparent, the appearance of deposited filaments and plain filament are not different. To proof that filaments were accomplished deposition with polyelectrolyte, filaments were immersed in Methylene blue that is positively charge and Moder acid red dye that is negatively charge thus Methylene blue can stick with filaments with PSS on top and Moder acid red can stick with filaments with PDAD on top due to the electrostatic interaction between the oppositely charge.



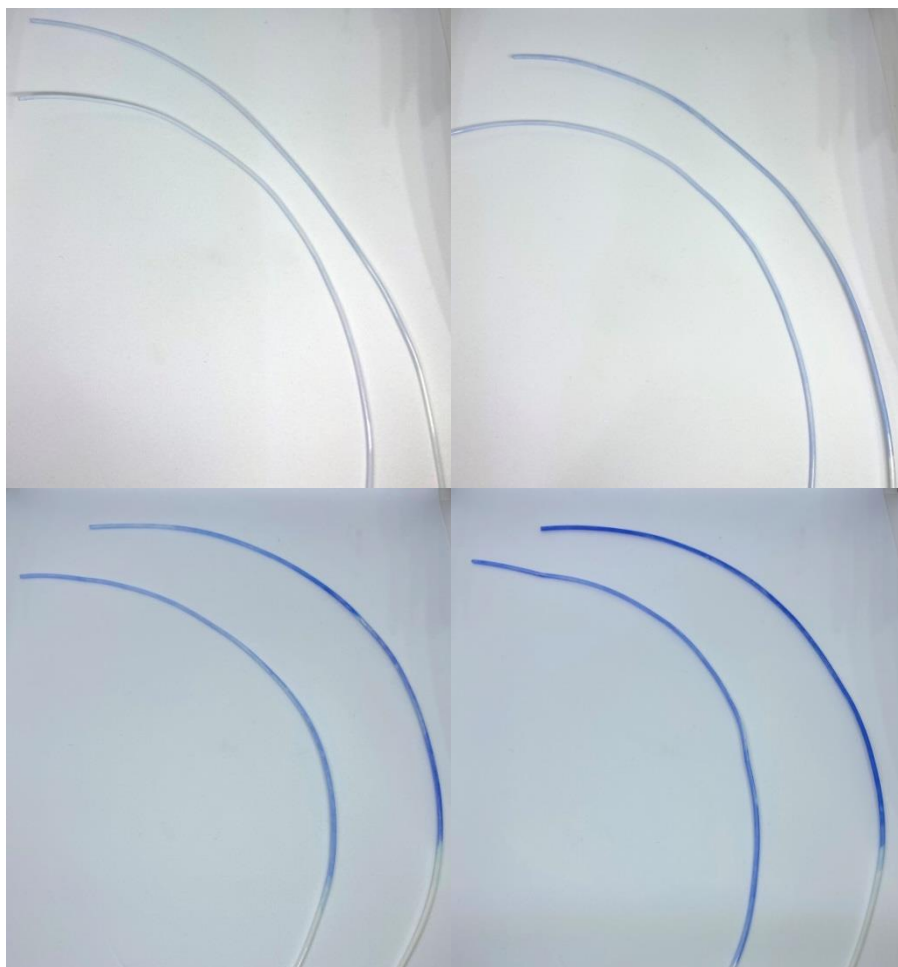


Figure 4.12 PLA (left) and ABS (right) filament with 2,4,6,8 layers of PEMs.

To compare the efficiency of PEMs adhesion on different PEMs deposited layer and type of filament. PLA and ABS were deposited with 2,4,6,8 layers of PEMs and investigated adhesion efficiency by immersed in Methylene blue dye. Figure 4.12 is shown the more layer of PEMs; the darker color of Methylene blue and ABS is darker than PLA all of layer of PEMs. It can be concluded that electrostatic interaction of PEMs is more effective with increasing of PEMs layer and ABS has higher surface adhesion than PLA.

4.3.2 3D printing PEMs Coated Filaments

Bare PLA, PLA with PDAD top layer, and PLA with PSS top layer were detected peak spectra by Fourier-transform infrared spectroscopy (FTIR) in order to compare peak spectra with printed samples.

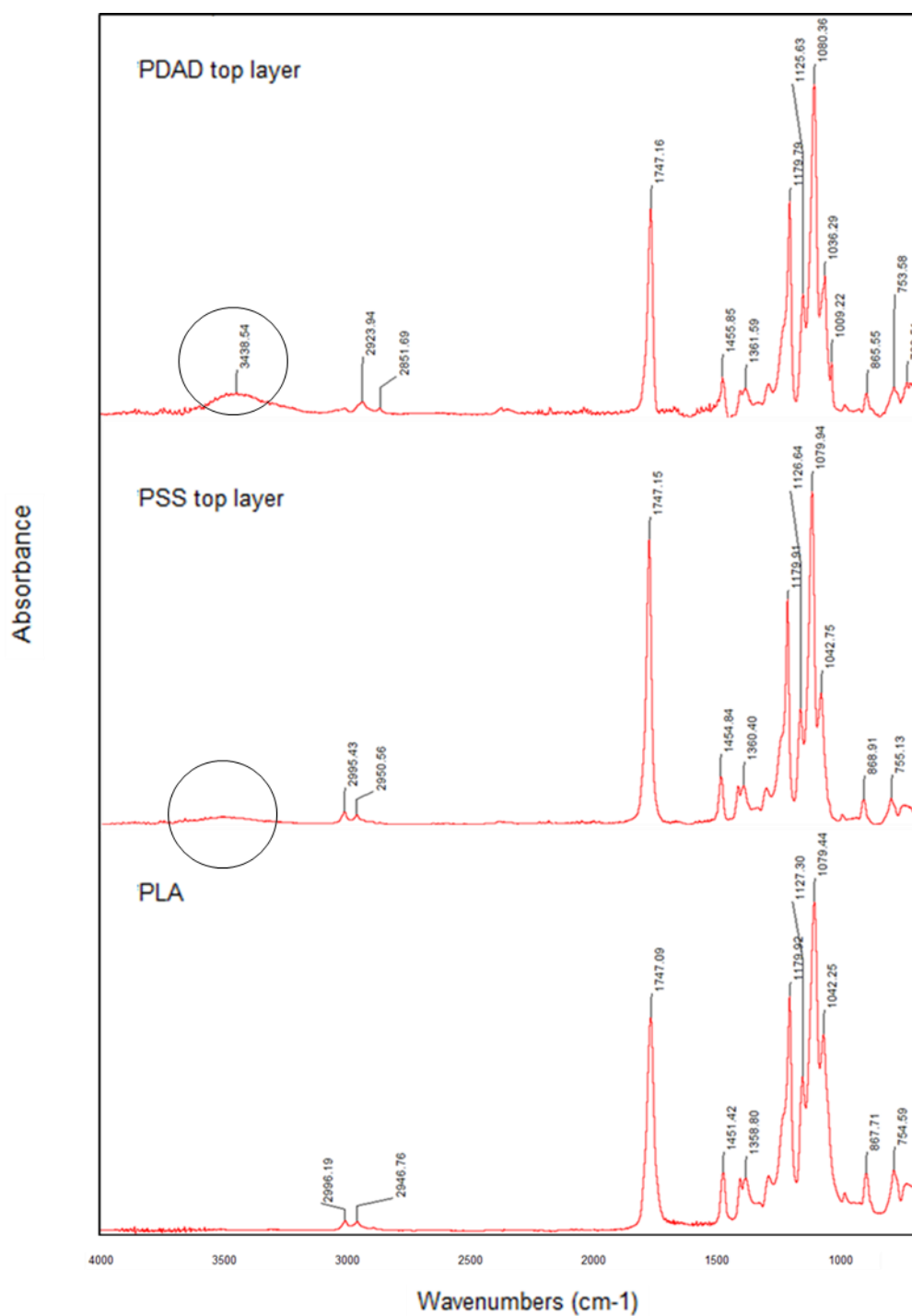


Figure 4.13 ATR-FTIR spectra of bare PLA, PLA with PDAD top layer, and PLA with PSS top layer.



2287006921

CD IThesis 6272032063 thesis / rev: 19072564 14:14:29 / seq: 8

In Figure 4.13 PLA with PDAD and PSS on top has broad peak of -OH at 3400-3500 cm^{-1} which is possible to be -OH of PDAD and PSS or moisture. Thus, the results from FTIR spectra cannot be concluded clearly.

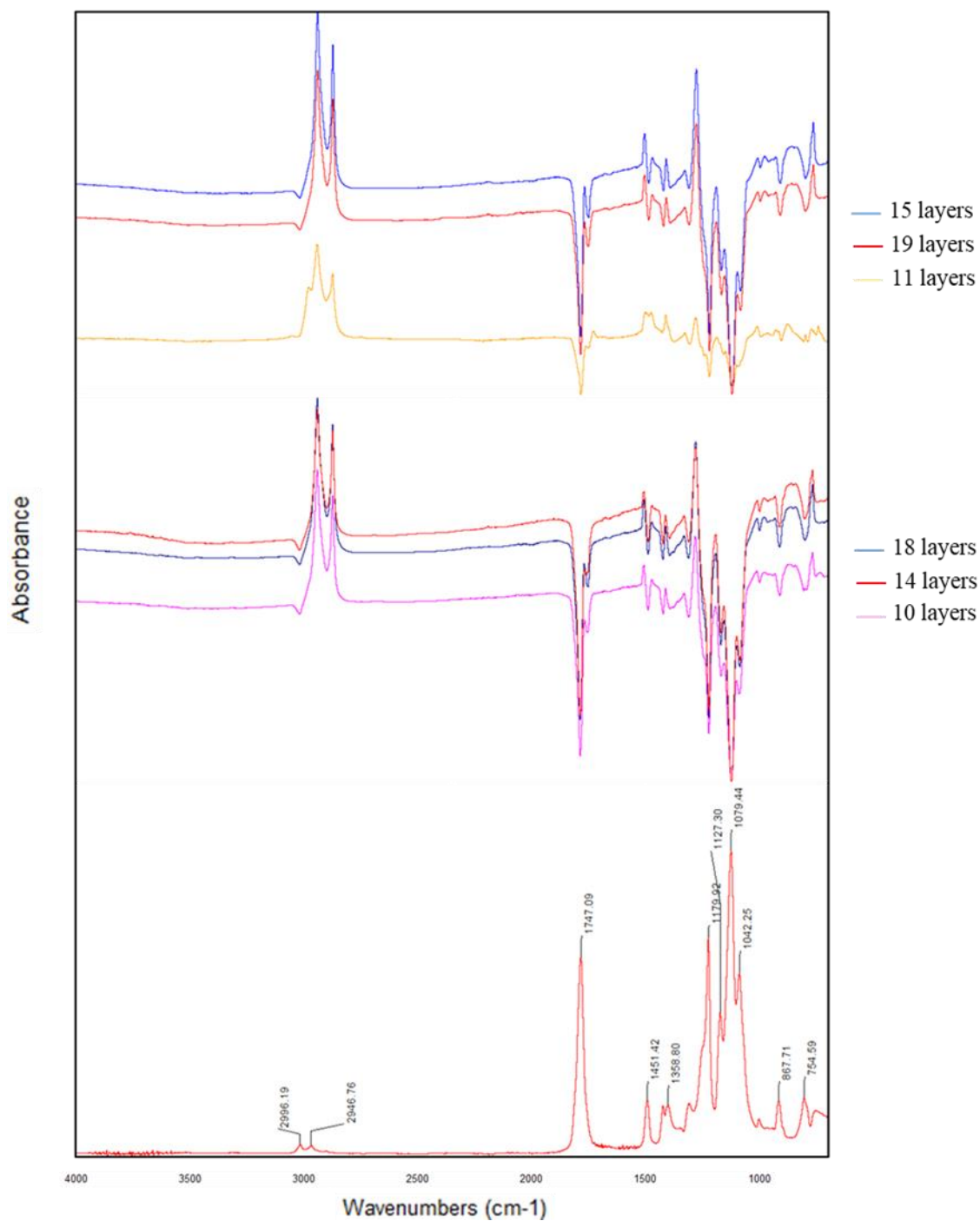


Figure 4.14 ATR-FTIR spectra of bare PLA, Polyelectrolyte multilayers coated PLA odd layer and even layer.

PLA was deposited with PEMs in several layers. Odd layers number such as 11,15,19 layers are PDAD on top and even layers number such as 10,14,18 are PSS on top. These 6 samples were 3D printed and then were detected peak spectra by Fourier-transform infrared spectroscopy (FTIR). As shown in figure 4.14 every layer's number variation cannot observe peak spectra of PDAD and PSS. It can be concluded that PEMs was peeled off by 3D printing process.

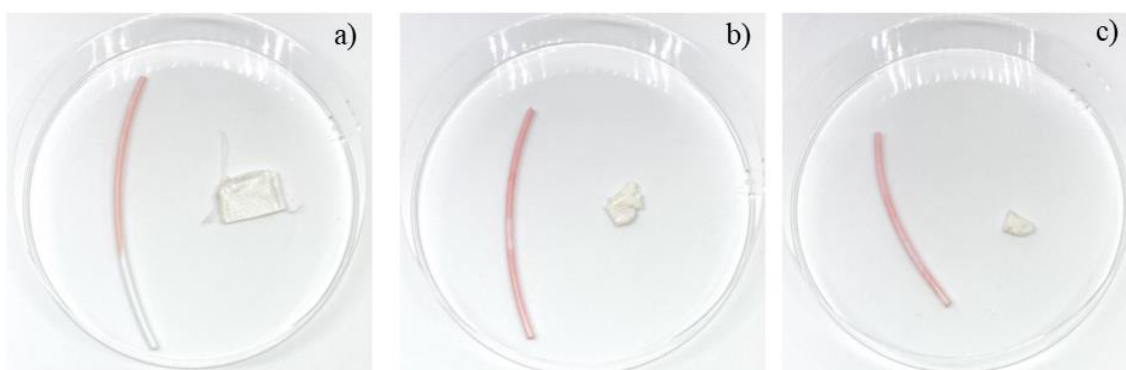


Figure 4.15 Dye absorption of before (left) and after (right) 3D printed polyelectrolyte multilayers coated filament. a) Untreated b) NaOH treated c) PEI treated.

To confirm that PEMs can be deposited on filament and PEMs was peeled off by 3D printer. PEMs coated filaments before and after 3D printing were immersed in oppositely charge dye (red solution). PEMs coated filaments can stick with dye but printed PEMs coated filaments cannot observe red color of dye. It can be concluded that PEMs was successfully deposited on filament but was completely removed from filaments surface by 3D printing.

4.4 Silver Nanoparticles Exsitu Loading on Polymer Filament

The substrates used are PLA and ABS filament that has physical properties such as opaque, solid white color, smooth surface and ABS filament is opaquer than PLA but still hard to differentiate.

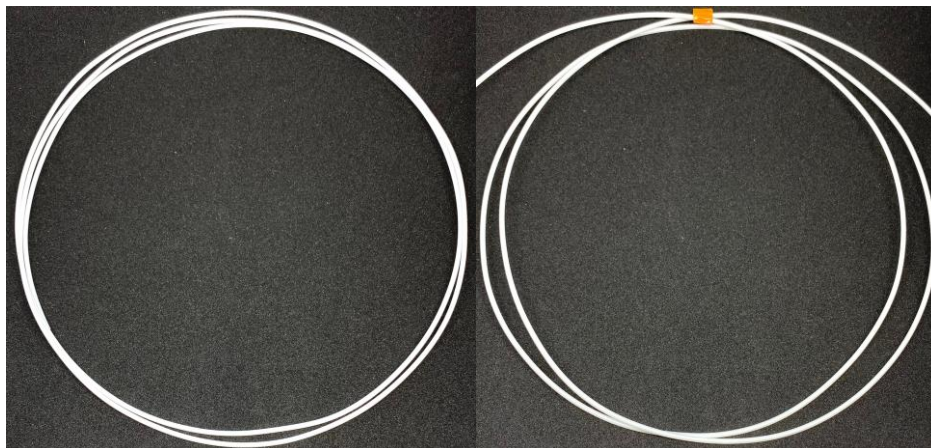


Figure 4.16 PLA and ABS filament respectively.

4.4.1 Silver Nanoparticles Loading



Figure 4.17 AgNPs coated PLA and ABS filament respectively.

The filaments were coated 7 layers of PEMs and then coated AgNPs with 0.01 mM capping agent as shown in Figure 4.17. The filaments have homogeneous silver color of metallic.

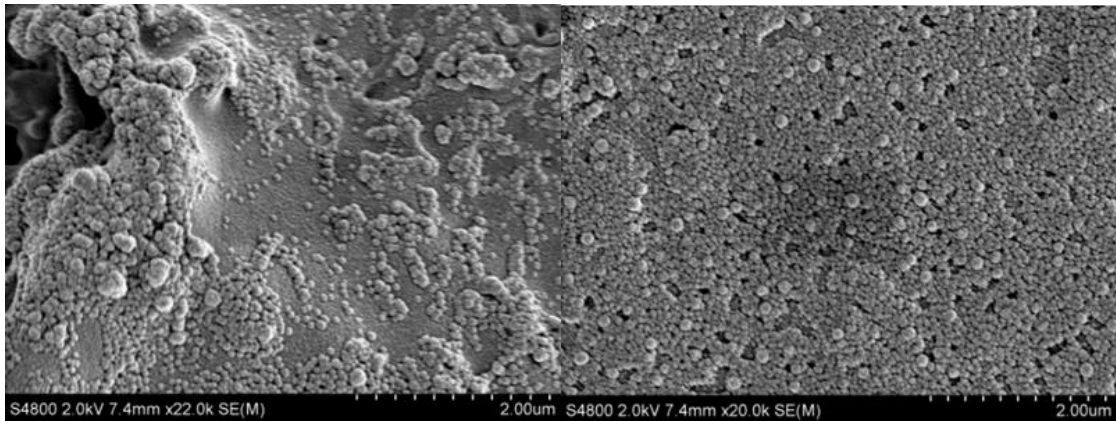


Figure 4.18 The morphology of AgNPs dispersion on PLA and ABS filament respectively.

In Figure 4.18 AgNPs were packed full on ABS but for PLA, AgNPs were not packed full. It can be concluded that AgNPs can disperse on ABS better than PLA because functional group on ABS make higher adhesion than functional group on PLA.

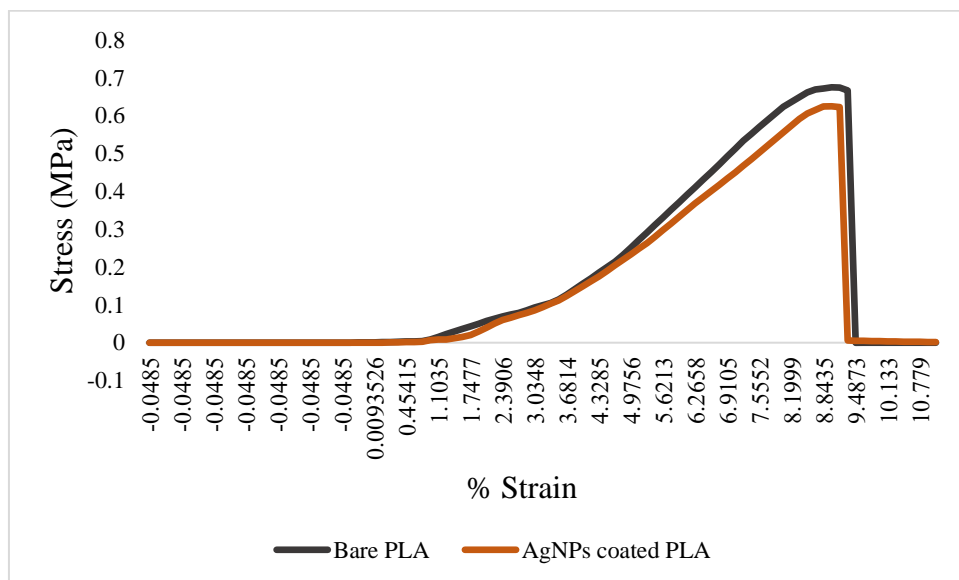


Figure 4.19 Stress and % strain curve of AgNPs coated PLA.

	Maximum Tensile Strength (Mpa)
Bare PLA	0.646147
AgNPs coated PLA	0.65242

Table 4.1 Maximum tensile stress of PLA

The effect of AgNPs coating on mechanical properties of filament was investigated by Universal Tensile Machine (UTM). From figure 4.19, stress and % strain was plotted to calculate maximum tensile stress of filament as shown in table 4.1. The results of average maximum tensile stress of neat PLA and AgNPs coated PLA have similar values. It can be indicated that AgNPs coating does not affect the filament.

4.4.2 3D Printing Silver Nanoparticles Coated Filaments

Short filament is facile to test or process. The printed specimens were designed in square shape, size 2x2 cm².



Figure 4.20 Printed normal PLA and ABS filament respectively.

Bare filaments were printed in order to compare the difference with AgNPs coated.



Figure 4.21 Printed AgNPs exsitu coated PLA and ABS filament respectively.

For exsitu coating can observe homogeneous grey color only in area with high deposition of printed filament.

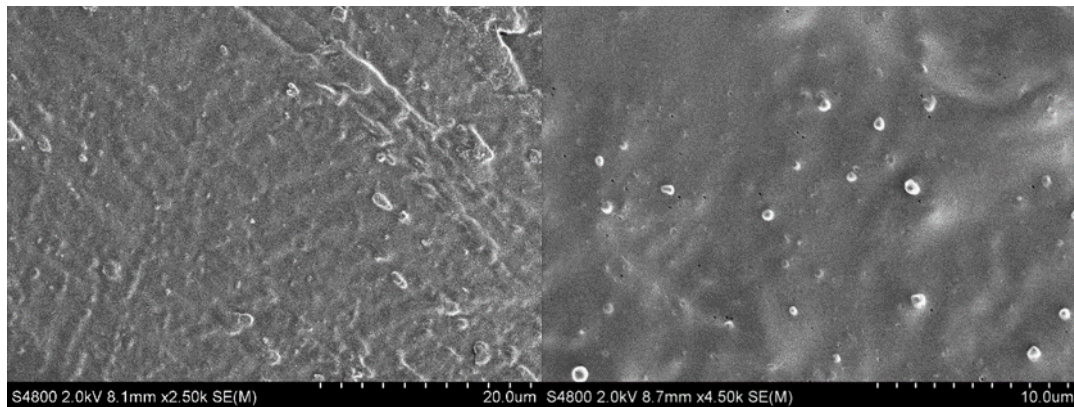


Figure 4.22 FE-SEM surface image of printed AgNPs exsitu coated PLA and ABS filament respectively.

The printed specimens were analyzed by Field scanning electron microscopy (FE-SEM). In Figure 4.22 AgNPs cannot be observed on the filaments surface because pressing filament through the gear inside extruder and nozzles that is 10 times smaller than the filament diameter cause high amount of friction between filaments surface and extrusion die make AgNPs was peeled off.

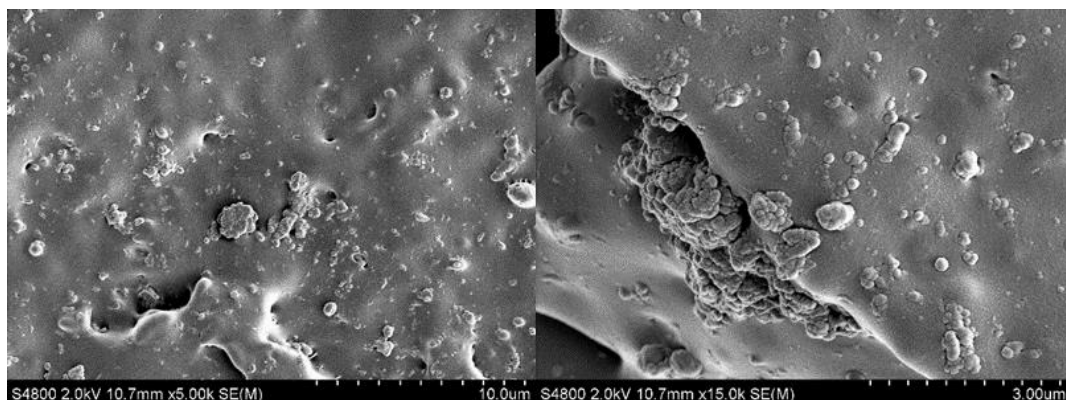


Figure 4.23 FE-SEM cross-section image of printed AgNPs exsitu coated PLA at x5.00k and x15.0k.

Printed specimens were analyzed in cross-section, cluster of AgNPs were found and disperse everywhere inside specimens. Indicate that AgNPs inside cause grey color of specimen.

4.5 Silver Nanoparticles Insitu Loading on Polymer Filament

4.5.1 Silver Nanoparticles Loading

Making insitu coating without treatment made poor quality of PEMs attachment result in AgNPs that was synthesized inside layers of PEMs occurred partially on filament. However, variety of experiments was performed to proof that which factor depends on PEMs attachment.

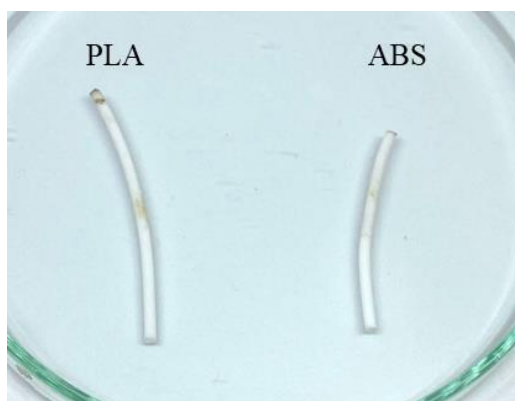


Figure 4.24 PDAD and PSS 10 mM in NaCl 1 M, AgNO₃ 10 mM, NaBH₄ 5 mM.

First, PDAD and PSS 10 mM in NaCl 1 M was used to assemble PEMs. AgNO₃ 10 mM, NaBH₄ 5 mM was used to synthesize AgNPs. Result in poor attachment of synthesized AgNPs.

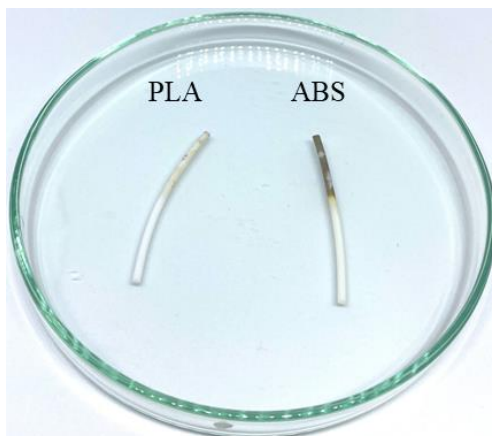


Figure 4.25 PDAD and PSS 50 mM in NaCl 2 M, AgNO₃ 10 mM, NaBH₄ 5 mM.

Second, PDAD and PSS 50 mM in NaCl 2 M was used to assemble PEMs. AgNO₃ 10 mM, NaBH₄ 5 mM was used to synthesize AgNPs. Results in better attachment of synthesized AgNPs on ABS only.

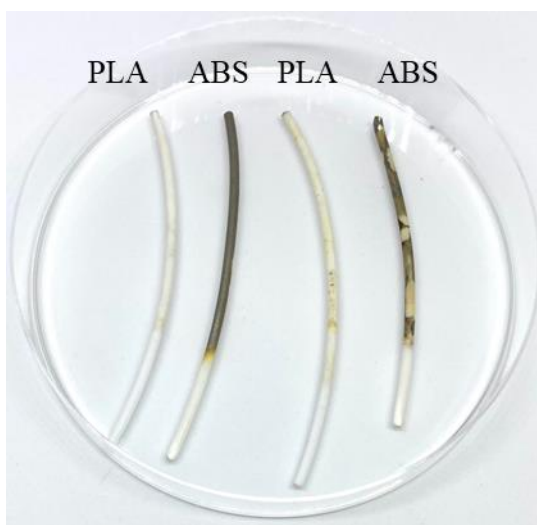


Figure 4.26 PDAD and PSS 50 mM in NaCl 2 M, AgNO₃ 20,30 mM respectively, NaBH₄ 5 mM.

Third, PDAD and PSS 50 mM in NaCl 2 M was used to assemble PEMs. AgNO₃ 20,30 mM, NaBH₄ 5 mM was used to synthesize AgNPs. From above mention experiment can be concluded that increasing PDAD and PSS concentration make better AgNPs synthesis while increasing AgNO₃ concentration cannot improve

AgNPs synthesis. ABS can be formed metallic but PLA hardly AgNPs was synthesized on.



Figure 4.27 PLA that soaked into 50 and 100 mM AgNO₃.

Next experiment focused on AgNPs insitu synthesis on PLA. First, PLA was soaked into 50 and 100 mM AgNO₃. Even though used high concentration of AgNO₃, PLA cannot be formed AgNPs. Thus, PEMs layers variation was demonstrated.



Figure 4.28 PLA with 8,10,12,14,16 PEMs layers using 10 mM AgNO₃ respectively.



Second, PLA with 8,10,12,14,16 PEMs layers were made. Result in 8 PEMs layers can be formed AgNPs indicate that the more PEMs layers, the more poorly PEMs deposition and smoothness.



Figure 4.29 PLA with 8 PEMs using 30,50,100 mM AgNO_3 respectively.

Third, PLA with 8 PEMs layers were loaded AgNPs using 30,50,100 mM AgNO_3 . It can be concluded that PLA cannot be loaded AgNPs throughout filament but ABS can be formed metallic. However metallic on ABS is completely different from exsitu. Insitu has higher roughness and flaky when blown because of PEMs layers has no smoothness.

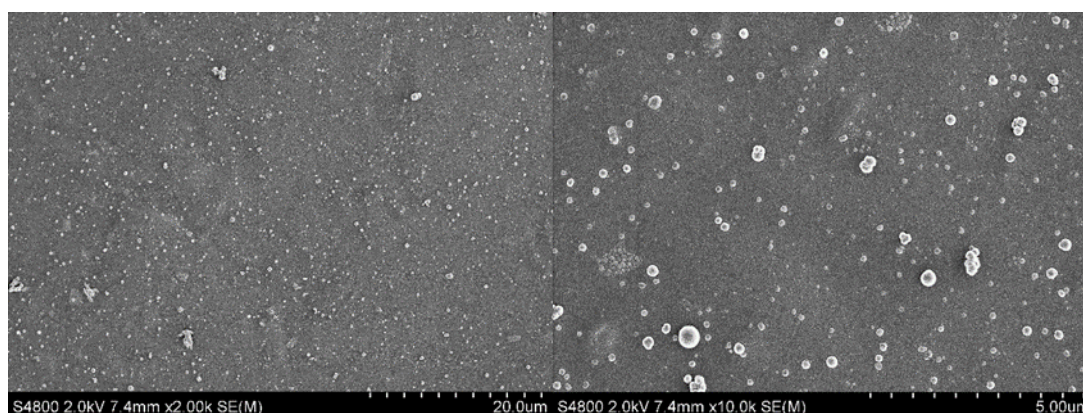


Figure 4.30 The morphology of AgNPs insitu synthesized on PLA.

PLA filament surface has very low amount of AgNPs dispersion and cannot form metallic due to the result of poor quality of insitu AgNPs synthesis on PLA from above mention experiment.

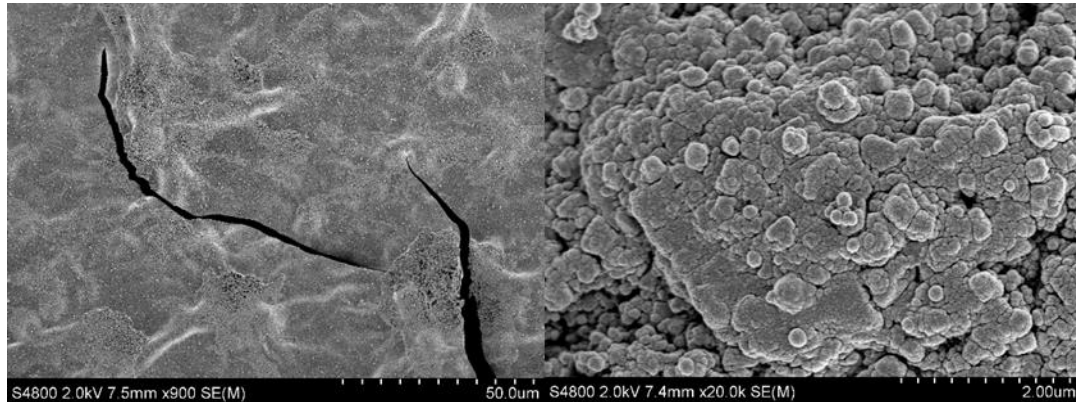


Figure 4.31 The morphology of AgNPs insitu synthesized on ABS.

AgNPs on ABS filament surface is in the form of a sheet that can be easily peeled off and break apart. However, it can form metallic.

4.5.2 3D Printing Silver Nanoparticles Coated Filaments

Due to AgNPs insitu method make low quality metallic coated filament. Nonmetallic (yellow color) and low amount of AgNPs dispersion for PLA filament. And easy peeled sheet metallic for ABS filament. AgNPs insitu coated filaments cannot be operated with 3D printing process.

4.6 Surface Treatment of Poly (lactic acid) and Poly (Acrylonitrile-Butadiene Styrene) Filament for Exsitu Silver Nanoparticles Loading

Poly (lactic acid) (PLA) and Poly (Acrylonitrile-Butadiene-Styrene) (ABS) filament are commonly used as a built-up material for Fused Deposition Modeling or 3D printing technology. There are thermoplastics with high flexibility and suitable toughness that facilitates the 3D printing. However, PLA and ABS filament have low surface energy and surface wettability, and poor adhesion. Even though they were surface modified by deposition of PEMs but after 3D printing, for exsitu AgNPs cannot be observed on them and for insitu they obtain low quality of AgNPs loading.

Thus, the surface treatment is introduced into filaments in order to improve surface adhesion for functionalization with metal nanoparticles coating.

4.6.1. NaOH Treatment

NaOH is strong based with negative charge able to erode plastic to rougher surface in order to make polyelectrolyte multilayer and metal nanoparticle attach firmly.

4.6.1.1 *PLA Filament*

Various concentrations of NaOH solution were prepared to demonstrate pH that PLA filament 3D printing grade can be modified without breaking due to strong alkaline etching.

Concentration (mM)	NaOH pH	Modified result
250	13.39	Break
150	13.18	Break
100	13.00	Break
50	12.69	Break
25	12.39	Break
15	12.17	Break
10	12.00	Break
5	11.69	Break
1	11	Not break

Table 4.2 NaOH concentration variation and result of PLA filament after modification

From Table 4.2 1 mM of base can be used to modify PLA filament. Due to PLA filament is very brittle and consist of ester bond that sensitive with nucleophilic attack of strong base causing PLA filament is broken apart easily.

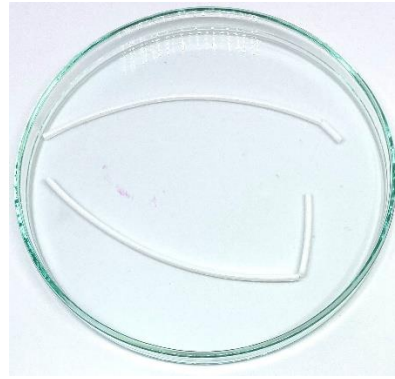


Figure 4.32 Broken PLA filament from modification.

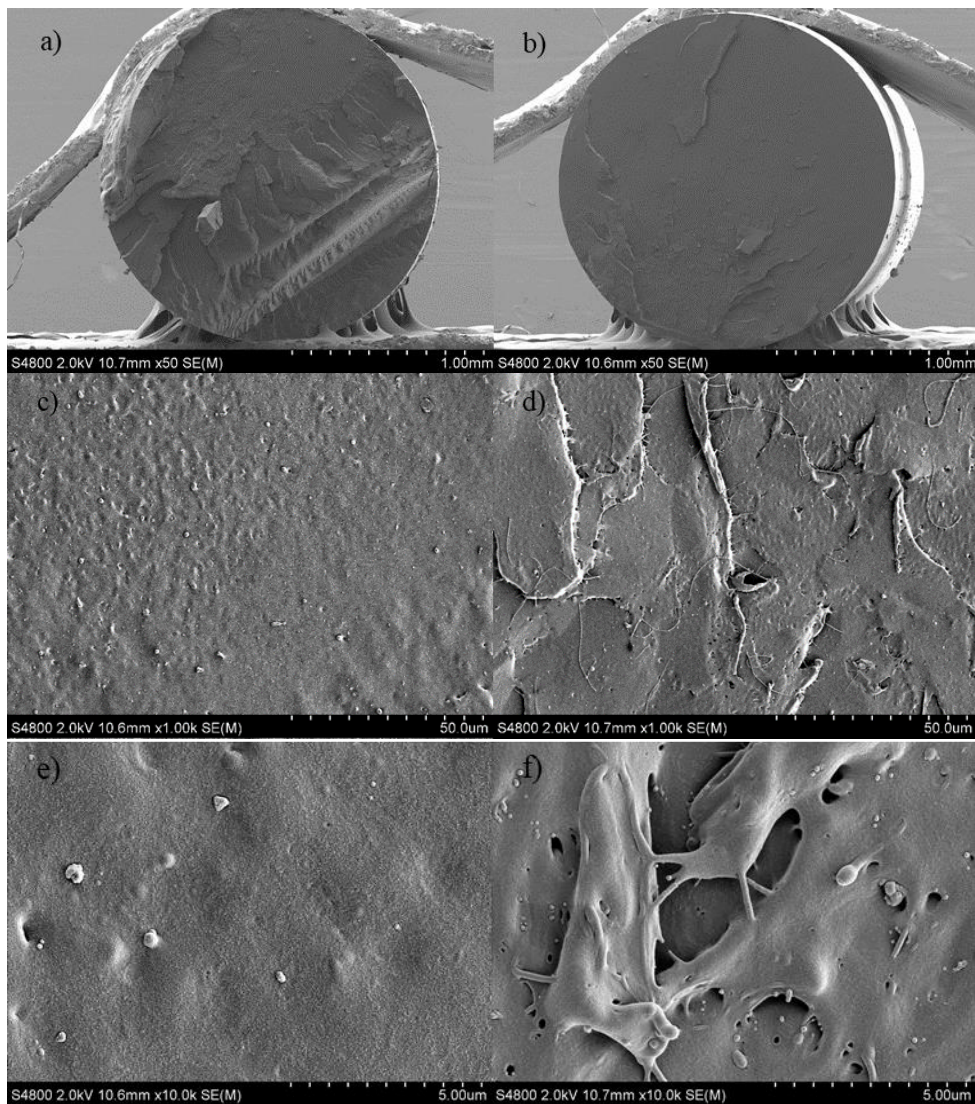


Figure 4.33 FE-SEM image of PLA filament cross section at different magnification.

- a) Untreated x50 b) Treated x50 c) Untreated x1.00k d) Treated x1.00k
 e) Untreated x10.0k f) Treated x10.0k

The morphology of broken filament in cross section from high pH alkaline treatment compared with untreated filament was investigated by Field scanning electron microscopy. Breaking apart of filament was occurred from too high degree of roughness that generated by basic etching. Therefore decreasing concentration of alkaline solution and increasing treated time is the key to modify filament to achieve appropriate degree of roughness and still maintain their mechanical properties.

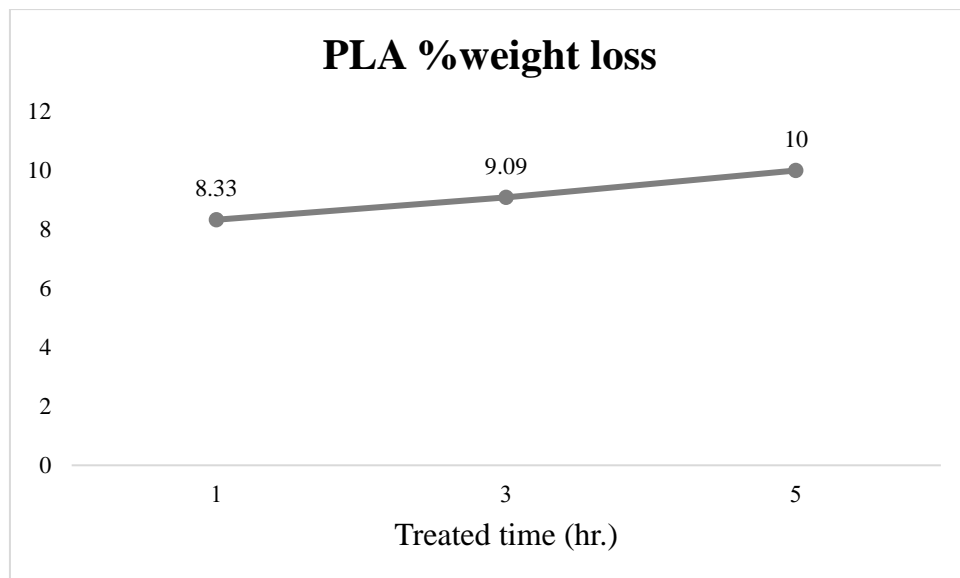


Figure 4.34 % weight loss of PLA after treated at various times.

PLA was treated by 1 mM NaOH with variation of time 1, 3, and 5 hr. Due to surface etching of strong base, the filament lost weight with increased treated time.

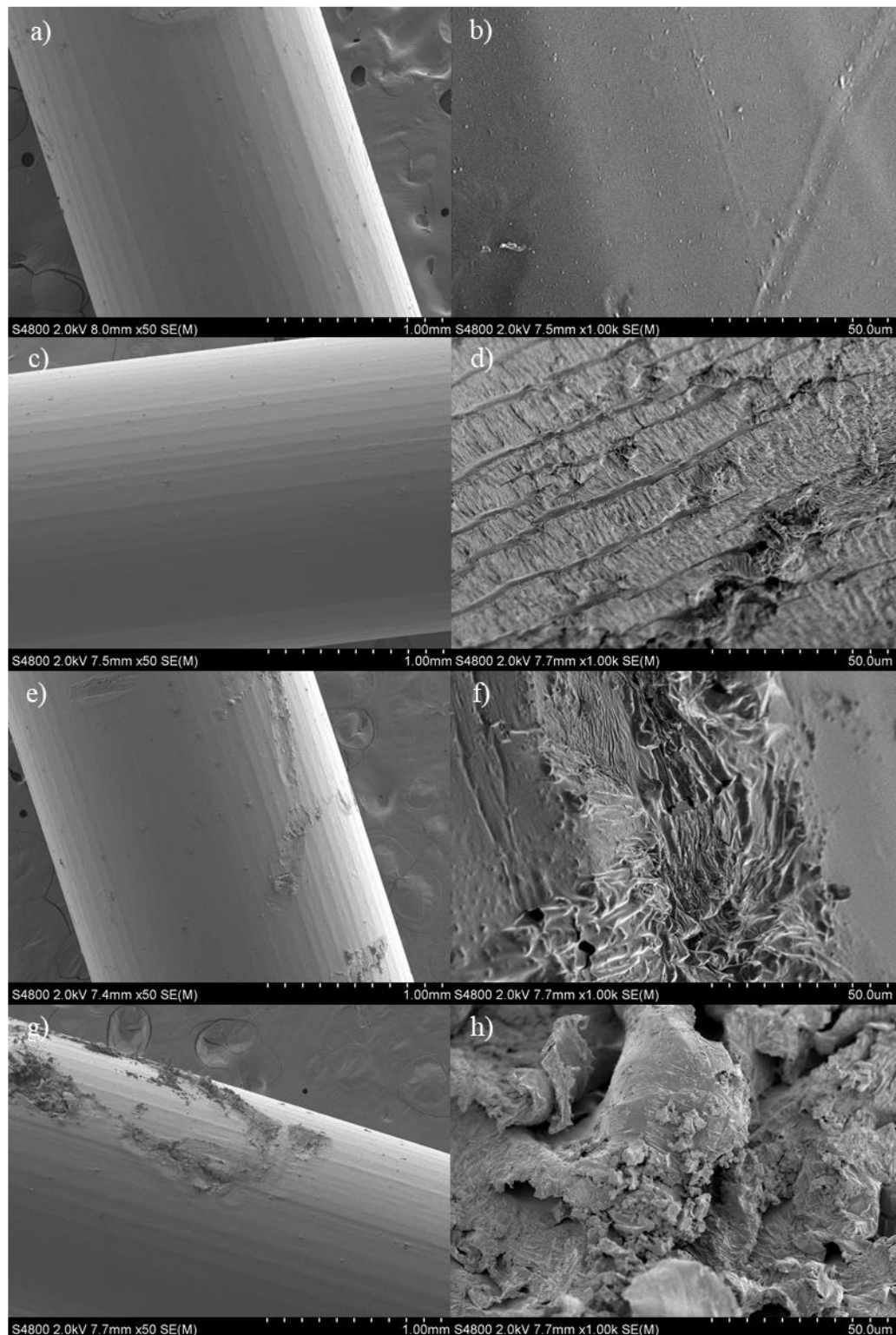


Figure 4.35 FE-SEM image of NaOH treated surface of PLA filament at different magnification.

a) Untreated x50 b) Untreated x1.00k c) 1 hr. treated x50 d) 1 hr. treated x1.00k

e) 3 hr. treated x50 f) 3 hr. treated x1.00k g) 5 hr. treated x50 h) 5 hr. treated x1.00k

From Figure 4.35 is shown comparison of surface morphology between untreated PLA and NaOH treated PLA at different time. It can be concluded that the degree of PLA surface roughness is increased with increasing of treated time significantly.

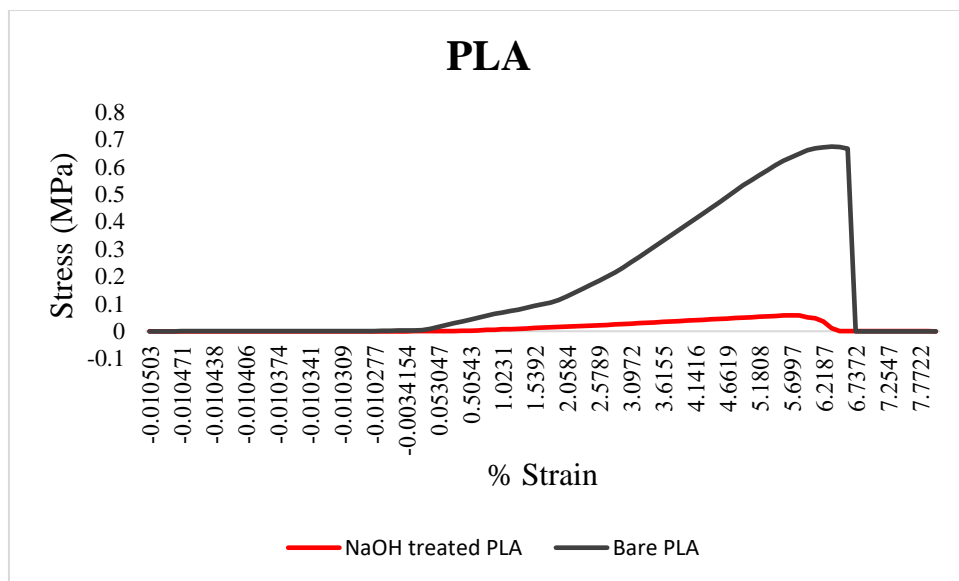


Figure 4.36 Stress and % strain curve of bare PLA and NaOH PLA.

	Maximum Tensile Strength (Mpa)
Bare PLA	0.646147
Treated PLA	0.067208

Table 4.3 Maximum Tensile Stress of PLA

PLA filaments were shape-shifted from rod shape to flat shape by Compression molding and then were investigated mechanical properties by Universal testing machine (UTM). In table 4.3 NaOH treatment made maximum tensile stress of PLA drop from 0.646147 to 0.067208 MPa. After surface treatment PLA by NaOH solution cause decreasing of mechanical property approximately 89.59 %

Next, the filament was immersed in 0.25 M NaOH solution before coated with PEM and AgNPs in order to make obvious difference between with and without treatment.



Figure 4.37 Untreated and Alkaline treated PLA

From Figure 4.37 surface of treated PLA is less shiny very much due to higher roughness. But roughness can cause more attachment of PEM and AgNPs.

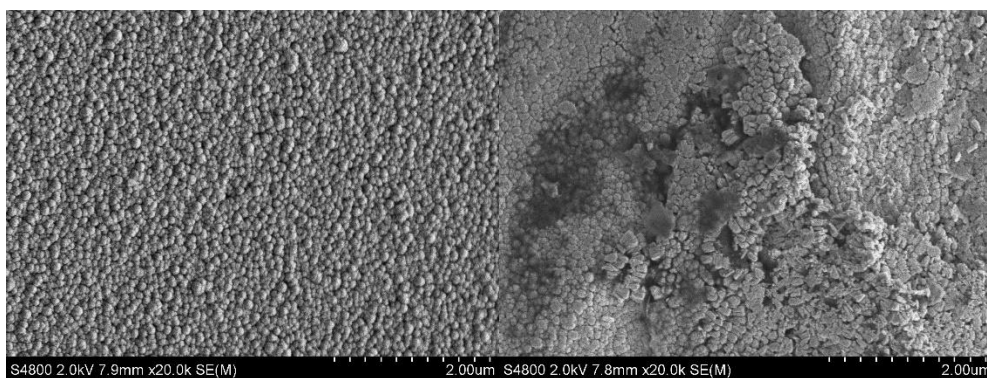


Figure 4.38 The morphology of AgNPs dispersion on alkaline treated PLA on low and high surface roughness respectively.



2287006921

CU Theses 6272032063 thesis / rev: 19072564 14:14:29 / seq: 8

From Figure 4.38 is shown AgNPs can be packed full on low surface roughness area and embedded in high surface roughness area of PLA. Alkaline treatment can be used to increase PLA surface adhesion efficiency with AgNPs significantly.

The efficiency of NaOH treatment was investigated by Peeling test and measured by Image J program. 1 mM NaOH was used to treat PLA filament with variation of time 1,3,5 hr. because this concentration can erode PLA surface without breaking. And then deposited with PEMs and AgNPs respectively.

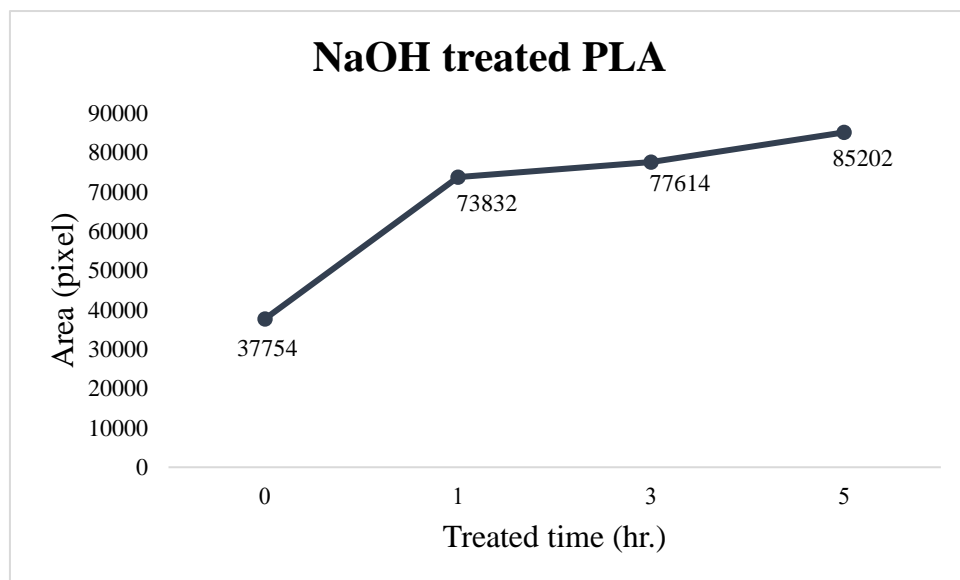


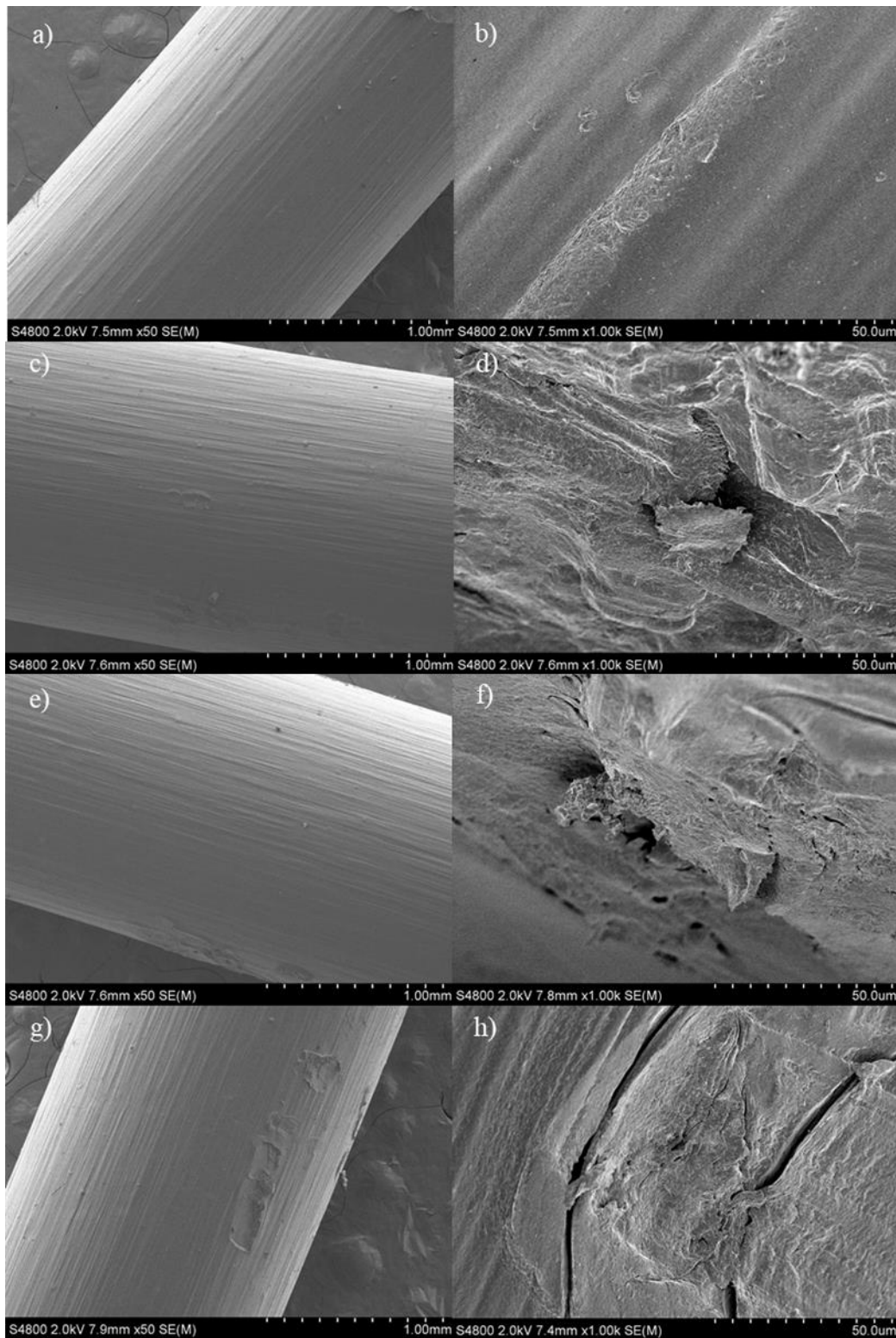
Figure 4.39 Peeling test of NaOH treated PLA.

Figure 4.39 representing the area of AgNPs that could not be removed from filament surface by scotch tape measured by Image J program in unit of pixel. The more treated time with NaOH, the more unremovable AgNPs area, indicating NaOH treatment can be used to increase PLA surface adhesion efficiency with AgNPs significantly.

4.6.1.2 ABS Filament

ABS filament properties are higher toughness, stiffness than PLA filament thus it is hard to be broken by alkaline treatment. ABS can be treated by

higher NaOH concentration than PLA. ABS was treated with variation of NaOH concentration 10 mM, 100 mM, 1000 mM.



2287006921

CU IThesis 6272032063 thesis / rev: 19072564 14:14:29 / seq: 8

Figure 4.40 FE-SEM image of NaOH treated surface of ABS filament at different magnification.

- a) Untreated x50 b) Untreated x1.00k c) 10 mM NaOH treated x50 d) 10 mM NaOH treated x1.00k e) 100 mM NaOH treated x50 f) 100 mM NaOH treated x1.00k g) 1000 mM NaOH treated x50 h) 1000 mM NaOH treated x1.00k

From Figure 4.40 is shown comparison of surface morphology between untreated ABS and NaOH treated ABS at different NaOH concentration. It can be concluded that the degree of ABS surface roughness is increased with increasing of NaOH concentration gradually.

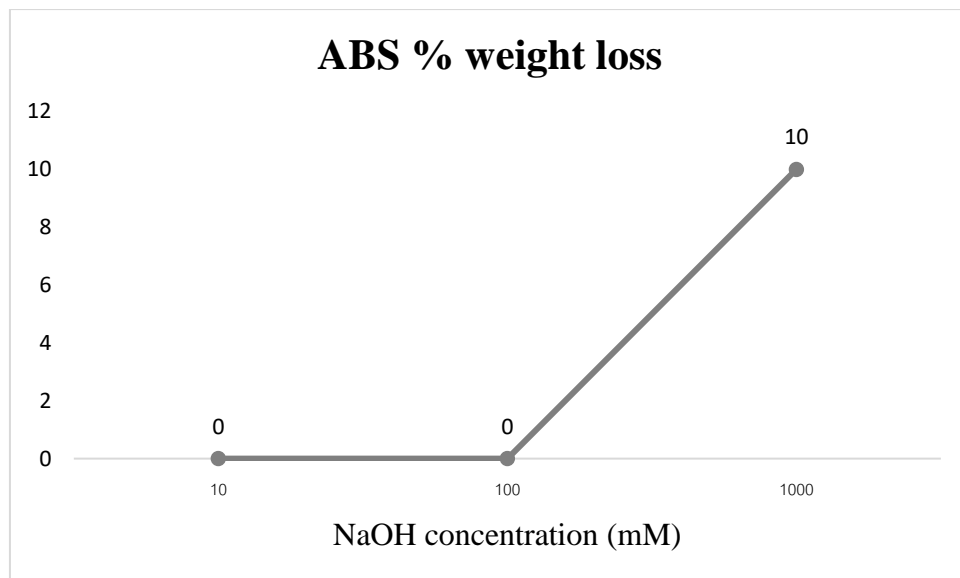


Figure 4.41 % weight loss of ABS after treated at various concentration of NaOH.

ABS was treated by NaOH concentration variation due to ABS is very tough and durable thus ABS can withstand the etching of strong base. At 10-100 mM NaOH ABS lost weight 0%. However, the filament lost weight at 1000 mM NaOH.

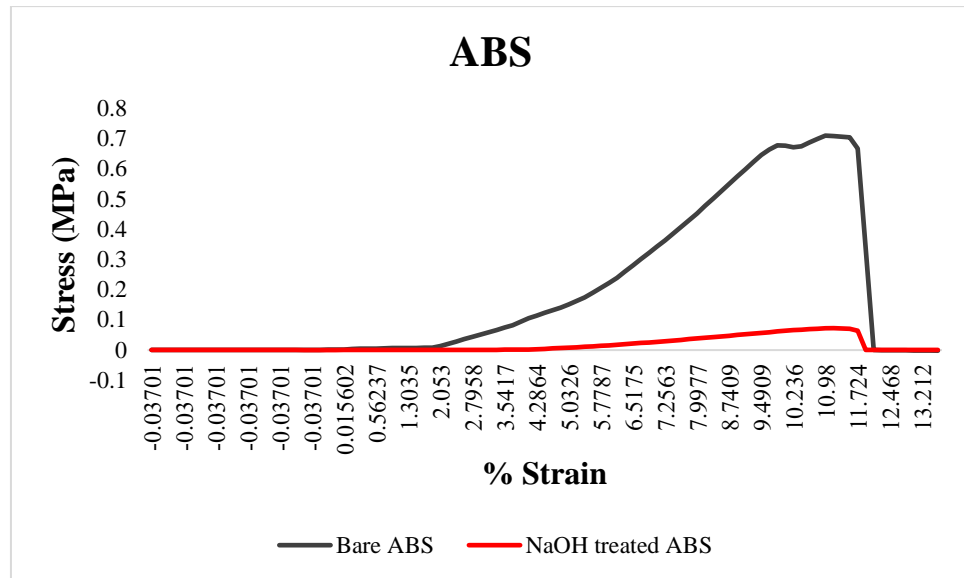


Figure 4.42 Stress and % strain curve of ABS.

	Maximum Tensile Stress (MPa)
Bare ABS	0.80779
Treated ABS	0.08762

Table 4.4 Maximum Tensile Stress of ABS

ABS filaments were shape-shifted from rod shape to flat shape by Compression molding and then were investigated mechanical properties by Universal testing machine (UTM). In table 4.4 NaOH treatment made maximum tensile stress of ABS drop from 0.80779 to 0.08762 MPa. It can be concluded that after modify PLA with NaOH cause decreasing of mechanical property approximately 89.15 %.



22870069321

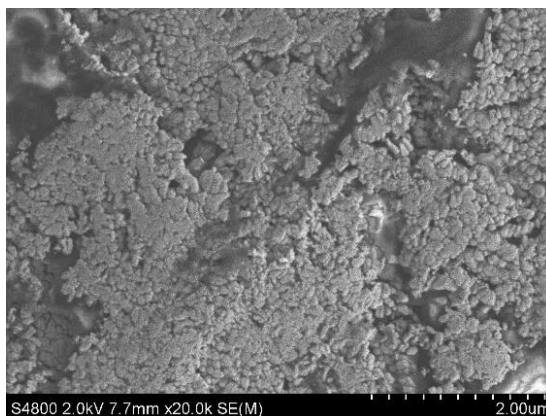


Figure 4.43 The morphology of AgNPs dispersion on alkaline treated ABS.

From Figure 4.43 is shown AgNPs can be packed full and embedded in surface roughness area of ABS. Alkaline treatment can be used to increase ABS surface adhesion efficiency with AgNPs significantly.

The efficiency of NaOH treatment was investigated by Peeling test and measured by Image J program. ABS was treated with variation of NaOH concentration 10 mM, 100 mM, 1000 mM.

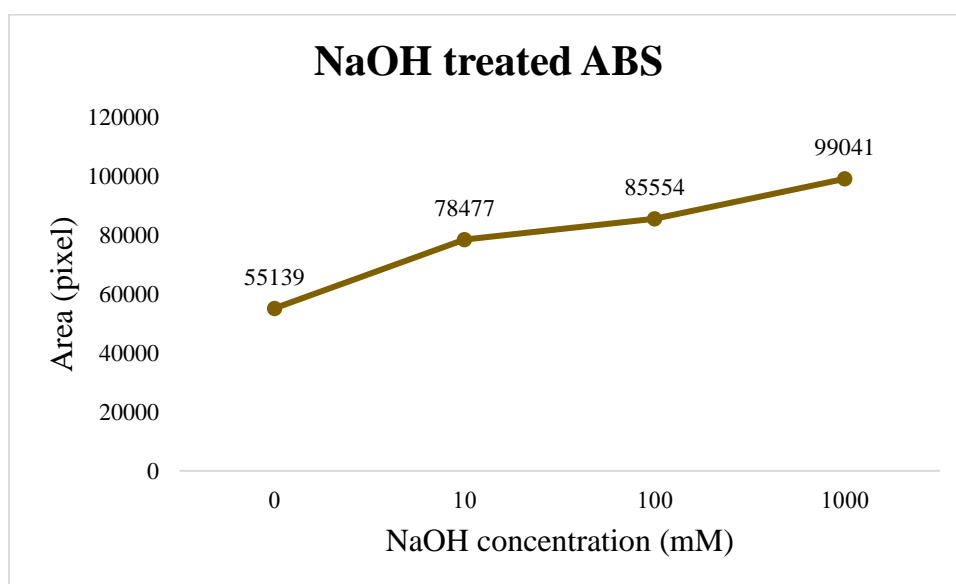


Figure 4.44 Peeling test of NaOH treated ABS.

For peeling test of NaOH treated ABS. The more treated time with NaOH, the more unremovable AgNPs area, indicating NaOH treatment can be used to increase ABS surface adhesion efficiency with AgNPs significantly.

4.6.1.3 3D Printed NaOH Treated PLA and ABS

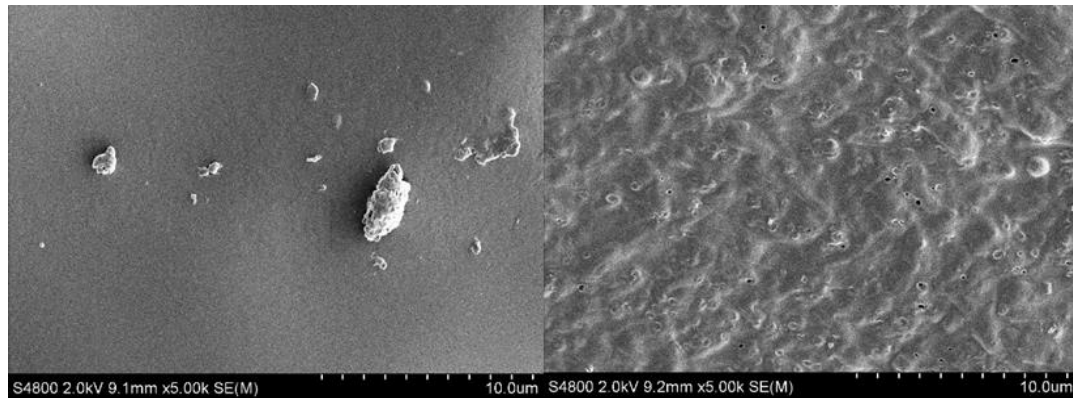


Figure 4.45 FE-SEM image of printed AgNPs exsitu coated on NaOH treated PLA and ABS.

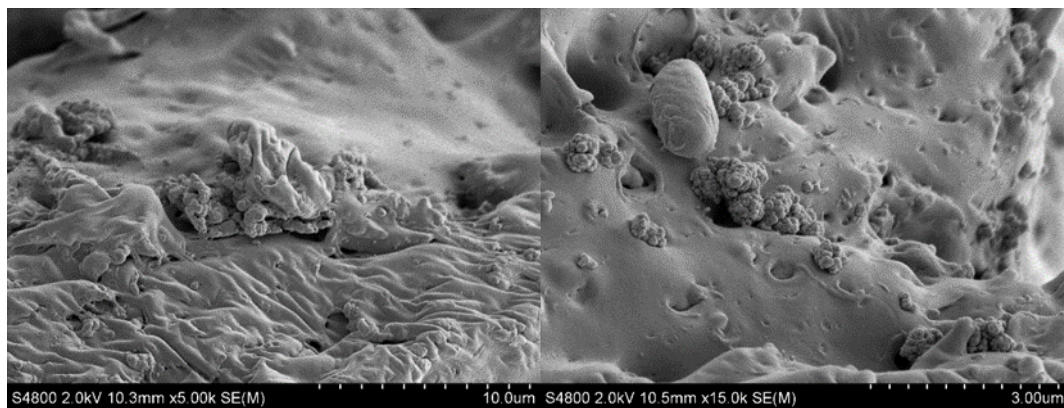


Figure 4.46 FE-SEM cross-section image of printed AgNPs exsitu coated on NaOH treated PLA at x5.00k and x15.0k.

AgNPs cannot be observed on NaOH treated PLA and ABS surface. However, cross-section can observe cluster of AgNPs dispersing everywhere inside specimens. It can be implied that after printing, all of AgNPs were not be removed by nozzle of 3D printer but some part of AgNPs concentrated inside specimen.

4.6.2 Polyethylenimine (PEI) Treatment

4.6.2.1 AgNPs Loading on PEI Treated PLA and ABS Filament

PEI solution was used due to high degree of branch, the efficiency of gripping with oppositely charge polyelectrolyte is excellent because of their strong positively charge, holding many layers of polyelectrolyte built up tightly. First, filament was emerged in 0.1% (w/v) PEI solution, varying time 1,3,5 hr. before deposition of polyelectrolyte multilayer of PDAD and PSS for monolayer treatment. And multilayer treatment was conducted by deposit PEI and PSS alternately before polyelectrolyte multilayer of PDAD and PSS, varying layer of PEI 2,4,6 layers. And then all samples were deposited with AgNPs.



Figure 4.47 PEI treated PLA and ABS filament respectively.

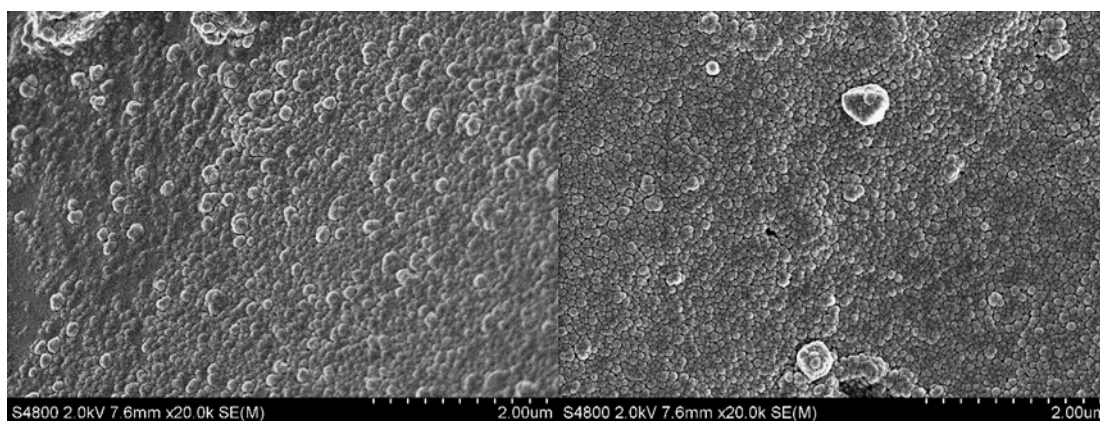


Figure 4.48 The morphology of AgNPs dispersion on PEI treated PLA and ABS.

From Figure 4.48 is shown AgNPs can be packed full on PLA and ABS surface. The distribution of AgNPs can occurred either well-dispersion or agglomeration.

The efficiency of PEI treatment was investigated by Peeling test and measured by Image J program.

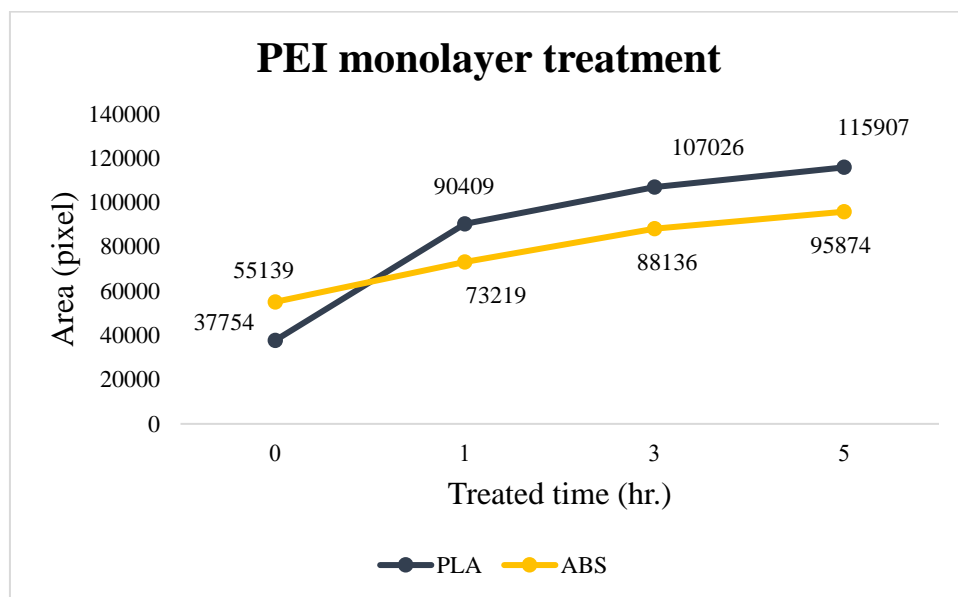


Figure 4.49 Peeling test of PEI monolayer treated PLA and ABS.

From figure 4.49 representing the area of AgNPs that could not be removed from filament surface by scotch tape measured by Image J program in unit of pixel. The more treated time monolayer PEI, the more unremovable AgNPs area, indicating PEI treatment can be used to increase PLA and ABS surface adhesion efficiency with AgNPs significantly.

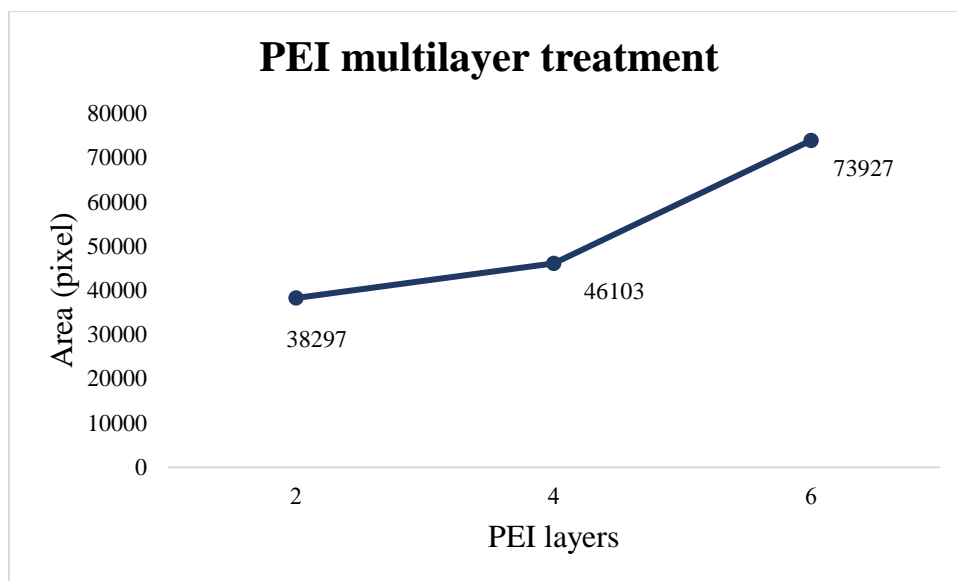


Figure 4.50 Peeling test of PEI multilayer treated PLA.

For multilayer treatment, the more PEI layers built up, the more unremovable AgNPs area. However monolayer treatment has higher surface adhesion improved efficiency.

4.6.2.2 3D Printed PEI Treated PLA and ABS

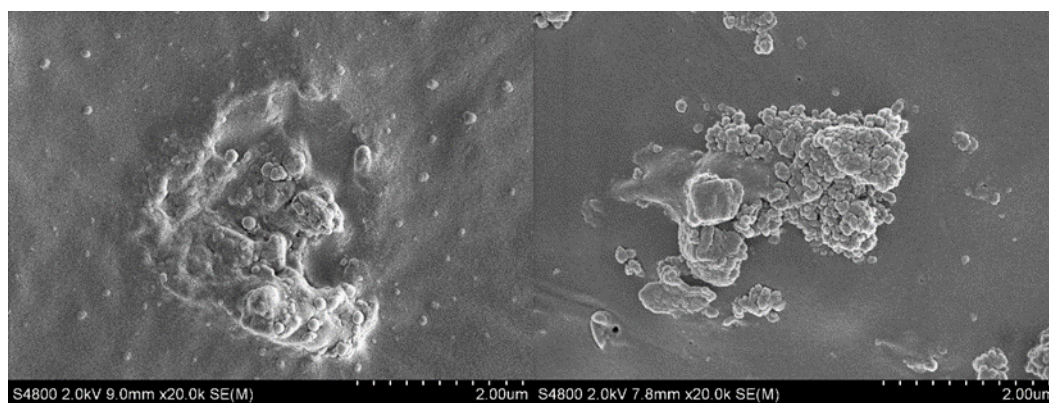


Figure 4.51 FE-SEM image of printed AgNPs exsitu coated on PEI treated PLA and ABS.

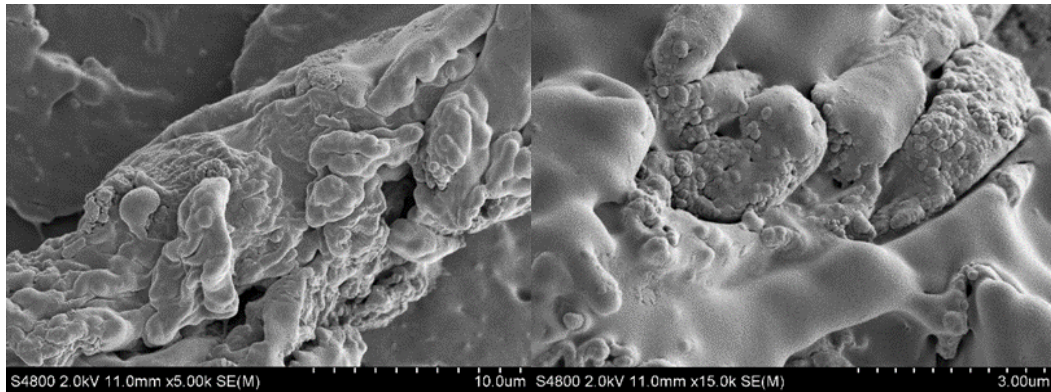


Figure 4.52 FE-SEM cross-section image of printed AgNPs exsitu coated on NaOH treated PLA at x5.00k and x15.0k.

AgNPs can be found on the surface and cross-section either. Due to PEI treatment cause higher attachment between AgNPs and filament.

4.7 Surface Treatment of Poly (lactic acid) and Poly (Acrylonitrile-Butadiene Styrene) Filament for Insitu Silver Nanoparticles Loading.

4.7.1 Alkaline Treatment



Figure 4.53 NaOH treated insitu coating.

NaOH can increase adhesion between filament and PEMS as shown in Figure 4.53 AgNPs can be loaded on PLA more than untreated. However, NaOH

cannot smoothen PEMs layers because AgNPs on filament still has high roughness and flaky when blown.

4.7.2 PEI Treatment

4.7.2.1 AgNPs Loading on PEI Treated PLA and ABS Filament

PEI or Polyethyleneimine was prepared 0.1% w/v and the filaments were immersed in PEI solution for 1 hr. before PEMs deposition and AgNPs loading respectively.

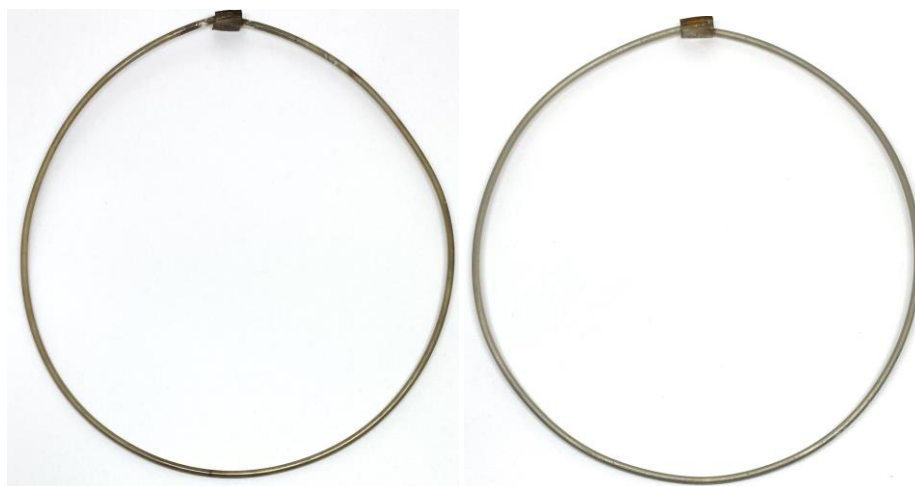


Figure 4.54 AgNPs insitu loaded PEI treated PLA and ABS respectively.

From Figure 4.54 AgNPs can be formed metallic and loaded throughout PLA and ABS filament smoothly. PEI has high amount of NH and NH₂ that will effectively increase adhesion between filament and PEMs and smoothen PEMs layers.

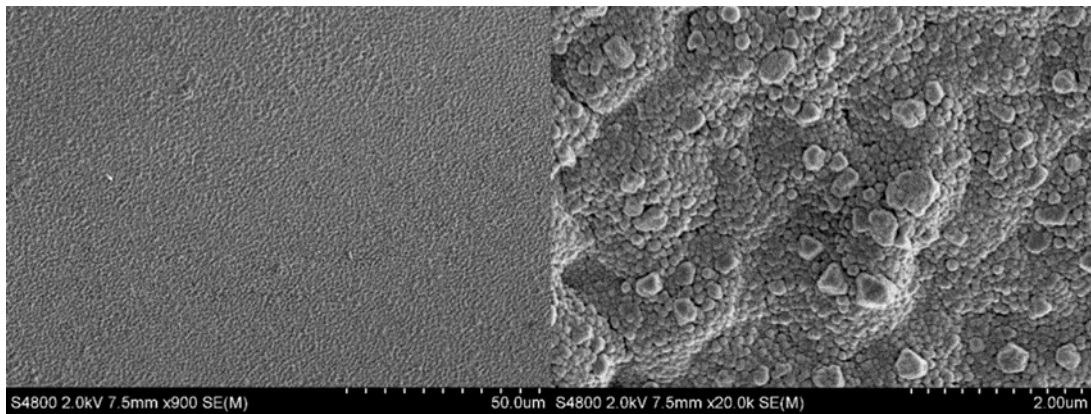


Figure 4.55 The morphology of AgNPs insitu synthesized on PEI treated PLA.

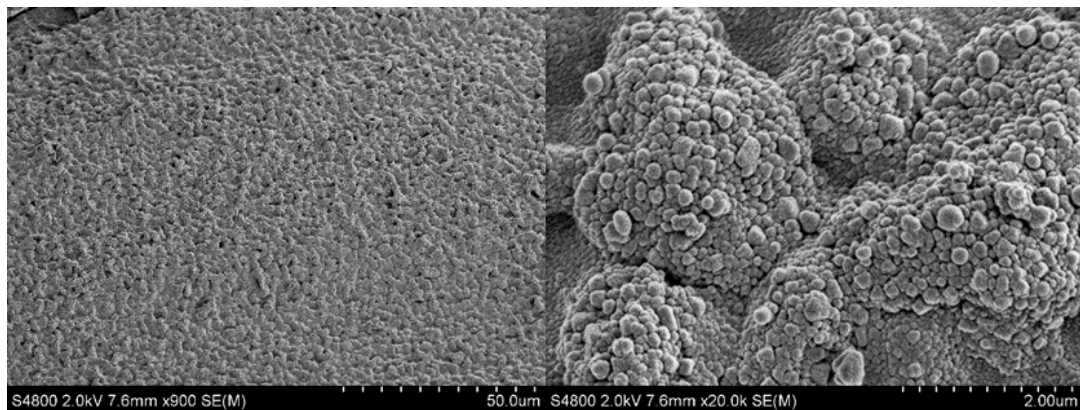


Figure 4.56 The morphology of AgNPs insitu synthesized on PEI treated ABS.

AgNPs can pack full as metallic form on PEI treated PLA and ABS without peeling off. Due to high degree of branch of PEI that has high efficiency to grip polyelectrolyte multilayer and AgNPs. It causes rough surface of AgNPs and disperse as a cluster.

4.7.2.2 3D Printed PEI Treated PLA and ABS



Figure 4.57 Printed AgNPs insitu coated PLA filament with and respectively.

While insitu coating has poor AgNPs dispersion causing aggregation due to PEI treatment before printing cause cluster of AgNPs.

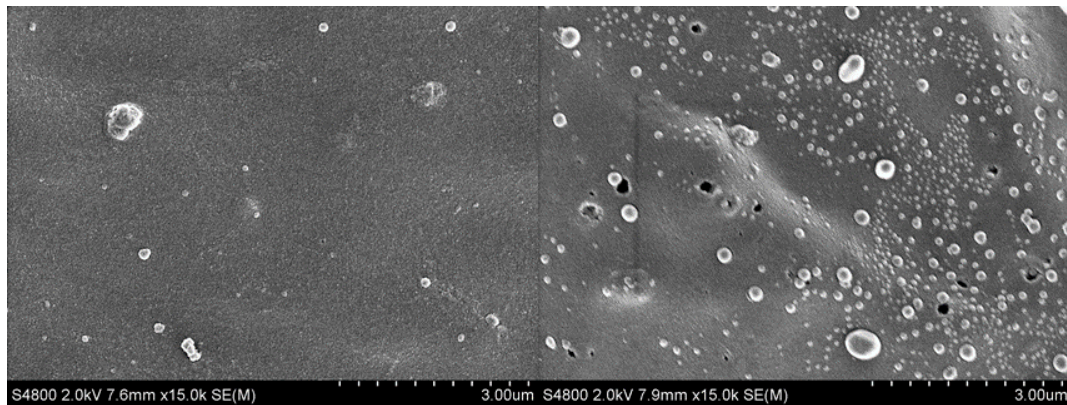


Figure 4.58 FE-SEM image of printed AgNPs insitu coated on PEI treated PLA and ABS.

Printed AgNPs insitu coated on PEI treated PLA and ABS can observe dispersion of AgNPs. It can be implied that PEI has efficiency to improve adhesion surface of PLA and ABS filament significantly.

4.8 3D Printing Confirmation

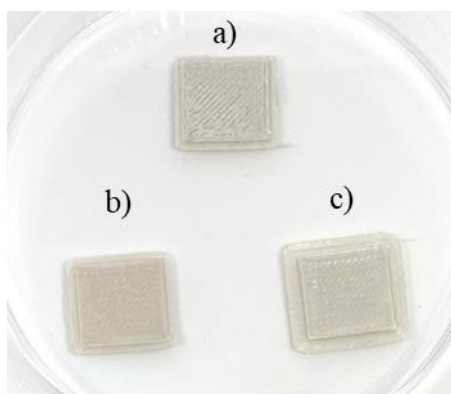


Figure 4.59 Printed AgNPs coated sample. a) Untreated b) NaOH treated c) PEI treated.

All of printed specimen including untreated, NaOH treated, and PEI treated has the same optical property that is homogeneous grey color from metallic. Thus, it infers that all of samples still have AgNPs.

The printed sample was characterized AgNPs by X-Ray Diffractometer (XRD) to confirm that they have AgNPs dispersion on the surface or inside printed samples.

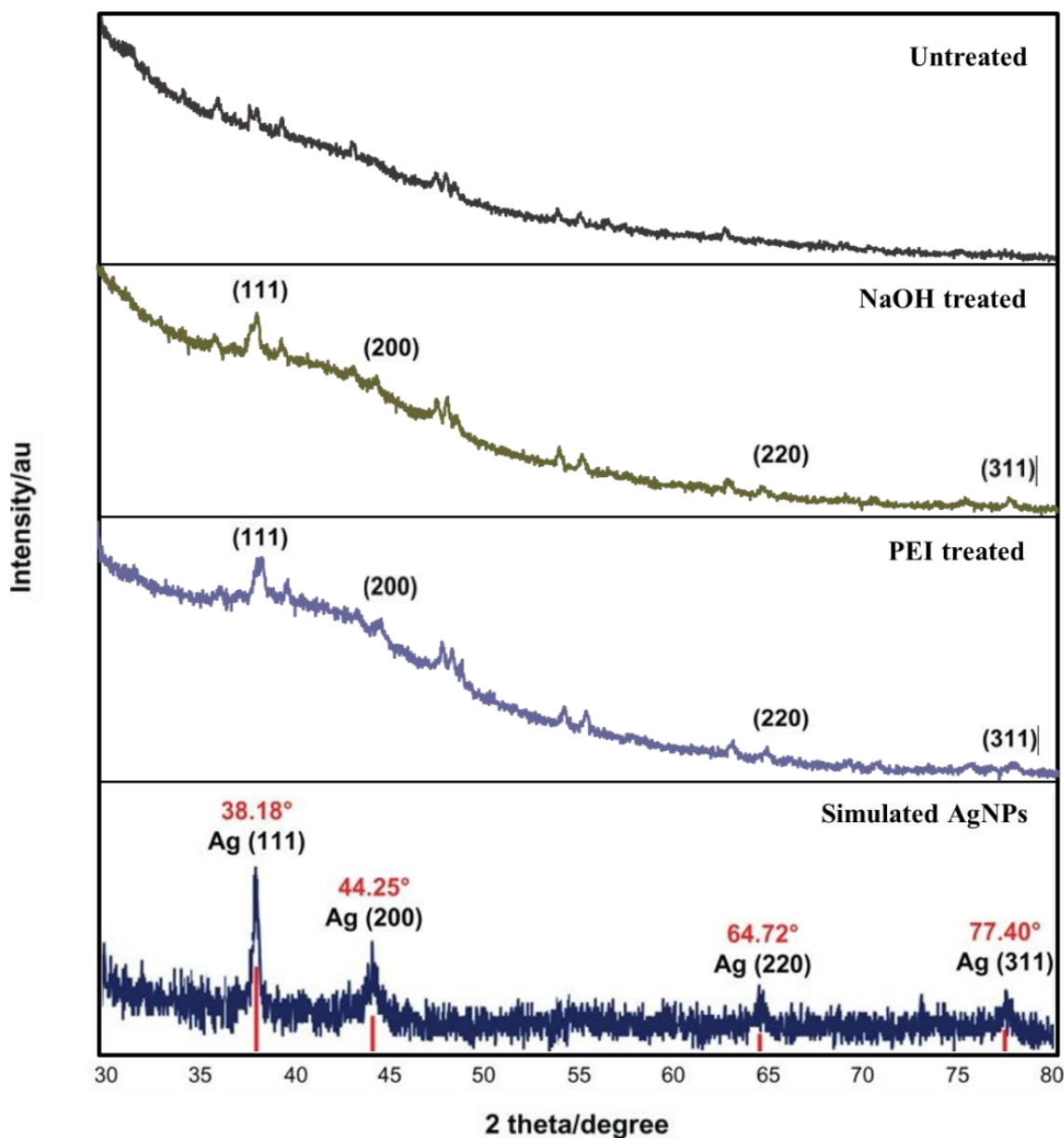


Figure 4.60 XRD patterns of printed samples. (Shameli, Ahmad et al. 2012)

Figure 4.60 is shown the XRD spectra of printed untreated, NaOH treated, and PEI treated samples compare with simulated AgNPs. The main peaks corresponding to $2\theta = 38.18^\circ$, 44.25° , 64.72° , and 77.40° which corresponding Miller indices, (111), (200), (220), (311). For untreated sample, it could not observe peaks match with simulated patterns of AgNPs. It implies that grey color and AgNPs dispersion that could observe from FE-SEM cross-section image of untreated sample comes from AgNPs within the sample that are very deep and could not be detected by

XRD. For NaOH and PEI treated samples, all peaks in spectra well match with simulated patterns of AgNPs. It implies that grey color and AgNPs dispersion that could observe from FE-SEM cross-section image of samples come from AgNPs within the samples that are not very deep enough to be detectable by XRD.

Part 2 ZIF-8 Particles Catalyst

4.9 ZIF-8 Particles Size Distribution

ZIF-8 was synthesized by using Zinc acetate ($\text{Zn}(\text{OAc})_2 \cdot \text{H}_2\text{O}$) and 2-methylimidazole (Hmim). The synthesized ZIF-8 is white fine powder. The ZIF-8 particle size has gained is narrow distribution. It can be seen stable particle size in Figure 4.61 and the calculated average size was 163 nm.

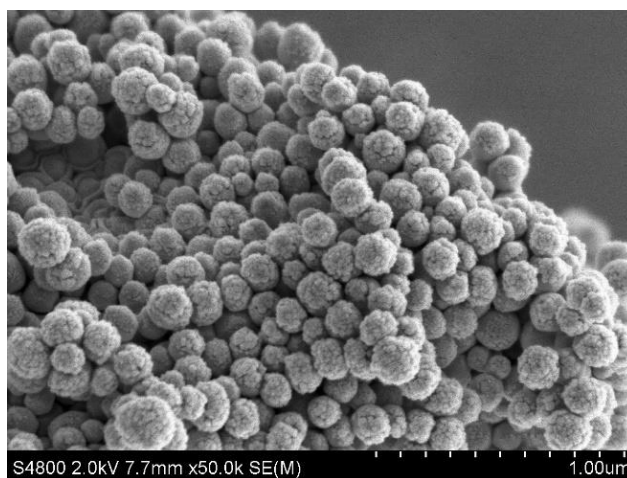


Figure 4.61 SEM image of synthesized ZIF-8.

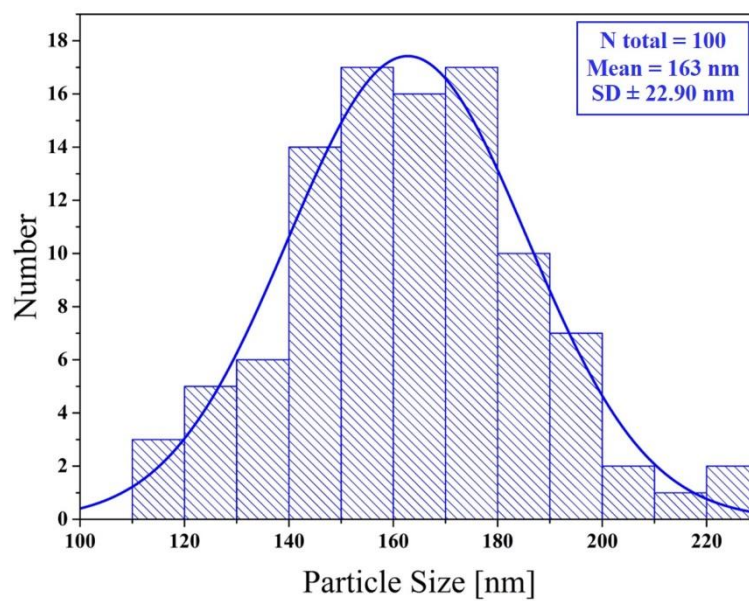


Figure 4.62 Size distribution of ZIF-8 particles.



Figure 4.63 ZIF-8 solutions.

4.10 ZIF-8 Crystal Morphology



22870069321

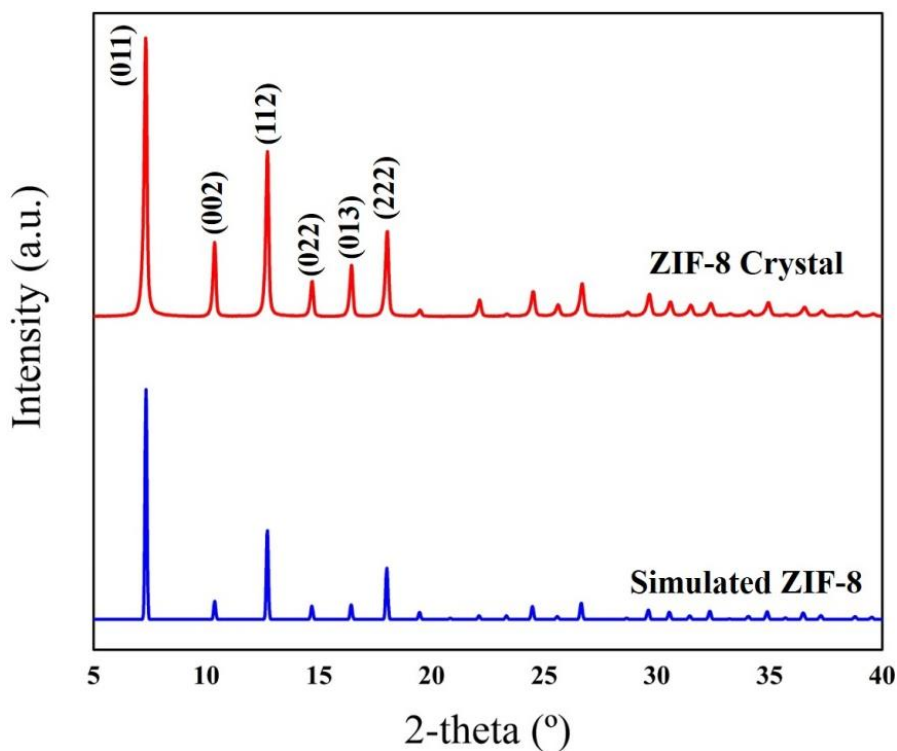


Figure 4.64 XRD patterns of synthesized ZIF-8 sample.

In Figure 4.64 shows the XRD spectra of synthesized ZIF-8 sample (red line) and simulated ZIF-8 (blue line). The main peaks corresponding to $2\theta = 7.4^\circ$, 10.4° , 12.7° , 14.7° , 16.4° and 18.0° which corresponding Miller indices, (011), (002), (112), (022), (013) and (222). All peaks in spectra well match with simulated patterns of ZIF-8 single crystal.

4.11 ZIF-8 Dispersion on Filaments

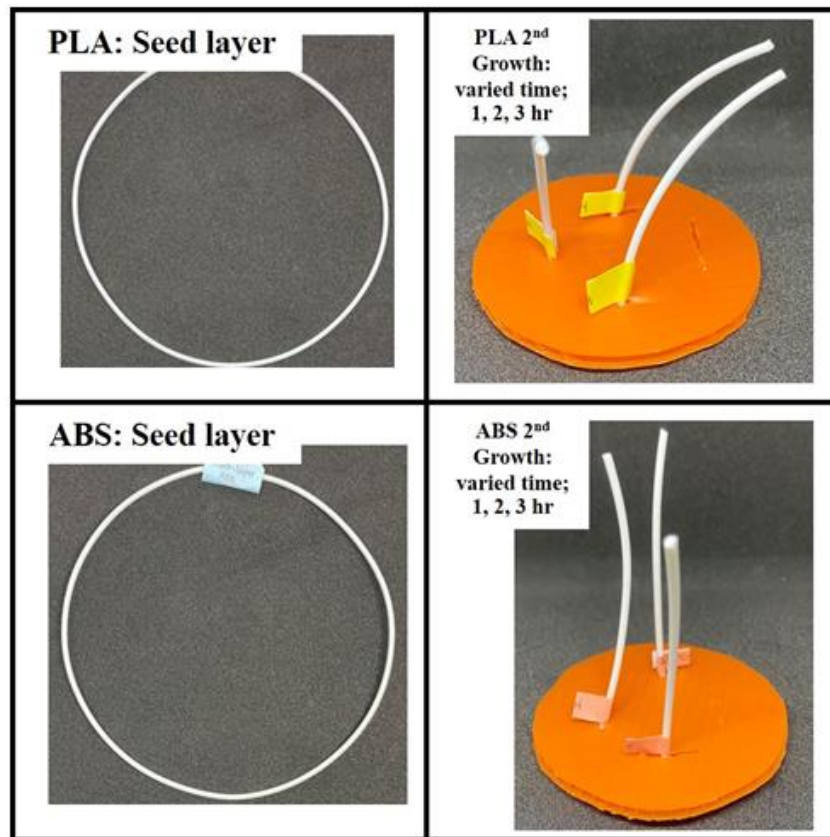


Figure 4.65 Optical images of PLA and ABS filaments; seed layer, and secondary growth.

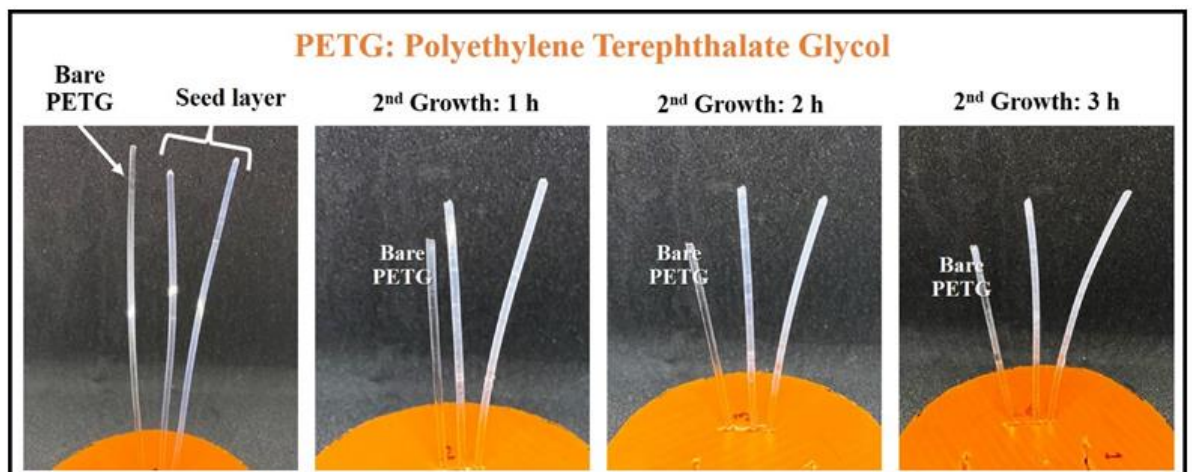


Figure 4.66 Optical images of PETG filaments; bare filament, seed layer, and secondary growth.

PLA and ABS filaments are solid white. Thus, after ZIF-8 coating including seeding and secondary growth steps, the changing color of filaments could not observe. Therefore PETG is another option to be able to observe whether ZIF-8 can be coated on the surface of the filaments because of their semi-transparent color. It can be seen in Figure 4.66 that bare PETG filament was changed from transparent into white after the seeding step, and more intense after the secondary growth process; as increasing in growth time, the white intensity was increased.

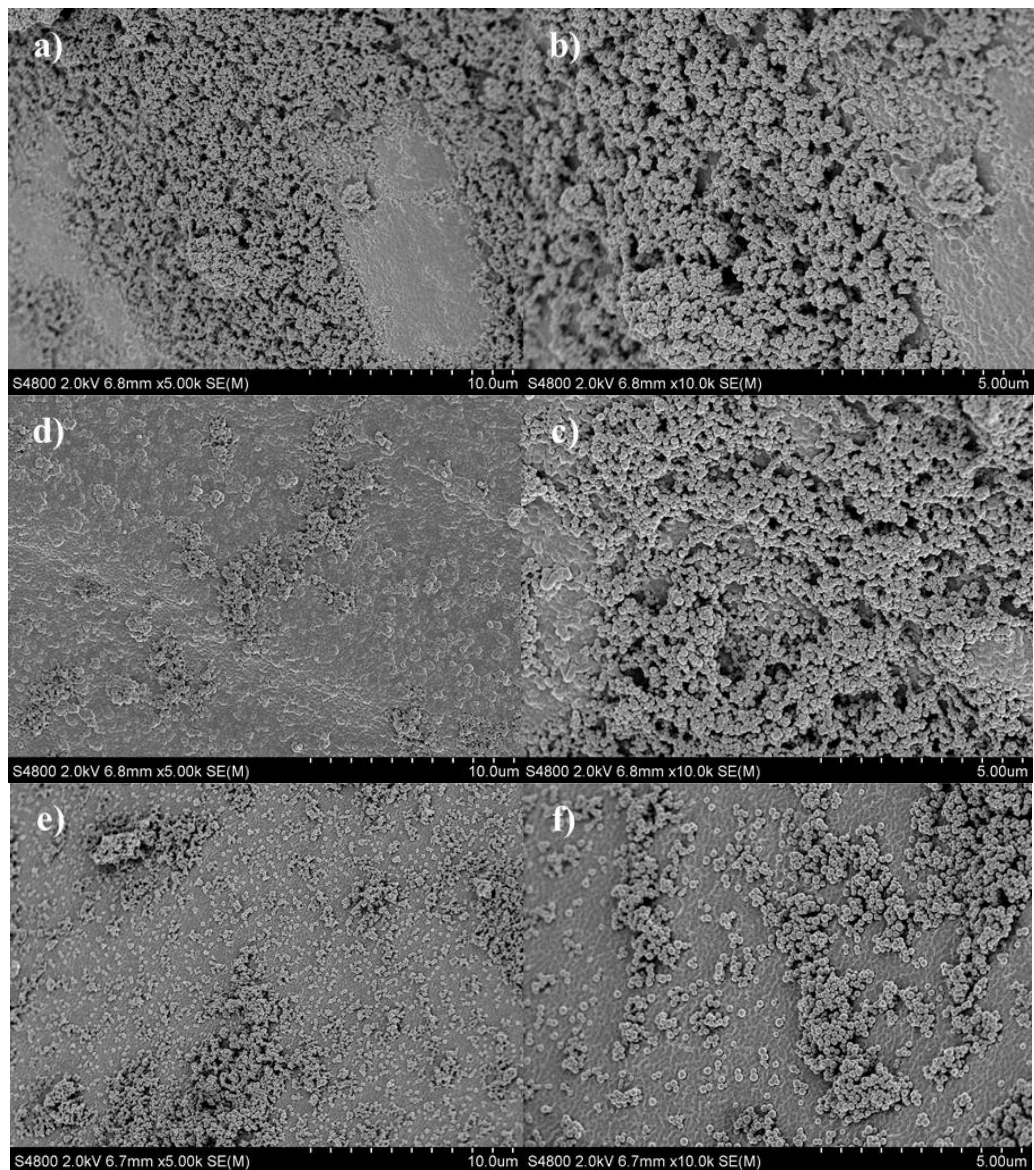


Figure 4.67 SEM images of ZIF-8 seed layer at different magnification; a) PLA x5.00k, b) PLA x10.0k, c) ABS x5.00k, d) ABS x10.0k, e) PETG 5.00k, and f) PETG x10.0k.

The surface morphology of ZIF-8 coated filaments were analyzed by Field scanning electron microscopy (FE-SEM) for observe ZIF-8 particles dispersion. As shown in Figure 4.67 ZIF-8 particles were successfully deposited on filaments. However, when determine the samples in low magnification scale, it can be observed that good homogeneous dispersion of seed crystals on the substrates cannot be prepared.

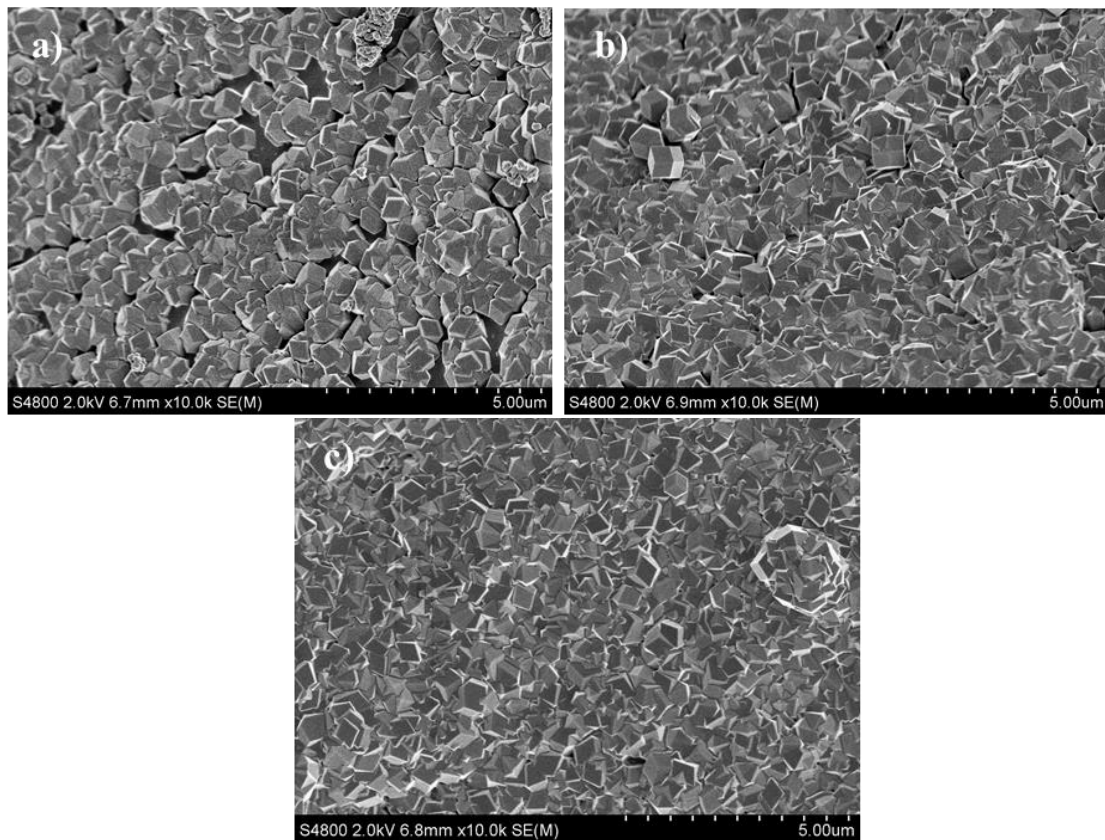


Figure 4.68 ZIF-8 dense thin film coated on PETG filaments obtained from secondary growth process in different growth time; a) 1 hr., b) 2 hr., c) 3 hr.

Figure 4.68 depicts the SEM images of ZIF-8 dense thin film coated on PETG filaments under different secondary growth time such as 1,2,3 hr. According to these results, the dense film can be obtained after 3 hours of growth time.

4.12 3D Printing

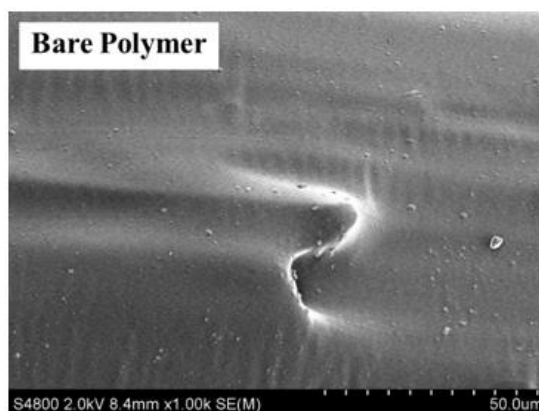


Figure 4.69 FE-SEM image of printed PETG surface.

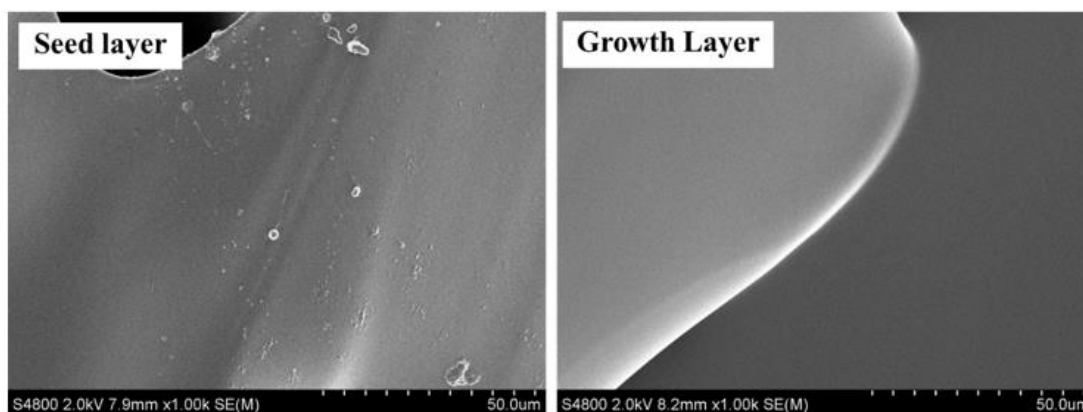


Figure 4.70 FE-SEM image of printed seed layer and growth layer of ZIF-8 coated PETG.

ZIF-8 particles could not observe on printed seed layer and growth layer of ZIF-8 coated PETG. Because ZIF-8 particles were peeled off by strong friction between filament and die during 3D printing process.

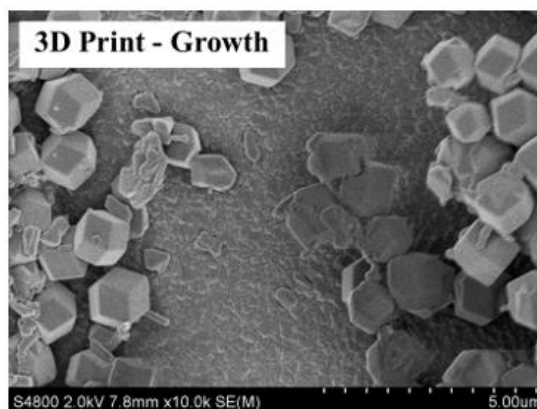


Figure 4.71 FE-SEM image of growth layer of ZIF-8 coated printed seed layer of ZIF-8 coated PETG.

In Figure 4.71 depicts successful preparation of dense ZIF-8 film on printed seed layer of ZIF-8 coated PETG.

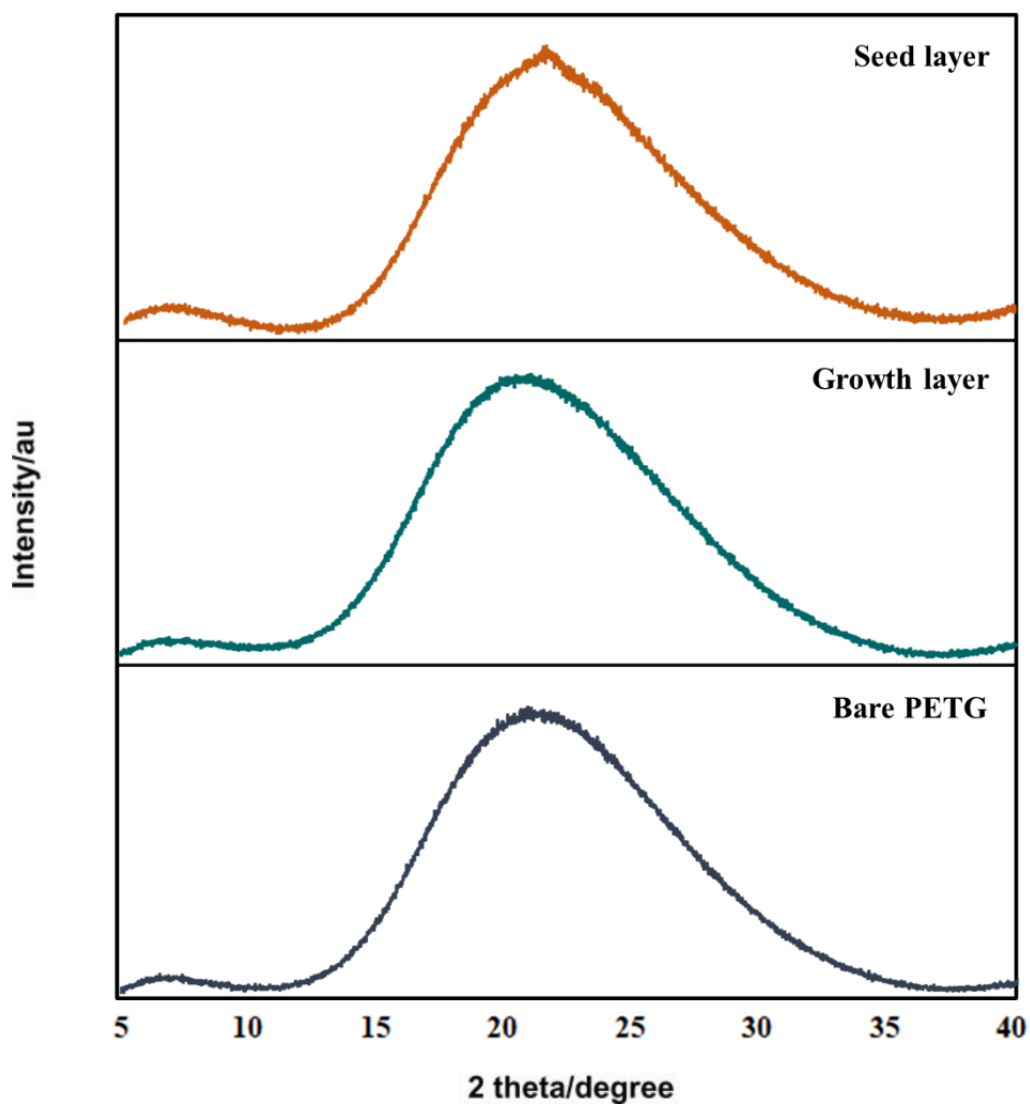


Figure 4.72 XRD patterns of printed samples.

Due to FE-SEM characterization could not observe ZIF-8 particles on printed seed layer and growth layer of ZIF-8 coated PETG. ZIF-8 particles were analyzed by X-Ray Diffractometer (XRD). In figure 4.72 could not observe peak because samples have no crystal phase of ZIF-8 particles. It can be concluded that samples have only amorphous phase of PETG.

CHAPTER 5

CONCLUSION

Catalyst were produced by synthesis of silver nanoparticles using NaBH_4 as a reducing agent and PSS-co-MA as a capping agent. Metallic could be formed by low concentration of capping agent while high concentration obtained yellow color. It was found that silver nanoparticles can be coated on surface modified filament well. However, poor adhesion between filaments and surface modification method like polyelectrolyte multilayers cause peeling off of silver nanoparticles during 3D printing process. Alkaline and Polyethyleneimine (PEI) treatment was introduced to increase filaments surface adhesion.

FE-SEM image has shown excellent silver nanoparticles dispersion on the filaments corresponding to optical property that is homogeneous metallic filaments. The results of filaments surface adhesion were demonstrated by Peeling test. Surface treated filaments obtain stronger silver nanoparticles attachment than surface untreated filaments. Peeling test show unremovable silver nanoparticles area after taping and removing by scotch tape that PEI treatment 5 hr. has the highest amount of unremovable silver nanoparticles and 3D printed PEI treated filament can be found silver nanoparticles on the surface while untreated and NaOH cannot. Thus, PEI treatment is the highest efficient method to surface treat filaments.

3D printed metallic filaments were investigated silver nanoparticles existence by XRD to confirm the result obtained from FE-SEM images. Surface treated filaments both NaOH and PEI show peak of silver nanoparticles while surface untreated filaments have no peak signal. However, for untreated and NaOH treated FE-SEM image could observe silver nanoparticles only cross-section but on the surface corresponding to optical property showing homogeneous grey color. It can be concluded that surface untreated filaments have no silver nanoparticles on the surface but very deep inside. NaOH treated filaments have no on the surface either but under the surface.



2287006921

CU Theses 6272032063 thesis / rev: 19072564 14:14:29 / seq: 8

Silver nanoparticles were successfully formed metallic on filament but for 3D printed out. However, there are a few that capable to adhere outside the surface of the filament even pressed through enormous friction between filaments and 3D printer nozzle. This research needs to be developed in order to constructed microreactors with high amount of catalyst loading and high catalytic activity reactor with high details customizing by 3D printing method.



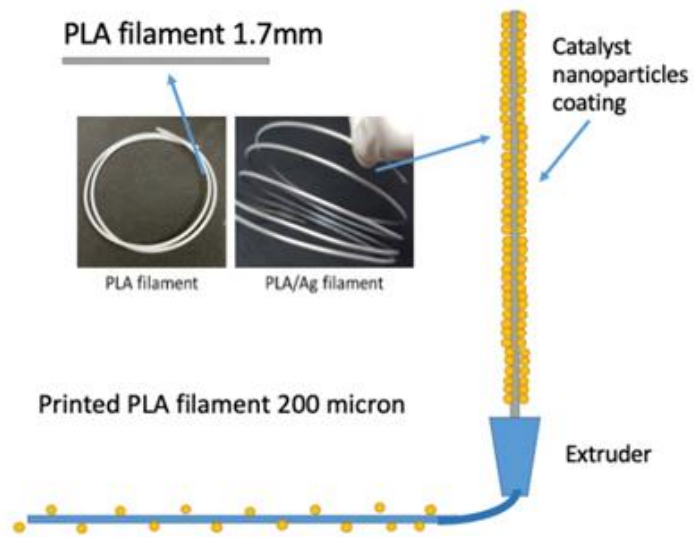
2287006921

CU iThesis 6272032063 thesis / recv: 19072564 14:14:29 / seq: 8

APPENDIX

GRAPICAL ABSTRACT

Appendix A



2287006921

CD IThesis 6272032063 thesis / rev: 19072564 14:14:29 / seq: 8

REFERENCES

- A Bhosale, M. and B. J. C. O. C. M Bhanage (2015). Silver nanoparticles: Synthesis, characterization and their application as a sustainable catalyst for organic transformations. Current Organic Chemistry, 19(8), 708-727.
- Açıkyıldız, M., et al. (2014). Electrocatalysis and the Production of Nanoparticles. Modern Electrochemical Methods in Nano, Surface and Corrosion Science, 171.
- Baran, E. H. and H. Y. Erbil (2019). Surface modification of 3D printed PLA objects by fused deposition modeling: a review. Colloids and Interfaces, 3(2), 43.
- Chen, X.-c., et al. (2016). Self-wrinkling polyelectrolyte multilayers: construction, smoothing and the underlying mechanism. Physical Chemistry Chemical Physics, 18(45), 31168-31174.
- Domínguez, M. I., et al. (2021). Current scenario and prospects in manufacture strategies for glass, quartz, polymers and metallic microreactors: A comprehensive review. Chemical Engineering Research and Design, 171, 13-15
- Dubas, S. T. and J. B. Schlenoff (1999). Factors controlling the growth of polyelectrolyte multilayers. Macromolecules, 32(24), 8153-8160.
- Dubas, S. T. and J. B. Schlenoff (2001). Swelling and smoothing of polyelectrolyte multilayers by salt. Langmuir, 17(25), 7725-7727.
- Iravani, S., et al. (2014). Synthesis of silver nanoparticles: chemical, physical and biological methods. Research in pharmaceutical sciences, 9(6), 385.
- Jian, M., et al. (2015). Water-based synthesis of zeolitic imidazolate framework-8 with high morphology level at room temperature. RSC Advances, 5(60), 48433-48441.
- Jose, P. A., et al. (2018). 3D printing of pharmaceuticals—a potential technology in developing personalized medicine. Asian Journal of Pharmaceutical Research and Development, 6(3), 46-54.
- Karakurt, I. and L. Lin (2020). 3D printing technologies: techniques, materials, and post-processing. Current Opinion in Chemical Engineering, 28, 134-143.
- Karakurt, I. and L. J. C. O. i. C. E. Lin (2020). 3D printing technologies: Techniques, materials, and post-processing. Current Opinion in Chemical Engineering, 28, 134-143.

- Kong, L., et al. (2017). Preparation of Palladium/Silver-Coated Polyimide Nanotubes: Flexible, Electrically Conductive Fibers. Materials, 10(11), 1263.
- Merindol, R. (2014). Layer-by-layer assembly of strong bio-inspired nanocomposites, Strasbourg.
- Merlin L. Bruening, M. A. (2020). Polyelectrolyte Multilayer Films and Membrane Functionalization. Material Matters, 6, 3.
- Neumaier, J. M., et al. (2019). Low-budget 3D-printed equipment for continuous flow reactions. Beilstein Journal of Organic Chemistry, 15(1), 558-566.
- Ramanjaneyulu, B. T., et al. (2018). Towards Versatile Continuous-Flow Chemistry and Process Technology Via New Conceptual Microreactor Systems. Bulletin of The Korean Chemical Society 39(6), 757-772.
- Rasal, R. M., et al. (2010). Poly(lactic acid) modifications. Progress in Polymer Science, 35(3), 338-356.
- Shahrubudin, N., et al. (2019). An Overview on 3D Printing Technology: Technological, Materials, and Applications. Procedia Manufacturing, 35, 1286-1296.
- Shameli, K., et al. (2012). Green biosynthesis of silver nanoparticles using Curcuma longa tuber powder. International Journal of Nanomedicine, 7, 5603.
- Song, Z., et al. (2016). Recent progress on MOF-derived nanomaterials as advanced electrocatalysts in fuel cells. Catalysts, 6(8), 116.
- Tham, C., et al. (2014). Surface engineered poly (lactic acid)(PLA) microspheres by chemical treatment for drug delivery system, Trans Tech Publ. Key Engineering Materials, 594-595, 214-218.
- Yuan, W., et al. (2020). Weak polyelectrolyte-based multilayers via layer-by-layer assembly: Approaches, properties, and applications. Advances in Colloid and Interface Science, 282, 102200.
- Zhang, L., et al. (2017). Facile immobilization of Ag nanoparticles on microchannel walls in microreactors for catalytic applications. Chemical Engineering Journal, 309: 691-699.
- Zhang, X., et al. (2013). Synthesis of hollow Ag–Au bimetallic nanoparticles in polyelectrolyte multilayers. Langmuir, 29(22), 6722-6727.

Zhang, Y., et al. (2018). Influence of the 2-methylimidazole/zinc nitrate hexahydrate molar ratio on the synthesis of zeolitic imidazolate framework-8 crystals at room temperature. Scientific reports, 8(1), 1-7.

VITA

NAME	Pornnutcha Thadasri
DATE OF BIRTH	4 May 1997
PLACE OF BIRTH	Chonburi
INSTITUTIONS ATTENDED	<ol style="list-style-type: none">1. Bachelor of engineering, Major in petrochemicals and polymeric materials, Silpakorn University, Nakornpathom, Thailand2. Master of science, Major in Polymer Science, The Petroleum and Petrochemical College, Chulalongkorn University, Bangkok, Thailand
HOME ADDRESS	37/15 Moo 6, Phob chok Village, Sattahip Sub-district, Sattahip District, Chonburi, 20180, Thailand



2287006921

CU ThesIs 6272032063 thesis / recv: 19072564 14:14:29 / seq: 8